Studies on Photoelectronic Phenomena in Undoped Semi-Insulating GaAs

By

ANIRBAN BHATTACHARYYA

MATERIAL SCIENCE PROGRAMME

INDIAN INSTITUTE OF TECHNOLOGY, KANPUR

DECEMBER, 1998

Studies on Photoelectronic Phenomena in Undoped Semi-Insulating GaAs

A thesis submitted in
Partial fulfillment of the requirements
For the degree of
Master of Technology

by

Anirban Bhattacharyya

to the
Materials Science Programme
Indian Institute of Technology (Kanpur)
December 1998

CERTIFICATE

It is certified that the work contained in the thesis entitled *" Studies on Photoelectronic Phenomena in Undoped Semi-insulating GaAs"* by Anirban Bhattacharyya has been carried out under our supervision and that this work has not been submitted elsewhere for a degree.

Dr Y. N. Mohapatra
Associate Professor,
Dept. of Physics & Materials Science
Indian Institute of Physics (Kanpur)

Dr. Satyendra Kumar
Associate Professor
Dept. of Physics
Indian Institute of Technology (Kanpur)

Dedicated to

My Parents

Acknowledgement

Writing the acknowledgement page is possibly the most pleasurable part of any thesis work, and in the hindsight everything seems to be rosy, as the setting sun lights only the peaks and leaves the valleys in the dark.

I would like to thank my thesis guides for introducing me to a topic, which has engineering utility, and also poses a challenge to the scientific mind. I am also grateful to them for their guidance and for giving me a "free run" in a lab with the most sophisticated instruments in this field that money can buy.

I would like to thank Dr. P. Gupta Bhaya for the use of his Source-Measure Unit K-236, which has played a vital role in the set-up.

I would like to thank the faculty of Materials Science Department for the knowledge I have gained in diverse fields from them.

Dr Ram Bilas has been a great help with his smiling presence and helping attitude, Mr. J. S. Sharma with his skillful hands and huge experience in the workshop.

With S. Narasimhan I have spent the major part of this two years in setting up the system, and sharing the ups and downs of the life. I would wish him the best of luck in seeking his dreams.

Dr. T. Som has been like an elder brother to me, and I have thoroughly enjoyed the scientific discussions we have had. I would also like to mention Amitranjan, Dr. P. K. Giri and Anirban Mitra in this regard.

I would like to thank all my friends in the lab, and in the M.Tech Program, Anjali, Sasmita, Sangeeta, P. G. Prasad, and specially Sanghamitra for making my stay in IIT Kanpur a pleasurable one.

Finally I would like to thank my parents for the enormous support I have received from them and especially from little Anshuman, without which it would have been difficult for me to complete the work.

List of Figures

42. 5.18 The Sample is exposed to IR radiation at low temperature Using a IR lamp with Si filter and Thermal Filter for 10 min The Photocurrent are recorded for different heating rates.

43. 5.20 Sample dark cooled to 20K, Exposed to light in the following sequence: 1) Monochromatic 676 nm, 2) Broadband IR, 3) Monochromatic 676 nm

44. 5.21 Sample dark cooled, and exposed to: 1) 676 nm from halogen lamp, 2) IR, 3) 676 nm

45. 5.22 Sample dark cooled, exposed to white light of high intensity, 676 nm light, IR lamp with Si filter and again 676 nm light.

46. 5.23 The samples are dark cooled to 20K, and then exposed to:
Sample1: 676 nm, IR, 676 nm in sequence.
Sample2: white light, 676 nm, IR, 676 nm in sequence.
Photocurrent-Temperature data taken with 676 nm

47. 5.24 Sample dark cooled, sequentially exposed to 1) Flash of white light 2) 676 nm, 3) IR, 4) 676 nm. TSC, PC measured, heating rate 15K/min

48. 5.25 Sample illuminated IR LAMP for 20 min at 25K TSC taken with heating rate = 15K/min, showing instabilities at 60K and ~130K

49. 5.25 Sample exposed to IR light for 20 min at 25KTSC taken at different heating rates

50. 5.27 The Sample is Exposed to IR for 10 min at ~26K, heated to 120K and kept for varying lengths of time, cooled, exposed to HeNe laser for 5 min, TSC done @ 15K/min Shows lower occurrence of instabilities at 60K

51. 5.28 Sample dark cooled, exposed to IR for varying lengths of time, exposed to 5 min of laser, TSC taken at 15 K/min. Shows Instabilities at 60K

52. 5.29 Decay transients at various temperatures.

53. 5.30 Oscillations in SI GaAs For different excitation wavelengths,
Temperature = 150K

52. 5.31 Oscillations in SI GaAs For different excitation wavelengths,
Temperature = 30K

List of Tables

Abstract

Semi-Insulating Gallium Arsenide has emerged as an important technological material apart from its privileged use as a substrate for a GaAs based Technology. This has necessitated a thorough understanding of its properties from the view of its growth and its applications. Standard literature attributes most of the photo-electronic properties of semi-insulating gallium arsenide to the presence of a mid-gap level due to a native defect termed EL2, which is usually present in very large concentration. However, in many samples depending on various factors, EL2 is present in a very low concentration. The aim of this work has been to focus on such a sample, where many other trap levels and recombination centres are present, and investigate the various photoelectronic phenomena in order to understand the role of these defect centers.

General characterization has been carried out to obtain an understanding of the various traps present in the material through thermally stimulated current (TSC) measurements. Steady state photoconductivity measurements were carried out for a large temperature range from 20K to room temperature, and for a wide range of excitation intensities. Time domain measurements, TSC and thermally stimulated photocurrent (TSPC) measurements have been done for different initial conditions of trap filling at low temperatures.

The sample exhibits the presence of traps normally present in semi insulating GaAs, showing six traps with two dominant ones with activation energies 0.32 eV and 0.45eV. The temperature dependence of photoconductivity due to intrinsic light (676nm), with intensity as a parameter shows that at low temperature (50K→25K) the temperature dependence is controlled by position of quasi-Fermi levels which in turn are controlled by light intensity. Two traps at 0.3eV and 0.45eV have been inferred from presence of two shoulders in the plot, these values being in agreement with the dominant traps observed in the TSC spectrum.

Little of no photoquenching is observed with high intensity IR light, an observation in direct contrast to behavior in samples containing large concentration of EL2. IR radiation tends to quench the TSC peaks simultaneously, and an isothermal anneal at temperatures of 110K - 120K recovers the peak heights. This can be explained on the basis of change in the occupation of lifetime controlling recombination centers with IR radiation and temperature and not due to any configurational changes of defects or metastability. The TSPC data for different heating rates show that of the two peaks observed, only one correspond to a thermally activated process.

Low temperature photoconductivity transients with specially designed sequence of operation with white light, IR and 676nm shows that intense white light desensitizes the photoconductor due to filling of centers in the gap. The sensitizing ability of IR radiation is dependent on the initial occupation distribution of centers, indicating that the dominant center controlling the lifetime can be changed with proper choice in initial conditions.

We have shown by focussing on a typical undoped SI GaAs sample that conventional Shockley-Read-Hall kinetics is adequate to explain IR quenching of trap activity in samples containing low concentration of EL2 centers

Contents

Chapter 1: Introduction

1.1 Why semi-insulating gallium arsenide.

1.2 Motivation of this work

1.3 Thesis layout

Chapter 1: Introduction

1.1 Why Semi-insulating Gallium Arsenide.

Among the technologically important materials that interests material scientists, gallium arsenide has been one of the most promising, and substantial part of the promise has now been translated into many applications unattainable using other semiconductors. In spite of two to three decades of its use in the industry and as a research material in the laboratory, several aspects of a gallium arsenide as a technological material continues to offer challenges to the material scientist. The role of various intrinsic defects in determining photoelectronic properties is one of many such problems where current understanding is far from coherent, despite forty years of research.

In the micro-electronic industry, the role of a suitable substrate is of importance, and one of the prime requirements of a substrate material is that it should be structurally identical to the epitaxial layer in terms of crystal parameters. In many applications it is required that its electrical conductivity should be extremely low. Theoretically the most straightforward, and practically the most difficult way to bring about high resistivity is to minimize the impurity concentration by minimizing impurity incorporation during growth or processing. The limitations posed by growth technology do not allow this. However in case of GaAs, it has been possible to obtain extremely high resistivity material irrespective of presence of impurities, under certain conditions of crystal growth wherein intrinsic defects play the role of compensating centers. In absence of a good native oxide layer of GaAs, the role of an *isolating material*, such as that played by SiO_2 in silicon based devices, has been taken up by this widely available material.

The materials science aspect of the problem is to optimize the growth conditions under which the high resistivity could be reproduced. The physics aspect, on the other hand, tries to investigate the origins of this particular behavior. The deluge of data highlighting various characteristics, all of them tentatively linked to a single unique source, has made it difficult to construct a single model that can coherently explain all the various aspects. It has been stated that with the increase of each electron volt of band gap, the complexity

increases manifold, as the presence of deep levels alters the property of the semiconductor to an extent that they control basically all the photoelectronic parameters.

In the special case of high resistivity, or semi-insulating GaAs, the presence of a single trap level with extremely high concentration has been detected in specially grown samples. The presence of this defect in not intentionally doped material tends to control almost all the electrical properties, as the Fermi level is firmly pinned to the associated deep level, calculated to be near the center of the band gap. However the system is made much more complicated due to the presence of other impurity centers, which also affect the properties of the crystal especially in samples where the concentration of this particular impurity is low.

There is a history of intense study of this material for over forty years, and over this period, there have been many changes in the general underatanding in the physics of the problem. In the 60's and 70's the property was thought to be due to the presence of impurities present in the material, incorporated during growth, and oxygen was thought to be a prime suspect. Various properties of the material, including the characteristic photoelectronic properties have been studied in detail at this time, and attributed to the oxygen doping. This was completely negated by works in the 80's when it was conclusively proved that the imperfection was a native defect, most probably a complex structure in which a native defect was a prime constituent. This imperfection had a characteristic level in the middle of the band gap, and was named EL2. This native defect was later proved to be an As_{Ga} antisite, and the general mechanism of the particular phenomena related to semi-insulating GaAs was also tentatively put down. The early 90's threw up yet another aspect of the problem when several groups showed diverse properties which could not be understood from existing theories. One major contributor to the apparent confusion is that the impurity incorporation in a material is extremely dependent on the crystal growth processes, and over the last few decades there has been a virtual revolution in this field. Also even within a single ingot there has been seen a distribution of imperfections, and hence a variation in the sample properties.

It is in this backdrop that we have decided to turn our attention to this enigmatic and yet consequential material. To study the different phenomena, and to try and present a cohesive picture of the mechanism which bring about these.

1.2 Motivation of this work

In spite of the understanding on the single most important defect center called EL2 in undoped semi-insulating GaAs, there has been a variety of interesting and not-so-well understood effects observed in the material. There has been a resurgence in the interest in these effects since their understanding would help standardizing characterization of these substances better. Further, most explanation of unusual phenomena in his material cannot be traced to some simplistic phenomenology involving EL2 alone.

During the course of earlier work on this material, we came across samples whose properties resembled normal undoped SI GaAs in many respects but did not show conventional signature of presence of the EL2 defect in large concentration. To date most experiments and explanations have centered around El2 so that samples with low or no EL2 concentration have been neglected. It appears that the investigation of such samples hold the key to the development of a more wide ranging phenomenology to account for various changes of observations regarding nature of compensating centers and their role in controlling lifetime and trapping.

This work was aimed at setting up a computer-controlled facility to be able to carry out conventional characterization such as

(i) Thermally stimulated current and its variations

(ii) Temperature dependence of photoconductivity and

(iii) Photocurrent decay and transient characteristics.

In studying trap related phenomena in undoped semi-insulating GaAs at low temperatures, the choice of excitation conditions in determining initial conditions play a vital role. In this work we have used white light, monochromatic light of energy larger than band-gap, and infrared subbandgap energy in varying intensities.

In other words we set out to investigate photoconductivity and trap related low temperature phenomena which would help characterize and understand deep levels better in this material.

In a nutshell it can be stated that if a sample of GaAs is taken to low temperatures and exposed to infrared light, the photoconductivity reduces drastically due to an effect

generally referred to as optical quenching. This optical quenching is normally seen for photoconductivity as well as in a trap characterization tool called thermally stimulated current spectroscopy. The mechanism for both these processes are usually taken to be identical, and a host of publications has come out on this topic.

Our results show primarily that, while the optical quenching of thermally stimulated current has been seen to be complete and substantial, under the same conditions and for same sample, the photoconductivity remains unquenched. This has important significance on the underatanding of the role of deep levels in the material. The entire experimental work, elaborate as it may appear at the first glance, basically are directly related in the pursual of this strange property, and in trying to describe and explain the reasons for the anomaly. Since the properties of this material is strongly dependent on various parameters, such as temperature, wavelength of excitation source, time, etc, as well as the history of sample excitation, some of the experiments performed has become rather involved. They can be called designer experiments, where one attempts to look at the dependence of properties on each of these parameters individually and also their cross-sensitivities. In a more ambitious scale, this work attempts to construct a possible phenomenological explanation invoking the structural and configurational changes of the dominant defects in the material.

1.3 Thesis layout

The photoelectronic properties exhibited by any material can be classified into a general, which is present in most of the similar type of materials, and the specific, which is unique to that material. Chapters 2 and 3 are devoted to briefly outline these. Chapter 2 gives an overview of general optoelectronic processes, the material parameters such as lifetime and conductivity, and linking them to the trap properties of type, density, energy position and capture cress section. Special emphasis is given to the description of impurity center behavior using concepts such as demarcation levels; and to the characterization of trap levels by various methods.

Chapter 3 gives a brief, quasi-chronological account on the development of the understanding of nature and origin of specific optoelectronic material properties of semi-insulating GaAs, specially those arising out of the presence of deep level traps. Stress has

been given on the divergence of opinions in various controversial aspects of the material. Also, it tries to prepare the stage for the experimental results and their explanations of this work.

Chapter 4 discourses the experimental set-up, the experiments conducted, and the raw data that has been obtained. In order to facilitate the explanation of the 'designed experiments', we have also presented a background, describing the general experimental procedures usually followed to characterize trap-related phenomena in photoconductors in general, and in SI GaAs in particular.

In chapter 5, the experimental results and discussions have been broken into three broad categories. The preliminary experiments provide the boundaries of the operating space, in terms of range of voltages currents and wavelengths to be used, and general characterization of the material. The main experimental section describes the different experimental procedures and results. The third section shows the experiments that have been performed, but not looked into in detail, and as such present a pointer to future direction of work. It also discusses at length the experimental results, and tries to explain in terms of a suitable simplified model, all the diverse phenomena.

Chapter 6 sums up the entire work, and tries to bring out the major points that the work tries to address.

Chapter 2: Photoelectronic Processes & Levels in Semiconductors

2.1 Electron Processes in Crystals
- 2.1.1 Absorption and excitation
- 2.1.2 Trapping and capture
- 2.1.3 Recombination

2.2 Fundamental relations in electron processes

2.3 Fermi-level analysis of conductivity.

2.3.1 The Quasi Fermi Level

2.4 Photoconductivity process

2.5 Traps and trap dependent photoconductivity in semiconductors.
- 2.5.1 Effects of trapping
- 2.5.2 Detection of Traps
  - Growth and decay curves: general
  - Thermally stimulated trap emptying
    - Quasiequilibrium Analysis
    - General Equations

2.6 Recombination processes
- 2.6.1 Recombination at an imperfection

2.7 Conclusions

Chapter 2 Photoelectronic Processes & levels in Semiconductors

This work is fundamentally based on the presence of deep levels in semi-insulating GaAs. These impurity centers, or intrinsic defects, cause the material to exhibit its characteristic properties. Some of these properties are common to most photoconductors with a band-gap similar to that of GaAs, such as GaSe, CdSe etc, while some are unique to this material. It is therefore imperative that the general behavior of deep levels in insulators and semiconductors, especially their effect on the photo-electronic processes, is understood clearly, before going into their specific behavior in GaAs.

This chapter attempts to give an overview of the different photo-electronic processes, specially those related to the presence of an impurity level. We list significant material parameters, such as *lifetime* and *sensitivity* and their dependencies on the trap parameters such as trap nature, density, energy level and capture cross section.

2.1 Electron Processes in Crystals

We begin with the question, "what can happen when a crystal is exposed to radiation?" The different processes that take place when a semiconductor is exposed to an exciting radiation can be classified according to the accompanying electron transitions. They are (1) Absorption and Excitation, (2) Trapping and Capture and (3) Recombination (fig 2.1).

2.1.1 Absorption and excitation

There are various possible types of absorption transitions, which result in photoconductivity. The band to band transition (a) is caused in the absorption of the photon in the crystal itself, resulting in the formation of a free electron and a free hole. The transition may be due to an absorption in a localized imperfection leading to a free electron and a hole bound in the locality of the imperfection (b). The other possibility is the raising of an electron from a valence band to the unoccupied imperfection level (c) leading to a free hole and a bound electron. The related spectra for these three and other related processes are given in fig (2.2).

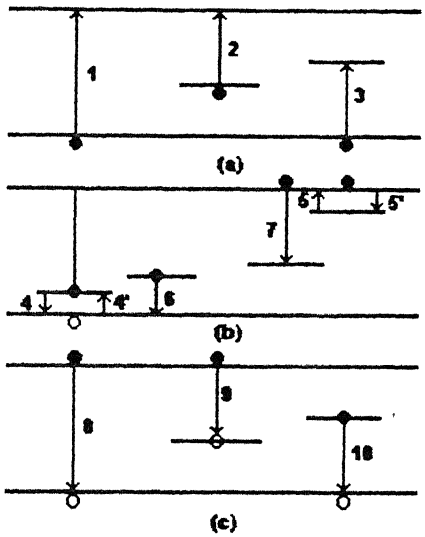

Fig 2.1 Common electronic transitions in photoconductors. (a) Absorption; (b) Trapping and capture; (c) recombination

2.1.2 Trapping and capture

This is the process in which the *carriers are temporarily localized at different imperfections that are called trapping centers before being re-excited to the free state.* This is more likely if the energy level of the center is near the band edge, but the final nature of the center is determined by kinetic conditions, that is temperature and excitation, and is not dependent on the nature of the centers themselves.

2.1.3 Recombination

This is a process in which the carriers recombine with another carrier of the opposite charge. This can be by recombination of free carriers, which can be radiative, emitting a photon of energy equal to the band gap. However, the usual case is when the this occurs through recombination centers, either a free electron being captured by a excited center containing a hole or vice versa.

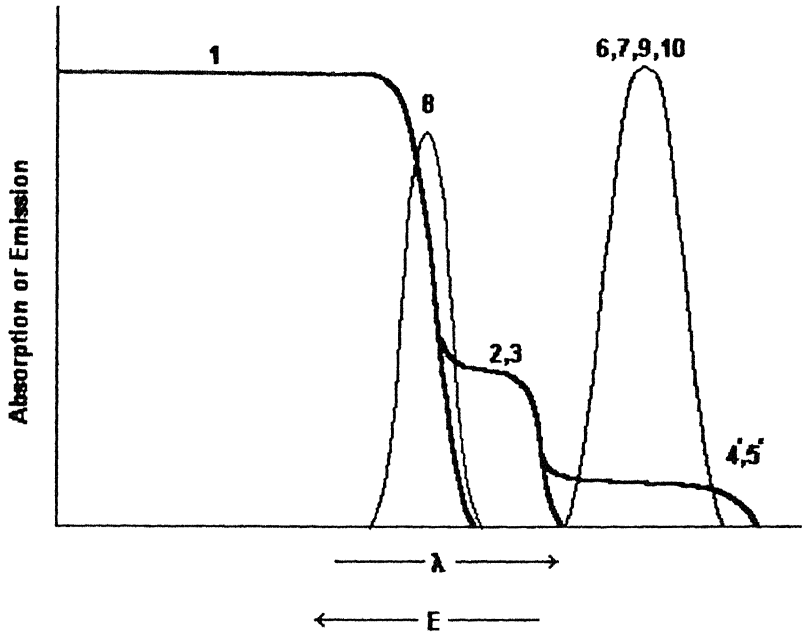

fig 2.2 representative Absorption spectra ——— and emission spectra ——— (1) Absorption transition from valence band to conduction band; (2,5') absorption from imperfection level to conduction band; (3,4') absorption transition from valence band to imperfection level; (8) Emssion transition for recombination betwee free electrons and free holes; (6,7,9,10) emission trnsition for recombination at an imperfection centre.

2.2 Fundamental relations in electron processes

The conventional way to describe the photo-electronic processes is through the position of Fermi levels, which gives the occupational probability of the different trap levels and the bands. We now derive the dependency of the electronic properties of a material on the Fermi level.

The number of occupied states in unit volume of a material (n), which again is the density of carriers in the conduction band, is given by the relation

$$n = \int_{E_c}^{\infty} f(E)N(E)dE \qquad (2.2.1)$$

Where the $f(E)$ in the occupational probability, and $N(E)$ is the density of states function. Substituting the values of these functions, under the conditions of (1) non degeneracy and (2) spherical constant energy surfaces we get

$$f(E)N(E) = AE^{\frac{1}{2}} \exp\left[-\frac{E + (E_c - E_0)}{kT}\right] \tag{2.2.2}$$

where the E is measured from the bottom of the conduction band.

The total number of electrons per unit volume in the conduction band is given by integration of eq 2.2.1, for all energies, then

$$n = 2\left(\frac{2\pi m_e kt}{h^2}\right)^{\frac{3}{2}} \exp\left(-\frac{E_c - E_0}{kT}\right) \tag{2.2.3}$$

$$p = 2\left(\frac{2\pi m_h kt}{h^2}\right)^{\frac{3}{2}} \exp\left(-\frac{E_0 - E_v}{kT}\right) \tag{2.2.4}$$

where m_e and m_h are the effective masses of electrons and holes.

The two equation given above can be simplified by using the effective density of states N_c and N_v, for the conduction and valence bands

$$n = N_c \exp\left(-\frac{E_{fn}}{kT}\right) \tag{2.2.5i}$$

$$p = N_v \exp\left(-\frac{E_{fp}}{kT}\right) \tag{2.2.5ii}$$

The E_{fn} and E_{fp} are absolute value of the energy difference between the Fermi level and the bottom of the conduction band or top of the valence band.

On the other hand, the electron concentration for imperfection levels is given by an expression of the form

$$n_I = \frac{N_I}{\frac{1}{2}\exp\left[\frac{E_{fn} - E_I}{kT}\right] + 1} \tag{2.2.6}$$

where N_I is the total number of traps having an energy level E_I and n_I traps are occupied at temperature T.

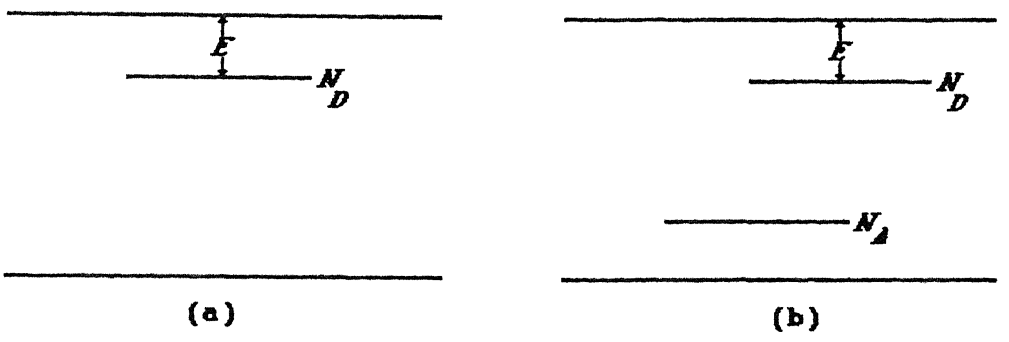

fig (2.3) Energy level diagram for (a) N_D donor levels (b) N_D donor levels and N_A acceptor levels

2.3 Fermi-level analysis of conductivity.

We now link the photoconductivity of a material with the position of the Fermi levels. In a simplified case, which nevertheless is the usual one in practice, we assume that the conductivity in a material is associated to one type of carriers only. The conductivity expression is given as

$$\sigma = ne\mu \tag{2.3.1}$$

$$= N_c e\mu \exp\left(-\frac{E_{fn}}{kT}\right) \tag{2.3.2}$$

Here σ is the conductivity of a material, and μ is the mobility of free carriers, here electrons.

Here, $N_c \propto T^{3/2}$ from eq(2.2.4, 2.2.5).. The dependence of μ with temperature is, if the mobility is only dependent on crystalline phonons and not on impurity scattering, as $\mu \propto T^{-3/2}$. Then the conductivity will vary with temperature as

$$\sigma = C\exp\left(-\frac{E_{fn}}{kT}\right) \tag{2.3.3}$$

where C is a constant.

From the relation we can see that the slope of ln(σ) vs. $1/T$ plot in given by $-E_{fn}/k$. So if the temperature dependence of conductivity is found, the position of the Fermi level can be determined.

We consider the case of a semiconductor, which has N_D donor concentration, and the donor level is at a distance E from the conduction band (fig 2.3). The equilibrium value of n, the carrier concentration, will be determined when the thermal excitation of the electrons from the donor level to the conduction band is equal to the rate of capture of the free carriers by the ionized donors. Here we are taking the case of an insulating material and neglecting the generation of carriers by band to band transition.

The rate of generation of free electrons by thermal excitation is given by $(N_D - n)\nu\exp(-E/kT)$ where the N_D-n is the numbers of donors not ionized, ν the attempt to escape frequency. The rate of capture of free electrons by ionized donors is given by $Sv_{th}\,n^2$, where S is the capture cross section for a free electron, and the v_{th} is the thermal velocity, given by $v_{th} = \left(2kT/m\right)^{1/2}$.

The equation for the equilibrium as discussed above is given by

$$(N_D - n)\nu\exp\left(-\frac{E}{kT}\right) = Sv_{th}n^2 \quad . \tag{2.3.4}$$

The relation for attempt to escape frequency is

$$N_C v_{th} = \frac{\nu}{S} \tag{2.3.5}$$

which, substituting for N_C is

$$\frac{\nu}{S} = 8me\left(\frac{\pi}{h^2}\right)^{3/2}(kT)^2 \tag{2.3.6}$$

which means that at any temperature the attempt to escape frequency for a particular center is directly proportional to the capture cross section for the carrier.

The equilibrium value for free electron concentration as given by (2.5) is substituted into the equation to get the relation for the equilibrium Fermi level

$$E_{fn} = \frac{E}{2} + \frac{kT}{2} \ln\left(\frac{N_C}{N_D}\right) \tag{2.3.7}$$

which is true for the initial assumption of a single donor type impurity level. For a crystal where there are donors as well as acceptors, we have the relation

$$(N_D - N_A - n)\nu \exp\left(-\frac{E}{kT}\right) = Sv_{th} n(n + N_A) \tag{2.3.8}$$

leading to a relation

$$E_{fn} = E + kT \ln\left(\frac{N_A}{N_D - N_A}\right) \tag{2.3.9 a}$$

in the common case of $n << N_A$. For $n >> N_A$, the relation is

$$E_{fn} = \frac{E}{2} + kT \ln\left(\frac{N_C}{N_D - N_A}\right) \tag{2.3.9b}$$

2.3.1 The Quasi Fermi Level

For steady state equilibrium under external excitation, there is exchange between free carriers in the conduction band and the electrons in trapping centers. We can define a quasi-Fermi level for each type of carriers, i.e. both electrons and holes, such that the position of which determines the occupancy level of the centers lying between it and the nearest band. The occupancy of the levels lying between the quasi-Fermi levels are determined by recombination processes.

The rate of change of carrier concentration during a constant rate of excitation f e-h pairs per second is given by

$$\frac{dn}{dt} = f - n(N_1 - n)v_{th} S_n + n_I N_C S_n \exp\left(-\frac{E_I}{kT}\right) \tag{2.3.10}$$

$$\frac{dp}{dt} = f - n_I p v_{th} S_p + (N_I - n_I) N_V S_p v_{th} \exp\left(-\frac{E_G - E_I}{kT}\right) \tag{2.3.11}$$

where n and p can be substituted by eqn.(2.2.5), to bring in the electron and hole Fermi levels.

For steady state conditions we have $dn/dt = dp/dt = 0$ the solution to the above equations for E_{fn} gives

$$\exp\left(-\frac{E_{fn}}{kT}\right)\left[1-\exp\left(-\frac{E_{fn_0}-E_{fn}}{kT}\right)\right]=\frac{f}{N_C(N_I-n_I)v_{th}S_n} \qquad (2.3.12)$$

where E_{fn_0} is the value of the thermal equilibrium in the dark (f=0). For sufficient excitation, $E_{fn_0} - E_{fn} >> kT$, the equation gives the approximate solution for E_{fn}

$$E_{fn}=kT\ln\left[\frac{N_C(N_I-n_I)v_{th}S_n}{f}\right]=kt\ln\left(\frac{N_C}{n}\right) \qquad (2.3.13)$$

$$E_{fp}=kT\ln\left(\frac{n_I N_v v_{th}S_n}{f}\right)=kt\ln\left(\frac{N_v}{p}\right) \qquad (2.3.14)$$

Adding the two, we get $E_{fn}+E_{fp}=kT\ln\left(\frac{N_C N_V}{np}\right)$

This can be substituted to give

$$E_{fn}+E_{fp}=E_G-kT\ln\left(\frac{np}{n_i^2}\right) \qquad (2.3.15)$$

This can be understood from (fig 2.4) which shows the position of the levels. The occupancy of the electrons are described by the electron quasi-Fermi level located at E_{fn} from the conduction band and the occupancy of the holes from the hole quasi Fermi level, at E_{fp} from the valence band. The difference in energy between the two is a function of the rate of e-h pair generation f.

For dark conditions $f = 0$, and we know that $np = n_i^2$, so (2.3.15) can be written as

$$E_{fn}+E_{fp}=E_G$$

Therefore the position of E_{fp} and E_{fp} are identical for the dark conditions, where all the free carriers are due to thermal excitations.

2.4 Photoconductivity processes

We now look into the process of photoconductivity, that is electrical conductivity processes in a crystal while being exposed to an photonic excitation. The basic principles of these phenomena and the various parameters associated are now discussed. The photoconductivity in most crystals is dominated by the various trapping centers that are usually present, and such phenomena as such form a major part of this work. These are treated in some detail in the next section.

2.4.1 Parameters involved in photonic excitation

The general mechanism for the photoconductivity mechanism in crystals is understood under the assumption that the material in question is homogenous in nature. The conductivity of an insulator or a semiconductor is stated as

$$\sigma = e(n\mu_n + p\mu_p) \tag{2.4.1}$$

The photoconductivity that results on excitation by an absorbed radiation, increasing the free carrier concentration is given by

$$\Delta\sigma = e(\Delta n\mu_n + \Delta p\mu_p) \tag{2.4.2}$$

In an insulator the value of Δn and Δp may be much larger than that corresponding to the free-carrier densities in the dark, and the opposite being true for a semiconductor where the effect of external excitation can be taken as a perturbation on a large dark carrier density.

There are two implicit assumptions made to simplify the calculations which are true for most cases.

1. The conductivity is dominated by one of the carriers
2. The crystal stays neutral during photoconductivity processes without a buildup of appreciable space charge in the crystal.

The ***free lifetime*** of a carrier can be defined as the time a charge carrier is free to contribute to the conductivity. It is the time an free electron excited to the conduction

band stays in the band, without undergoing recombinations and without being extracted from the crystal by an applied field.

This can be expressed as

$$f\tau_n = \Delta n$$

$$f\tau_p = \Delta p \tag{2.4.3}$$

Where the τ_p and τ_n are free carrier lifetimes for holes and electrons

$$\Delta\sigma = fe(\mu_n\tau_n + \mu_p\tau_p) \tag{2.4.4}$$

The ***photosensitivity*** of a material is defined as the photoconductivity per unit excitation intensity. The ***photoconductivity gain*** G is the number of carriers which pass between the electrodes of the photoconductor per second by absorption of each photon.

$$\frac{\Delta I}{e} = GF \tag{2.4.5}$$

where ΔI is the photocurrent, F is the total number of e-h pairs being created, i.e. $F = f \times (volume)$. The gain can be expressed as the ratio of the free lifetime of a carrier to the time required to move between the electrodes, called transit time.

$$G = \frac{\tau_n}{t_n} + \frac{\tau_p}{t_p} \tag{2.4.6}$$

where the t_n and t_p are the transit times of the holes and electrons.

The free carrier lifetime of a carrier is dependent on the presence of recombination centres and trapping centres.

$$\tau = (v_{th}SN)^{-1} \tag{2.4.9}$$

where v_{th} is the thermal velocity and S is the capture cross section of a recombination centre.

2.4.3 Recombination kinetics in the absence of trapping

The simplified model of a recombination in a photoconductor, where trapping centres are neglected is now discussed.

For steady-state conditions, the total rate of free-carrier generation is equal to the total rate of free carrier recombination. In the dark

$$\sum_i g_i = n_0 v_{th} \sum_i S_i N_i \tag{2.4.8}$$

where n_0 is the concentration of free carriers, and g_i the rate of thermal generation from i-type centres.

If an additional density of Δn is now introduced by optical generation of rate f, we have

$$f + \sum_i g_i = (n_0 + \Delta n) v_{th} \sum_i S_i N_i \tag{2.4.9}$$

If we assume a single recombination centre, from which both optical and thermal generations take place, we obtain

$$n_0 + \Delta n = \left(\frac{f + g}{v_{th} S} \right)^{1/2} \tag{2.410}$$

$$\tau = [v_{th} S (n_0 + \Delta n)]^{-1} \tag{2.4.11}$$

For an insulator, $n_0 << \Delta n$ and $g << f$,

$$\Delta n = \left(\frac{f}{v_{th} S} \right)^{1/2} \tag{2.4.12}$$

$$\tau = [v_{th} S (n_0 + \Delta n)]^{-1} \tag{2.4.13}$$

The photocurrent varies as the square root of the light intensity, and the lifetime is inversely proportional to the photocurrent. The simple picture is unable to explain most of the experimental results, where the photocurrent varies as light intensity between 1/2 and 1, and sometimes more than 1.

For a semiconductor, $n_0 >> \Delta n$, and we get

$$\Delta n = \frac{f}{n_0 v_{th} S} \tag{2.4.14}$$

$$\tau \approx (n_0 v_{th} S)^{-1} \tag{2.4.15}$$

Here the photocurrent varies directly as the first power of light intensity, and to a first approximation lifetime is independent of light intensity and equal to the lifetime of free carriers of an unilluminated semiconductor.

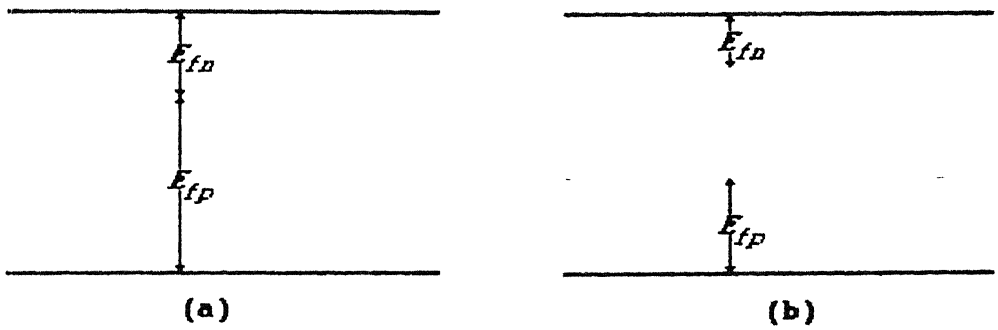

fig (2.4) (a) Fermi level for thermal equilibrium:
(b) Quasi Fermi levels for steady state optical excitation

2.5 Traps and trap dependent photoconductivity.

Traps are impurity centers in a material, which capture and release carriers but do not take part in the recombination process. They play a fundamental role in the energy storage, in all electronically active materials by spatially localizing an excited carrier. The carrier is held immobile, till excited optically or thermally.

The demarcation between a trapping and a recombination center depends on the relative magnitudes of the probability of the carrier being thermally freed from a trap after capture to the probabiiity of recombination with a carrier of opposite charge occurring at the center. This can be put mathematically that for a center to behave as a electron trap rather than a electron recombination center is,

$$n_I p v_{th} S_p << n_I S_n v_{th} N_c \exp\left(-\frac{E_I}{kT}\right) \qquad (2.5.1)$$

and vice versa.

This can be further understood by use of demarcation levels, as given in fig (2.5). This is true for an insulator, where the density of photoexcited carriers is much larger than thermally generated carriers.

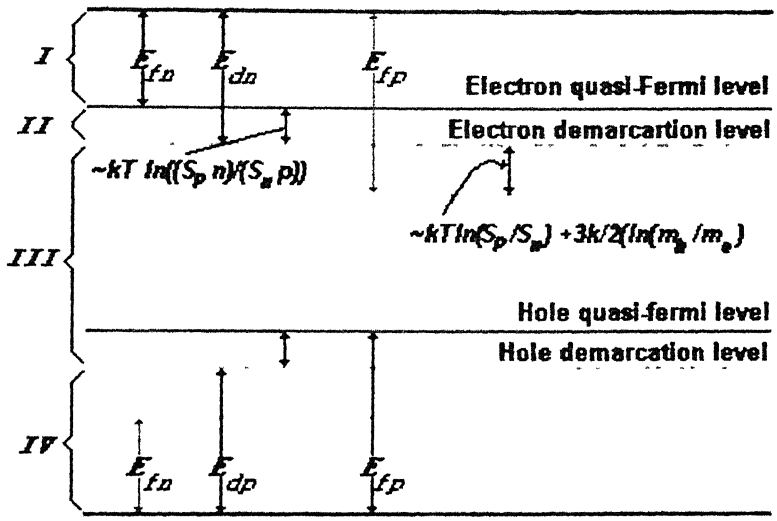

fig (2.5) quasi-Fermi levels and demarcation levels of a insulator

When the electron is at a electron demarcation level, it has equal probability of getting detrapped by thermal energy, and of recombination with a free hole. The occupation of a state lying above the electron demarcation level is determined by the conditions of thermal equilibrium between the levels and the conduction band. The occupation of states lying between the hole and electron demarcation level is determined by recombination kinetics of the material.

The demarcation level for electrons are given by definition as

$$n_1 S_n N_C v_{th} \exp\left(-\frac{E_{dn}}{kT}\right) = n_1 p v_{th} S_p \qquad (2.5.2)$$

which is eq(2.5.1) with E_I replaced by E_{dn}, the energy from the bottom of the conduction band to the demarcation level.

The relations between the electron quasi-Fermi level and the electron demarcation level is given by replacing N_C

$$E_{fn} = E_{dn} + kT \ln\left(\frac{S_p p}{S_n n}\right) \qquad (2.5.3)$$

which shows the dependence of the capture cross section in the designation of a center, and so each type of carriers will have its own demarcation level associated with it.

The hole demarcation level and the electron quasi-Fermi level both depend on the density of free electrons, and can be related as

$$p_1 n S_n v_{th} = p_1 S_p N_v v_{th} \exp\left(-\frac{E_{dp}}{kT}\right) \qquad (2.5.4)$$

where p_1 is the density of holes captured at the centers. This can be further calculated by substituting for n

$$E_{dp} = E_{fn} - kT \ln\left(\frac{S_p}{S_n}\right) + \frac{3kT}{2} \ln\left(\frac{m_h}{m_e}\right) \qquad (2.5.4)$$

Thus when the electron Fermi level goes up, in a material due to optical excitation, the hole demarcation level goes down, an effect which will be looked into in some detail in the later chapters.

In figure (2.5), the levels in region I are electron traps, in IV are hole traps. The levels in III are recombination centers by definition. Those in region II are above the electron demarcation level but below the quasi-Fermi level, so even though these are in equilibrium with the conduction band, the density of occupied levels is high, and recombination with free holes is possible.

The corresponding case for a semiconductor is shown in figure (2.6) where the density of thermally free carriers is greater than that of optically excited carriers.

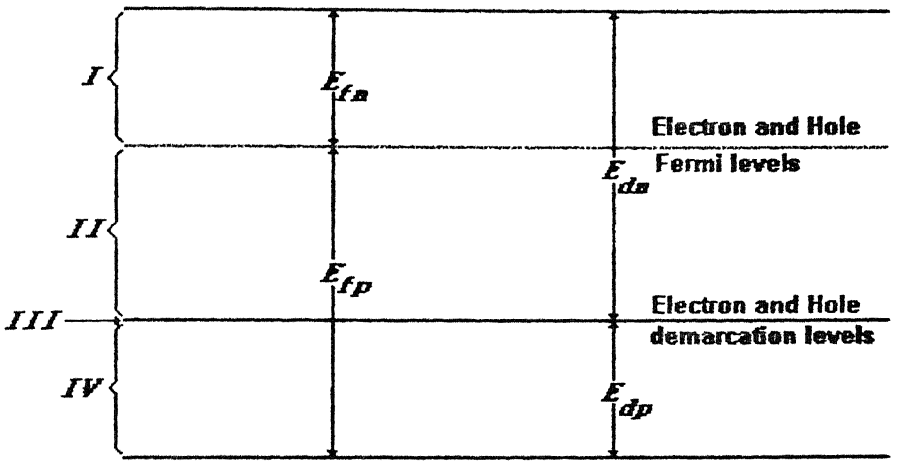

fig.(2.6) Fermi levels and demadcation lavels for a semiconductor

2.4.1 Effects of trapping

The presence of traps have a predominant effect on the electron transport and other related phenomena in a material, and often the study of photoconductivity and related effects in a insulator or a semiconductor entails a detailed study of the presence of traps in the material.

If traps are absent, all carriers in a material are free, and the presence of traps decreases the number of free carriers in a material. This can be considered as a change in the mobility of carriers, and an effective drift mobility μ_d^* of the carriers can be defined as

$$(n+n_t)\mu_d^* = n\mu \tag{2.5.5}$$

In insulators, where $n_t >> n$, we get

$$\mu_d^* = \frac{N_c}{N_t}\exp\left(-\frac{E_t}{kT}\right)\mu \tag{2.5.6}$$

Thus the major contribution of the presence of traps is to decrease the mobility of carriers, basically by localization.

A major effect is to make the experimentally observed decay time of the photocurrent after the excitation has been turned off, longer than the carrier lifetime. If the free carrier concentration is comparable to the number of trapped carriers, there is a prolongation of the decay transient as the trapped carriers are freed thermally. This phenomenon will be looked into with more detail at a later stage.

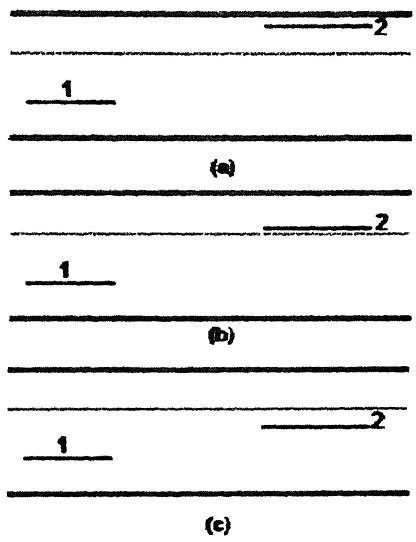

fig 2.7 Relations betwwe the location of trapping and recombination centres, and the Fermi levels
1: Recombination centre
2: Trapping centre
Dark Fermi level
Quasi Fermi levl

The presence of traps can also decrease the sensitivity of the photoconductor. This can be understood in reference to fig(2.7) where we have a semiconductor with n type photoconductivity associated with the majority carriers, and where the minority carriers are captured immediately. Also we consider the dark conductivity to be negligible. The figure shows the presence of a recombination center 1 and a trapping center 2. When the quasi-Fermi level for electrons is raised in presence of light, the occupancy of electrons in the trapping centers is decreased, and the loss of sensitization occurs. Now, as in (a), if

the trapping level lie considerably above the light Fermi level, then this change is negligibly low. In (b) however, the level lie near the Fermi level, and the change is considerable. The figure (c) shows that the *trapping level is above the dark Fermi level, but is below the light Fermi level.* This case is of importance, as there will be a large desensitization, but the *centers are no longer trapping centers under illumination.* This is a phenomena which leads to many interesting properties of semiconductors.

The exact form of the expression for the observed decay time will depend on the trap distribution in energy. The effect of traps on the electronic properties of a one-carrier insulator is given in ref 1.

2.5.2 Detection of Traps

There are various methods used to detect and characterize the various traps in insulators and semiconductors, that is, give direct information about their identity, density and identity of traps. We now summarize the various methods that has been employed in this work.

(1) ***Growth of photoconductivity after the beginning of the excitation.*** In a crystal which is initially de-excited, the increase of the number of free carriers in the material, and hence the photoconductivity, increases to the equilibrium value after a considerable time, as a portion of the carriers excited is trapped in various centers. If there is no thermal detrapping, as in deep levels at low temperatures, the area between the growth curve and the steady-state value of photocurrent gives a measure of the trap density.

(2) ***Decay of photoconductivity after cession of excitation.*** The traps filled during excitation will slowly empty, depending on their capture cross section and the ionization energy. If it is assumed that the retrapping of carriers is neglected, then exponential decay is expected. If there are more than one traps present, then the time dependence can be expressed as $I = I_0 t^{-n}$, where n may vary in different ranges of t. The photocurrent decay is proportional to the rate at which the carriers are freed from the traps, multiplied by the appropriate lifetime of the carriers.

(c) ***Thermally stimulated trap emptying,*** If the traps are filled by excitation at low temperature, they may be emptied by raising the temperature. This is usually carried out at a constant rate, to facilitate the analysis. The intensity of the thermally stimulated

conductivity is proportional to rate of trap emptying multiplied by the recombination lifetime.

We now look into each of these processes in some detail.

2.5.2.1 Growth and decay curves: general

There is a plethora of work on experimentally determination of growth and decay curves of photocurrent versus time. If trapping is important, as is in most cases, their data can be generally fitted as

$$\Delta i = \frac{\Delta i_0}{(1+at)^b} \tag{2.5.7}$$

where a and b are fitting constants, and may vary with temperature and time, even with time during the decay itself.

In most cases the description of the growth and decay of photocurrent in a material depends exhaustively on the trapping and detrapping of carriers. The probability of an electron escaping from a trap at a depth E and with a cross section S_t, at temperature T is given by

$$P = N_C v_{th} S_t \exp\left(-\frac{E}{kT}\right) \tag{2.5.8}$$

. The rate of change of trapped electrons during decay is given by

$$\frac{dn_t}{dt} = -n_t P \tag{2.5.9}$$

If the retrapping of freed carriers is neglected. The solution of the above equation is

$$n_t = n_{t0} \exp(-Pt) \tag{2.5.10}$$

The variation of the density of free carriers can be approximated, for short time lengths, by considering

$$\Delta n = -\frac{dn_t}{dt}\tau \tag{2.5.11}$$

where the lifetime $\tau = (v_{th} S_r N_r)^{-1}$, can be considered a constant, especially if $\Delta n \ll N_r$, the density of holes in recombination centers. The decay equation can be written as

$$\Delta n = n_{t0}\tau P \exp(-Pt) \tag{2.5.12}$$

If there are different kinds of traps, with different E values, then the resulting decay curve can be considered as a sum of many such exponential curves.

If the retrapping is to be included, the rate of trap emptying has to be multiplied by the ratio of capture probability for recombination centers to the sum of capture probabilities of recombination centers and empty taps.

$$Ratio = \frac{S_r N_r}{S_r N_r + S_t(N_t - n_t)} \tag{2.5.13}$$

Where N_t is the total trap density. Since $N_r = n + n_t$, and assuming $n << n_t$,

$$\frac{dn_t}{dt} = -\frac{S_r n_t^{\,2}}{S_t N_t + n_t(S_r - S_t)} P \tag{2.5.14}$$

For special case of $S_r = S_t$, and when the traps are saturated at the beginning of the decay, so that $n_{t0} = N_t$, the equation equivalent to 2.3.12 is

$$\Delta n = \frac{N_t \tau P}{(1 + Pt)^2} \tag{2.5.15}$$

which is similar to eq.(2.3.7).

In many materials there can be an assumption of a essentially uniform distribution of traps in energy, and the distribution of traps around the Fermi level is to be taken into account to determine the necessary theoretical relations. We will however not go onto the details of these trap distribution studies.

There are definite cases however that the analysis of the decay curves of photoconductivity exhibits the validity of a discrete trapping level. If an exponential decay is found, the measurement of decay at several temperatures permits the determination of both trap depths and capture cross sections. If the log of τ_0 (time required to decay to $1/e$ of the original value of photocurrent) is plotted as a function of $1/T$, a straight line is obtained with slope of E/k and intercept of $(N_C v_{th} S_t)^{-1}$.

2.5.2.2 Thermally stimulated trap emptying

At low temperatures, the deep level impurities in a high resistance semiconductor can be studied by measurement of the thermally stimulated current. The sample is initially

heated to a high enough temperature to empty all the traps, and then cooled in the dark, so as to keep the traps empty. At low temperature it is exposed to light to fill all the traps, and at that temperature thermal energy is not sufficient to empty the traps, so this remains in a non-equilibrium state.

If the sample is now heated at a constant rate, then each traps get emptied at temperatures where there is sufficient thermal energy, and the resulting current-temperature plot shows peaks, the position of each of which serves as the signature for each particular trap.

There has been several theoretical publications dealing with the interpretation of the Thermally Stimulated Current spectra[3-4], however we present here the more simple ones,

1. Quasiequilibrium Analysis

The theoretical analysis due to Bube, (1960) requires the following assumptions:

1. The recombination in the material involves retrapping of the emitted carrier by the level under consideration.

2. The level is initially completely filled.

3. Equilibrium is assumed between the conduction band and the trap, so that a Fermi level can be defined throughout the temperature range.

4. The peak occurs when the Fermi level crosses the trap level.

Under these conditions, the energy level of the trap is given by

$$\Delta E_T = kT_m \ln\left(\frac{N_c(T_m)}{n_m}\right) \qquad (2.5.16)$$

where ΔE_T is the level of trap below the conduction band edge, T_m is the temperature of the conductivity peak, and n_m is electron concentration at T_m.

The drawbacks to the approach is that (2) is unlikely to be true, and ΔE_T can be derived for general considerations, independent of (4). The eq. (2.4.1) is true only if the traps are half filled at T_m.

2.5.2.2.2 General Equations

A more fundamental approach was (*Randall and Wilkins(1945)*, and *Saunders and Jewitt (1965)*)[5] based on the following equations:

$$\frac{dn_I}{dt} = -n_I N_c S_I v_{th} \exp\left(-\frac{\Delta E_I}{kT}\right) + n(N_I - n_I) S_I v_{th} \qquad (2.5.17)$$

$$\frac{dn}{dt} = -\frac{n}{\tau} - \sum_I \frac{dn_I}{dt} \qquad (2.5.18)$$

where n_I is the density of electrons in the I^{th} level, N_I is the density of the I^{th} level.

Here (2.4.2) equates the net change of electrons in the I^{th} level, and this is equal to the rate of capture of electrons in the trap level minus the thermal release of the trapped electrons to the conduction band.

The eq. (2.4.3) involves the recombination of conduction electrons. The rate of change of electrons in the conduction band is equal to the rate at which it gets trapped, having a effective lifetime of τ, minus the rate of detrapping from all the trap levels..

These are a set of $N+1$ coupled nonlinear equations, where N is the number of trap levels, and can be only solved by a using a number of simplifying assumptions.

The analysis of Saunders and Jewitt (1965), assumes that the current peaks are sufficiently apart, for the following assumptions to be valid

1. The recombination from all traps except one can neglected.

2. The occupancy of all other traps are sufficiently constant, so that the retrapping by these levels may be accounted for in the term τ, and is temperature independent.

The summation can now be neglected. If we assume $n << n_I$ and $n_I << N_I$, then the eq(2.4.2) and eq(2.4.3) can be solved, and conductivity can be found as

$$\sigma(T) = \frac{e\tau\mu_e N_C S_I v_{th}}{1+\tau N_I S_I v_{th}} \hat{n}_I \exp\left(-\frac{\Delta E_I}{kT} - \frac{1}{\beta}\int_{T_0}^{T} \frac{N_C S_I v_{th} \exp\left(-\frac{\Delta E_I}{kT}\right)}{1+\tau N_I S_I v_{th}} dT\right) \qquad (2.5.19)$$

where β is the rate of temperature rise, defined as

$$T(t) = T_0 + \beta t \qquad (2.5.20)$$

and $\hat{n}_I$ is the initial occupancy of the I^{th} trap level, at temperature T_0. If the explicit temperature dependencies are assumed

$$N_c \propto T^{\frac{3}{2}}$$

$$v_{th} \propto T^{\frac{1}{2}}$$

$$S_I \propto T^{-b}$$

$$\tau = const. \qquad (2.5.21)$$

Then eq(2.4.4) can be shown to have a maximum at $T = T_m$ such that

$$\frac{\Delta E_I}{kT_m} = \ln\left(\frac{T_m^2}{\beta}\right) + \ln\left(\frac{N_c S_I v_{th}^k}{\Delta E_I}\right) - \ln\left(1 + \tau N_I S_I v_{th}\right) \qquad (2.5.22)$$

provided that $\Delta E_I > kT$.

Two cases can be distinguished:

Case 1. Slow retrapping: $\tau N_I S_I v_{th} << 1$

In this case 2.4.6 becomes

$$\frac{\Delta E_I}{kT_m} = \ln\left(\frac{T_m^2}{\beta}\right) + \ln\left(\frac{N_c S_I v_{th}^k}{\Delta E_I}\right) \qquad (2.5.23)$$

and if $S_I \propto T^{-2}$, as is often assumed, then the second term on the right side becomes independent of temperature, since $N_c \propto T^{\frac{3}{2}}$ and $v_{th} \propto T^{\frac{1}{2}}$. Then a plot of $1/T_m$ versus $\ln\left(T_m^2/\beta\right)$ for various heating rates should give a straight line of slope $\Delta E_I / k$, and the intercept yields the capture cross section.

If $b \neq 2$, then (2.4.7) becomes

$$\frac{\Delta E_I}{kT_m} = \ln\left(\frac{T_m^{4-b}}{\beta}\right) + C \qquad (2.5.24)$$

where C is independent of temperature. The value of b must be found by trial and error, so that a straight line is obtained in a plot of $1/T_m$ versus $\ln\left(\frac{T_m^{4-b}}{\beta}\right)$. Then we can proceed to determine ΔE_I and S_I as above.

Case 2. Fast retrapping. $\tau N_I S_I v_{th} >> 1$ (2.5.25)

The equation becomes $\frac{\Delta E_I}{kT_m} = \ln\left(\frac{T_m^{3.5}}{\beta}\right) + C'$ (2.5.26)

Where C' is independent of temperature and

$$C' = \ln\left(\frac{N_c}{\tau N_I}\right) - \frac{3}{2}\ln(T_m) - \ln\left(\frac{\Delta E_I}{k}\right) \quad (2.5.27)$$

In this case, no information can be derived about S_I, but the quantity can τN_I can be computed.

In experimental situations, the heated rate β is altered to see a corresponding change in peak position (T_m). Then the procedure described above is used to find out the parameters of the trap levels such as the activation energy and the capture cross section. A single run of TSC experiment can map out the various trap levels of a system,

2.6 Recombination processes

The change in photoconductivity resulting from excitation is normally terminated by the recombination of the photoexcited carriers electrons and holes, a process determining the lifetime of carriers and hence the sensitivity of a photoconductor.

Such processes can be a direct one, or may be due to the recombination of a free carrier with a carrier bound to imperfection. Normally recombination through an imperfection is dominant for low carrier densities, and direct recombination for high carrier densities.

2.6.1 Recombination at an imperfection

Th rate of recombination through an imperfection center depends on the occupancy of the imperfection centers, which in turn is related to the free-carrier densities through the

capture cross sections. The statistics of recombination through a single type of imperfection levels have been considered by Hall[6] and Shockley and Read[7]. Fig (28) shows one such centre and the four processes connected to it

1. Electron capture by a neutral center
2. Electron emission by a negatively charged center
3. Hole capture by a negatively charged center
4. Hole emission by such a center

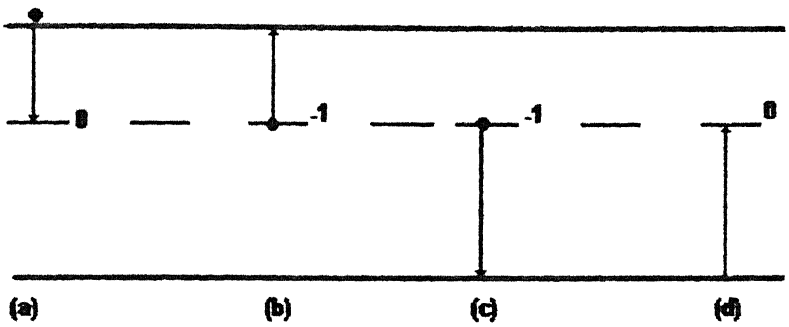

fig 2.8 The four electon emission and capture processes connected with a single imperfection level.
(a) Electron capture by a neutral centre
(b) electron emission from a negatively charged centre
(c) hole capture by a negatively charged centre
(d) hole emission from a neutral centre
The arrows indicate electron transitions

The SHR model tries to calculate the lifetime of excess carriers as a function of the location and density of recombination centers, and as a function of the location of the Fermi level. A qualitative picture is given by Rose[**] in the same direction, and this is being described below.

The minority lifetime of a semiconductor under the condition that recombination center density greater than that for density of thermally activated carriers, is given for different

locations of the Fermi level and Demarcation level (fig 2.9). The recombination center is chosen for $E_r < E_i$ and N_r is calculated for all such centers between the Fermi level and demarcation level. We now discuss special cases when the Fermi level moves from the conduction band to the valence band, and the demarcation level moves at the same rate in opposite direction.

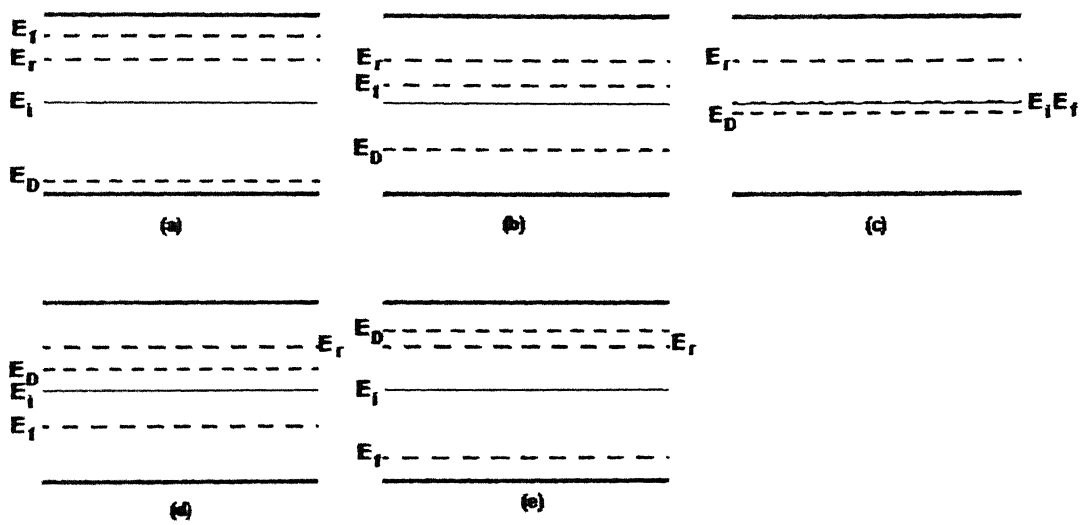

fig 2.9 The five relationships among the Fermi level, recombination level, centre of band gap, and demarcation level in a semiconductor

(a) The material is n type, the Fermi level being above the centers. The center is between the E_f and E_D. The minority carrier lifetime is given by

$$\tau_{po} = \frac{1}{v_{th} S_p N_r}$$

As the Fermi level moves away from the conduction band towards the recombination levels, the lifetime remains the same.

(b) The material is still n type, but the Fermi level is below E_r. The N_r centers are only partially occupied by electrons. As the Fermi level moves from E_r to E_I, the lifetime increases exponentially

$$\tau_p = \tau_{po} \exp\left(\frac{E_f - E_r}{kT}\right)$$

(c) The material is intrinsic, as the Fermi level lies at the same location as the intrinsic level, and the difference between E_f and E_D is $kT\ln(S_n/S_p)$. The maximum lifetime for n-type material is achieved in this condition. As the Fermi level moves below E_i the material becomes p type and minority carriers become electrons. There is a discontinuity in minority-carrier lifetime if S_n is not equal to S_p.

(d) The demarcation level now lies above Fermi level in p material. Those centers lying between E_r and E_D are not by definition behaving as recombination centers, and the lifetime decreases as the demarcation level move towards the E_r. If τ_{no} is the lifetime when all centers lie between E_D and E_f, then

$$\tau_n = \tau_{n0} \exp\left(\frac{E_D - E_r}{kT}\right)$$

(e) The N_r centers now lie between E_D and E_f, so the lifetime is

$$\tau_{n0} = \frac{1}{v_{th} S_n N_r}$$

The relations are graphically represented in fig (2.10)

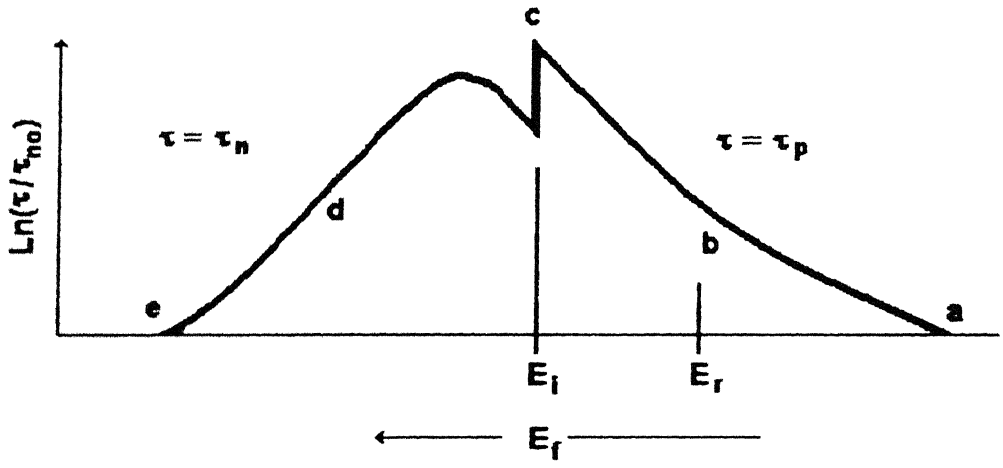

fig 2.10 Dependence of minority carrier lifetime on location of Fermi level.

2.7 Summary

In this chapter we have reviewed the general photo-electronic properties of a crystal, and its dependence on the properties of impurity levels. An effort has been made to trace the material properties through various parameters such as the quasi-Fermi level and the demarcation levels. Lastly we have looked at in some detail at the effect of the presence of traps in a crystal, and ways and means of evaluating the trap parameters experimentally. Finally recombination processes and the Shockley-Read-Hall recombination processes through a single type of impurity level is discussed.

Chapter 3: Semi Insulating Gallium Arsenide, a review

Chapter 3: Semi Insulating Gallium Arsenide, a Review

The material in this chapter attempts to trace briefly the development of understanding of the unique properties of semi-insulating GaAs and recount changes that has been brought about in our perception of the origins of this behaviour since the late seventies. This has been traditionally a well-studied material, and currently there is a general consensus regarding various phenomenological properties of the material as well as about their origins. However there has been many observations, which do not quite fit into the framework of phenomenology. There has been recently renewed interest in these aspects of numerous interesting photoelectronic phenomena in this light. In the later half of this chapter we bring out the necessary backdrop against which our experiments and their discussions must be viewed.

3.1 Semi Insulating Gallium Arsenide

The semi-insulating condition of GaAs was recognised but not understood in the early '60s, when *Hilsum*[8] *commented that it was fairly easy to make strongly n or p type GaAs,* but very hard to make weakly doped material reproducibly. Whereas semi-insulating crystals by undoped procedure could be formed by specific growth conditions, it was difficult to produce bulk material with a room temperature carrier concentration n_0 or p_0 in the range 10^{14} to 10^9 per cm^3. Therefore the fig (3.1) shows large areas of the ranges of carrier density as dashed rather than solid lines, indicating the ranges not readily accessible.

In the semi-insulating region the Fermi level is pinned to the intrinsic location, forcing ambipolar conditions, that is where both the holes and electrons take part in the conduction, The RT conductivity is in the range 10^5 -10^9 Ω cm. This material is of enormous technological applications as a substrate material due to its high resistivity, and is of interest to the scientific community because of its unique properties.

3.2 GaAs :O a review

Oxygen belongs to the sixth column of the periodic table, and is basically expected to be a donor impurity in the III-V compound semiconductors, a contention that has been firmly established in the material properties of GaP.[9] The O is found out from the low temperature ionisation studies to be a typical deep level impurity.

In GaAs, however, the similarities are not very clear, and no definite evidence for an electronically active centre has been found, that is closely related to oxygen doping. In 1962, several laboratories[10-12] reported that very high resistivity GaAs can be grown by horizontal Bridgemann technique, provided that the growth was carried out in a oxygen atmosphere. Various deep level characterisation techniques, such as thermally stimulated current, optical transient current spectroscopy study [13-14] revealed the presence of a deep donor level located at E_c-0.75 eV. The idea that the trap E_c-0.75 is due to oxygen gained ground, as shown in the following section

3.2.1 Photoelectronic properties of high resistivity GaAs: 0 (Review of Linn and Bube (1975)[15]

A thorough and pathbreaking work was conducted by Bube (1975), that looked into the unique properties of GaAs in the semi insulating state, specially the optical quenching properties of this material.

The spectral response of *photoconductivity and photo-Hall mobility* (fig 3.2, 3.3) has been taken for three temperatures of 295K, 213K and 82K. It can be immediately seen that there is very little difference of character in the two spectral responses at 295K and 213K. There is a band edge peak at 1.4eV, and a typical lower than band gap excitation with an absorption edge at 0.7 eV. The photo-Hall mobility is n type for all photon energies, indicating a extrinsic excitation from a level 0.7eV below the conduction band.

The spectral response at 82K is vastly different (fig 3.4). The photoconductivity was measured 3min and 15 min after photo-excitation for spectral scans in two different directions, low to high energy and high to low energies on a previously heated and dark cooled sample, a process which ensures the traps to be initially empty.

The results show a sharp fall in the photoconductivity, after the sample has been exposed to infrared radiation at low temperatures. This can be interpreted as to indicate two different states of the crystal: a higher sensitivity n-type and a lower sensitivity p-type. The higher sensitivity n type is encountered if the sample has not been previously exposed to photons in the 1.0-1.3eV range, and the lower sensitivity p state to which the higher sensitivity state is transferred, on exposure to 1.0-1.3eV light. The photoconductivity of the p-type is about two orders of magnitude smaller than that of the n-type state, and the process of transition is called *optical quenching.*

The temperature dependence of photoconductivity for intrinsic photoexcitation an the corresponding Hall mobilities are shown in fig 3.5. Curve 1 represents the high sensitivity state; at low temperatures the $\ln(\sigma)$ increases with 1/T with a slope consistent with the Shockley-Read-Hall one-level recombination model, for a level of about 0.65 below the conduction band and $\tau_{n0} = 6\times10^{-10}$ sec. In the low sensitivity state, the quenching persists at low temperature, and upon heating makes a rapid recovery to the high sensitive state when the temperature exceeds 105 K and is complete by 125 K.

The ***optical quenching***, as given by percent decrease of intrinsic-excited photoconductivity, is given in fig 3.6 as a function of the wavelength of the quenching light. At 82K, it is shown that the onset is about 0.5eV with an abrupt increase at about 0.77eV. Above 1.03eV, there are three processes found: (1) a fast excitation, (2) a fast quenching, of about 7%, and (3) a slow quenching accounting for 98% in a hour.

The thermally stimulated current experiments, as described in an earlier chapter, gives trap levels as reproduced in table 3.1. The work by Bube et.al. also touches upon ***non-Ohmic behaviour of contacts*** and ***low frequency oscillations.***

3.3 Direct evidence of nonassignment of oxygen to the main electron trap in GaAs.

The first questions against the oxygen behaviour began to arrive when attempts to create E_c - *0.75* level in GaAs grown by Liquid Phase Epitaxy (LPE) by incorporation of Ga_2O_3 were repeatedly unsuccessful [16-17]. But it was finally established by Huber Linh et.al.[18] that the O has no role to play in the trap level of GaAs. This was done by simultaneously looking for the trap density and spatial trap distribution in a horizontal

Bridgman grown not intentionally O doped sample. The doping profile was measured by C-V at two different temperatures, and along the spatial extent of the wafer. The O content and its distribution was measured by SIMS at precisely similar locations on similar samples. The comparison of SIMS and electrical characterisation show that (1) The concentration of the trap EL2[19] was one order of magnitude higher than concentration of oxygen. Also (2) there is a large difference in the trap distribution along the sample, and the distribution of O.

Thus one can unambiguously say that oxygen is not involved, either directly or in a complex defect in the origin of electron trap at E_C-0.75eV.

3.4 Linking of EL2 with the As_{Ga}^{+} antisite

The identification of EL2 was carried out by a comparative study of the electrical properties of EL2 and the EPR studies of the As_{Ga} antisite in 1983-1985. The EPR of As_{Ga} in plastically deformed GaAs [20] showed an energy state of 0.47 eV in the double donor state, from weak photoenhancement of the signal. Further analysis was carried out by Lagowski and Gatos [21] on a native trap denoted by them as HM1. Deep level transient studies and photocapacitance measurements indicated that the trap has two charge states with energies 0.54 +/- 0.02 eV and 0.77 +/- 0.02eV. This is in direct consonance with theoretical calculations that predict that the charge-state levels for As_{Ga} antisite to have a separation of 0.25eV, and so the trap HM1 can be directly identified with the antisite. The upper level, which has been identified with EL2, shows the photoexcitation to a metastable state. This provides the missing link for the working As_{Ga} defect. Detailed comparative study of the photoresponse of EL2 in undoped sample and the EPR study of the As_{Ga} antisite [22,23] further strengthen the argument.

It should be clearly stated that despite the erroneous assumption regarding the origin of the opto-electronic properties, all the phenomenological observations made by Bube are perfectly valid, and as such form the basis of study of defects and their peculiar behaviour in semi-insulating GaAs. The optical quenching effect and its recovery has been observed in photoluminescence, photocapacitance, photoconductivity, photo-EPR and other related phenomena. There has been a sustained effort by several groups to model these properties.

3.5 Modelling the Optical Quenching Phenomena

The first model was put forward by Levinson[24], where it was proposed that a the defect is basically "*a multi-charged complex defect which leads to a charge-state controlled electrostatic interaction between two or more defects in a complex. The minimisation of electrostatic and lattice strain energy gives rise to structural re-arrangements, which lead to transformations between two possible configurations of the complex.*" The two configurations of course would correspond to the two sensitivity states.

Further work was carried out by several groups, and we would highlight the work done by Jimenez et al. in this direction.

Jimenez reported in 1984[25] several detailed studies in photoquenching behavior at low temperatures (down to 4K). There were two distinct phenomena observed, and they could be classified as (1) Extrinsic quenching and (2) Near intrinsic quenching. Extrinsic quenching is achieved in the 1-1.25 eV photon range by these very photons, in a self-quenching phenomenon. This is the classical optical quenching generally reported. Near intrinsic quenching is achieved by 1.17eV light causing a decrease of near intrinsic photocurrent, in this case due to 1.45eV light. Both these two quenching can be shown to thermally evolve at around 125K with the extrinsic quenching evolving at slightly higher temperatures, leading to the understanding that they are due to the same cause. It is important to mention that there is a definite time lag that the near intrinsic quenching compared to the extrinsic quenching. These results lead to the model of the quenching phenomena as put forward by Jimenez, as given in fig (3.6).

The first step is the formation of EL2 into EL2* by means of the 1-1.25 eV radiation. This produces the typical extrinsic optical quenching. The second step is the capture of a neighbouring defect X (shallow level) after the EL2* was generated, to form a new complex, which accounts for the quenching of the near intrinsic light. The thermal evolution is first accomplished in the releasing of X, and then relaxation of the EL2* to EL2. This result shows the existence of *defect reactions* in a straightforward way.

This is a typical model that has been used to try to explain most of the phenomena relating to the optical properties of EL2. However, there are several more recent works that tend to question these seemingly simple mechanisms.

3.6 Enhanced and persistent photoconductivity in GaAs

It was reported by the same group, in the same year (1984)[26,27] that "among the great variety of Horizontal Bridgmann bulk GaAs samples tested by us, we have observed in some of them a striking photoconductivity behaviour, which consists of a strong enhancement of the photocurrent (EPC) after long excitations with phonons in the 1-1.35 eV spectral range at temperatures below 135 K. The result is opposite to the expected optical quenching (PCQ)".

The optical enhancement (fig 3.7) takes place after a fast increase, and a decay to an apparent steady state has taken place. There is a slow and continuous increase in the photocurrent until a steady state is reached. More intense the flux, the faster the steady state is reached. If the excitation source is switched off, and again applied, the steady state is reached in a very short time. The thermal quenching of photocurrent is observed very sharply at temperatures higher than 125 K.

Similar behavior was seen in the phenomena of long-lifetime persistent photoconductivity (PPC), which extends for more than an hour, and follows a non-exponential law. This can also be seen to completely erased by a heating to beyond 135 K[28]. This however was present only in LEC grown samples. Generally the PCQ, EPC and PPC are strongly sample dependent, and are not in any way directly correlated to the presence or absence of EL2.

Attempt was made at explanation of these phenomena through the presence and metastable transformation of a new trap, similar to El2 in structure[29]. It was observed that "in spite of the important role played by these traps (that is EL2), many other band gap levels control the properties of the material".

3.7 Topics relevant to present work

We now present a review of current literature directly relevant to the present work. Most of the works reviewed are of phenomenological nature. They question the established model described earlier on various counts, but fall short of offering a cogent structure in understanding of the diverse and often conflicting results reported. However this much is clear that there is a single underlying mechanism that is responsible for the seemingly

complex behavior. The current work is in a way an extension of the matter now presented.

3.7.1 Optically enhanced photoconductivity: an alternate view

The *optically enhanced photoconductivity* described earlier by Jimenez has been studied in detail by Desnica et. al. They demarcate two different phenomena, one for low intensity light and the other for high intensity light. It is shown that for low intensity light for all photon energies there is an increase in the photoconductivity with exposure time, as opposed to high intensity light, where quenching takes place.[30] The photocurrent evolution with time for low intensity light is studied. The much larger than band gap light show an almost instantaneous jump in the photocurrent, and then a saturation, whereas the band-gap light increases more slowly. For extrinsic light, there is continuous increase for up to six orders of magnitude.

The thermally stimulated current spectra is a standard technique employed to study the trap parameters. Here the TSC spectra is taken for different filling times and for different energy excitations. The trap filling, as given by the area under the peaks, is plotted for the different filling times. This plot is shown to be, within small discrepancies, identical to the photocurrent-time plot described earlier. This would suggest that the photocurrent evolution is entirely describable in terms of trap filling parameters.

For larger than band-gap light, initially there are equal number of holes and electrons, and so after the initial rise the current becomes steady. Now, as the electrons get trapped, the free hole become larger in number, and their lifetime increases, increasing the photocurrent. However, eventually most of the traps are filled, the photoconductivity reaches a steady-state value.

For sub-bandgap light, the dynamics are more complicated. There are free electrons created by photoexcitation of EL2 defects, and then these electrons are trapped. Later both electrons and holes are created through a two step process through the EL2 centers. Finally all traps are filled and the photoconductivity reaches a steady state.

The theory attempts to explain the increased photosensitivity without use of low temperature complex defect creation and annihilation.

3.7.2 Trap induced photoconductivity

The effect of the presence of traps on the photoconductivity has been studied in great detail[31] as a further proof of the mechanism of enhancement of photocurrent thought to be due to the increased hole lifetime brought about by trapping of free holes.

The temperature dependence of photoconductivity has been studied for various light intensities, after initially filling the traps. The plot (fig 3.8) shows the trap dependence on the photoconductivity as apparent by the similarity of the low intensity photocurrent data where the peaks are well defined with that of the TSC.

Very different results are shown if the photocurrent data is shown as a function of temperature taken for traps completely empty. The below the band-gap I_{pc} is very small, as opposed to the above band-gap light. It has also been shown that if the traps are selectively filled by varying the filling time (as confirmed by TSC data from identical filling schedules) the photocurrent at the temperature corresponding to a TSC peak varies as the trap filling conditions for that particular peak. The increase in I_{pc} above the empty trap value is proportional to the charge trapped in these deep traps

Similar results are seen after the traps are emptied by thermal annealing. It is seen that the photoconductivity at low temperatures is much lower if a major trap has been emptied by annealing at a suitably high temperature. This gives an alternative reason for the thermal evolution of the enhanced photocurrent as put forward by Jimenez. Instead of the theory involving the formation and disintegration of complex defects, the phenomena is now explained in terms of filled or empty traps. At low temperature, since most traps are electron traps, there are a large number of free holes present after the traps are filled thereby removing the free electrons. This leads to the increase of the photocurrent. At 120-135 K all the major traps are emptied, and the electrons are then free to recombine. This brings the photocurrent down.

However, the exact mechanism for the dependence of high intensity photconductivity on the trap level is not offered. The difference of results for high and low intensity light is also not addressed.

3.7.3 Quenching and Enhancement of Photoconductivity: a possible alternative mechanism

The understanding of the quenching of the photoconductivity has been presented earlier in terms of metastability of defects. It has been observed that the effect is inefficient needing high photon intensities and specific wavelengths (1.0-1.2eV).

Desnica et al.[32] describes a different type of quenching phenomena, which has been observed in LEC SI GaAs, when it is exposed to light in the range 0.7-1.38eV. For very low intensity light, there is a very slow enhancement, and quenching is not observed. For moderately low intensities, the quenching curve is well defined in the first few minutes, while enhancement comes later (fig 3.9). For higher light intensities, the onset of quenching is faster, and for still higher intensities it is obscured, or even wiped out.

These results makes it clear that the quenching is entirely different from that described in conjunction to EL2-EL2* transformation, as this can be seen only for *low* intensities, and for energies as low as 0.7eV.

The TSC spectra, taken after different illumination times of the light intensity which show the quenching phenomena provides an explanation for the photocurrent data. It is seen that while the deep traps exhibit a monotonic increase in trapping with illumination time, the shallower traps show a peculiar behaviour where they first increase, then decrease and finally increase with trap filling times. Since it has been shown earlier that the photocurrent is directly dependent on trap fill-rates, this phenomena of photocurrent quenching has been sought to be explained in terms of anomalous trap filling rates. Why the traps should behave in this fashion has not been addressed.

3.7.4 Light Intensity Dependence of Optical Quenching in SI GaAs

The photoquenching phenomena described earlier have been shown to be only a part of the entire spectral dependence of optical properties of GaAs. The slow quenching and other related phenomena are present only for the lowest excitation intensity, for light in the range 1.05-1.18 eV (fig 3.10)[33] For intensities several orders larger, there was only a quenching observed, and this took place for over four orders of magnitude. The temperature evolution of the photocurrent shows that for quenched PC for high intensity light, there is a very sharp recovery at 125 K. For low intensity there are various peaks

shown for different temperatures. This is the signature for the EL2*-EL2 transformation and thus the quenching for high intensity light is totally different in nature and in origin from the low intensity one.

The TSC data taken after different illumination times of the high intensity light shows that for prolonged exposure to the light, there is a continual decrease in the peak heights for all the peaks, though more pronounced for the low temperature peaks. If a quenching and recovery experiment is carried out by (a) prolonged illumination at 80K with high intensity light (b) anneal at a high temperature T_a (c) fast cooling and short exposure at low temperature and (d) normal TSC run. These experimental results shown in fig (3.11) show that [34] there is an identical sharp recovery at 125K. The conclusions that can be drawn form the above results are that the transformation EL2→EL2* is the mechanism for PC quenching, and that the TSC peaks are also closely related to this phenomenon. It has been conjectured that the *different traps are all due to various complex defects in the material, of which EL2 in included.*

The quenching and recovery of TSC data is now looked at more closely.

3.7.5 Infrared Quenching and Thermal recovery of Thermally Stimulated Current Spectra

This work by Fang and Look[35,36] is of relevance to this current work. Here the source used is a broadband IR from a tungsten lamp with a silicon filter to cut off light of energy above 1.12eV. The photocurrent due to this source shows (1) a rapid build-up to a magnitude proportional to EL2 concentration; (2) a quenching to two and a half orders of magnitude and (3) an enhancement of I_{pc}.

The TSC spectra taken for maximum illumination intensity and different times are shown in figure (3.12). For low illumination time, the basic structure of the TSC did not change, but the peak height reduced. Then there was a drastic change, and a new feature with new peaks-sets in evolved. Further increase of the illumination increased the peak-heights of this feature to saturation levels.

For annealing runs conducted at different temperatures, it can be noticed that beyond 124 K, a dramatic reversal takes place, and the old feature is brought back. This is in good agreement with the transformation temperature for EL2 defect.

The TSC peak would be visible if two conditions are fulfilled (1) There are enough free carriers to be trapped at low temperatures (2) electrons and holes emitted during the heating cycle have a lifetime long enough to be measured. The first case can be thought to be the reason for quenching, on the transformation of EL2 to EL2*. The EL2 when excited by IR light provided the electrons in the conduction band to fill the traps. EL2* would not take part in the process, and this could have been thought to be the reason for absence of peaks in the TSC. However if the sample is bathed in intrinsic light, there would be band to band transition, providing enough free electrons. However this condition also failed to produce a peak in the TSC. The other possibility of a very small carrier lifetime is difficult to eliminate. Also it is possible that he traps themselves undergo transformation on exposure to light, causing them to disappear from TSC plots.

The exact mechanism for any of the data is still unknown, and there are several directions in which further studies can be conducted in order to answer these questions raised.

3.7.6 Electrical field enhanced thermal quenching of a prominent thermally stimulated current peak

This work done by the same group,[37] looks into a peculiar behavior present in "*certain samples*". The TSC spectra, taken after filling the traps at 90K with 1.45 eV light, show a quenching of the prominent TSC peak at140K, denoted here by T_5. The other peaks are unaffected. On changing the rate of heating, which would shift the TSC peaks, shows that both the quenching and recovery temperature shifts the same amount.

The effect of bias voltage is large on the thermal quenching, and the phenomena become more prominent with bias, that is with field. This field-enhancement is explained by the formation and movement of a high resistivity domain. While it is present, the current decreases abruptly, and is regenerated when the domain reaches an electrode.

3.8 Summary and Questions raised

The sheer variety of phenomena observed earlier can be quite confusing, due to the looseness in use of the term "quenching". We have seen that it has been used to describe various unrelated phenomena arising from various mechanisms. The quenching seen for

high intensity light in the range 1.0-1.3 eV, and which recovers sharply at ~125K also exhibit three different properties, which need to be looked at differently: (1) quenching of intrinsic photoconductivity, (2) quenching of bandgap-light induced photoconductivity and (3) quenching of TSC peaks. Though there exist several models for the first two, the third is still unclear. Authors differ in designation of either only peak at ~140K to EL2, or in assigning all the peaks to it. The mechanism is also not established.

The other "quenching", arising from low intensity light of any wavelength, has been seen to be entirely different from the phenomena talked of earlier, and is due to trapping and detrapping of carriers. This is regenerated at higher temperatures where the traps are thermally emptied.

The third "quenching" is the field enhanced thermal quenching, and has been attributed to the formation of high resistance domains.

There are several questions that can be raised about the phenomena described, and the explanations offered. The first is that all the papers talk about "some samples" behaving in a different way. What is the actual reason is yet to be pinned down, whether it is a complex mechanism dependent on various growing techniques, or is due to any simpler reason. It needs to be mentioned that the earlier work was based on Horizontal Bridgman techniques, while the more recent works employ Liquid Encapsulated Czochralsky (LEC) or the Vertical Gradient Freeze (VGF) technique. Also almost all the results described earlier can be distinguished into either low intensity or high intensity excitation phenomena, with a very large difference between the two outcomes. This also needs to be pinned down to a single model.

It is with this background in mind that the current work has been designed and carried out.

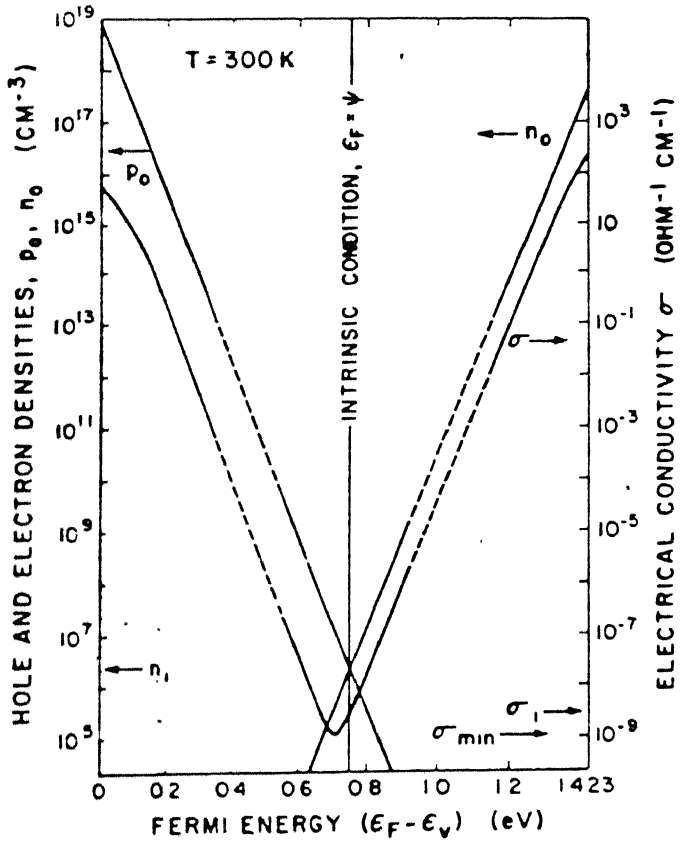

Fig(3.1) Variation at T=300K of Thermal Carrier densities n_o and p_o and resultant electrical conductivity with Fermi energy location.
J. S. Blakemore J.Appl. Phys 53, Oct 1982

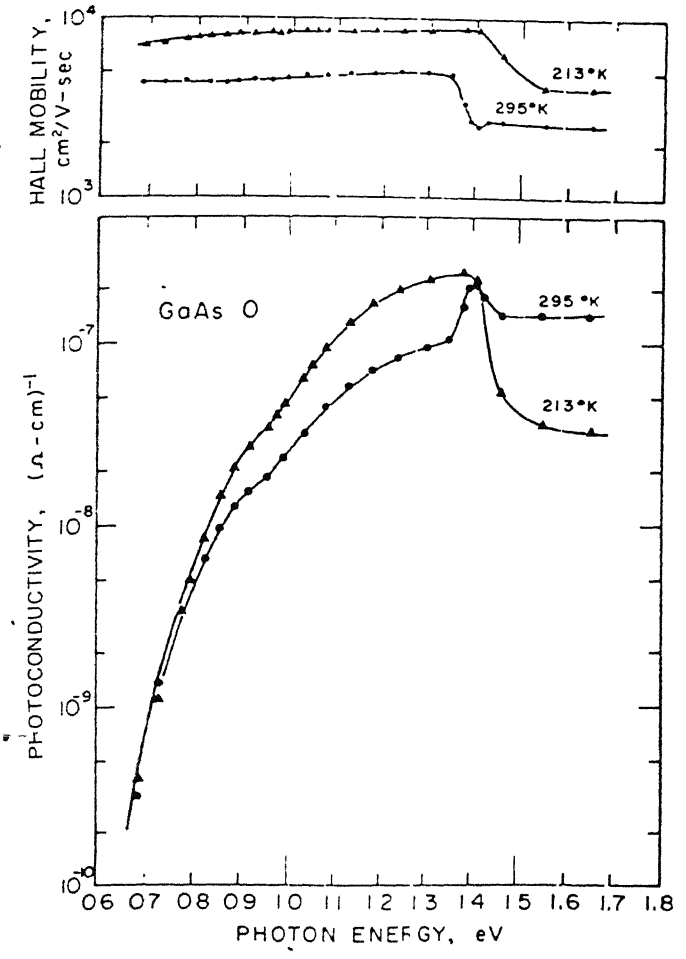

FIG. 2. Photoconductivity spectral response and variation of photo-Hall mobility with photon energy for GaAs :O at 295 and 213 °K.

Fig(3.2,3.3) Photoconductivity spectral response and variation of photo-Hall mobility with photon energy for GaAs:O at 295 °K
Lin, Omelianovsky and Bube[15]

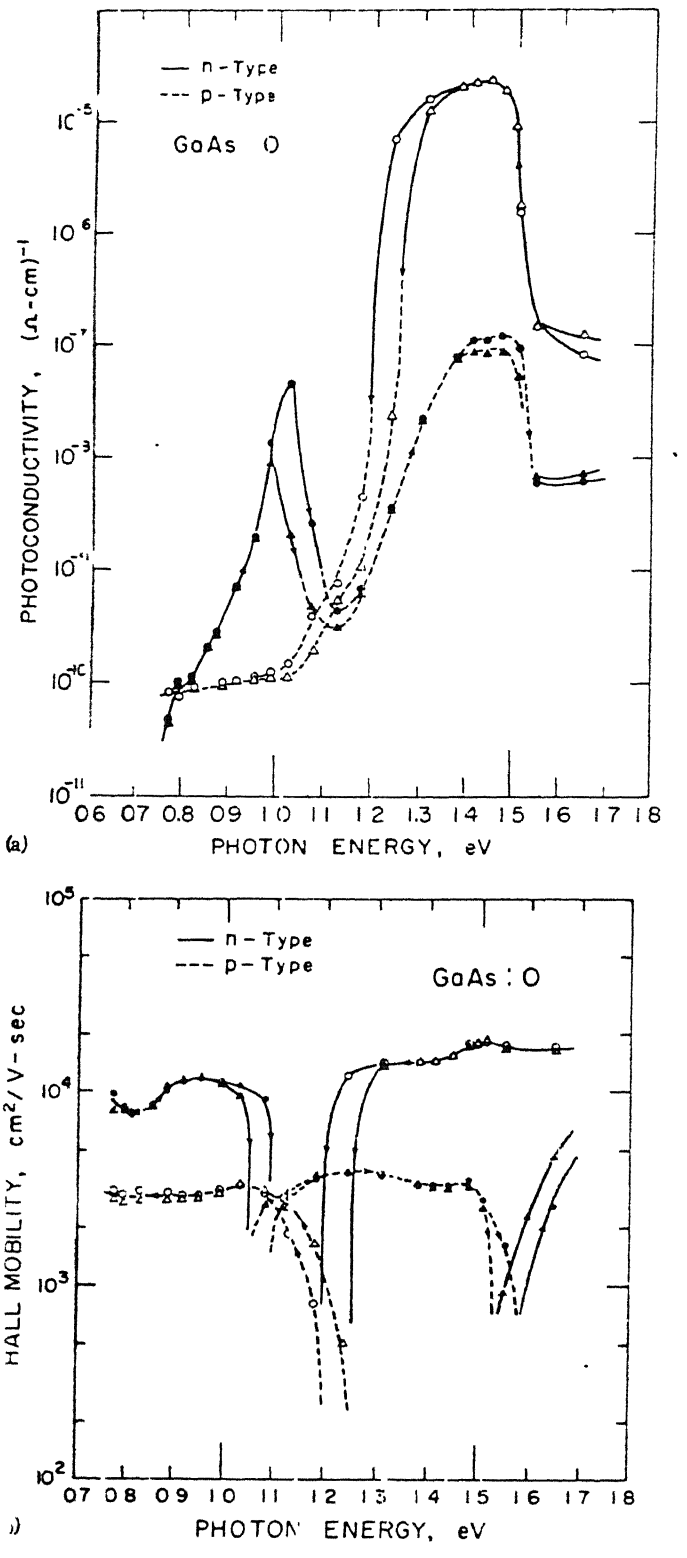

IG. 3. (a) Photoconductivity spectral response curves measured at 82 °K for GaAs :O: measured from high to low photon nergies, reading after 3 min (○) and after 15 min (△); measured from low to high photon energies, reading after 3 min (●) and after 15 min (▲). (b) Photo-Hall mobility vs photon energy for GaAs :O at 82 °K. Symbols are the same as in (a).

Fig(3.4) Photoconductivity spectral response and variation of photo-Hall mobility with photon energy for GaAs:O at 82 °K
Lin, Omelianovsky and Bube[15]

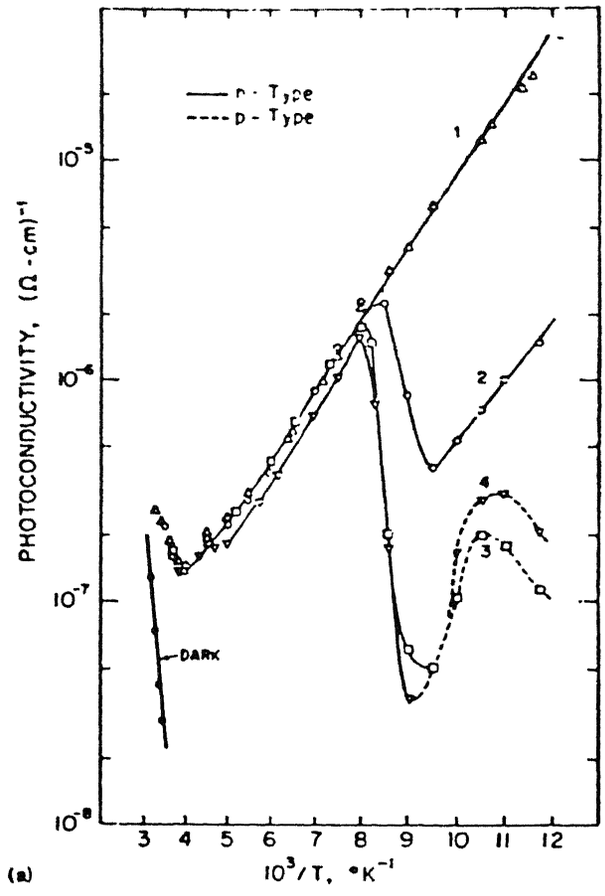

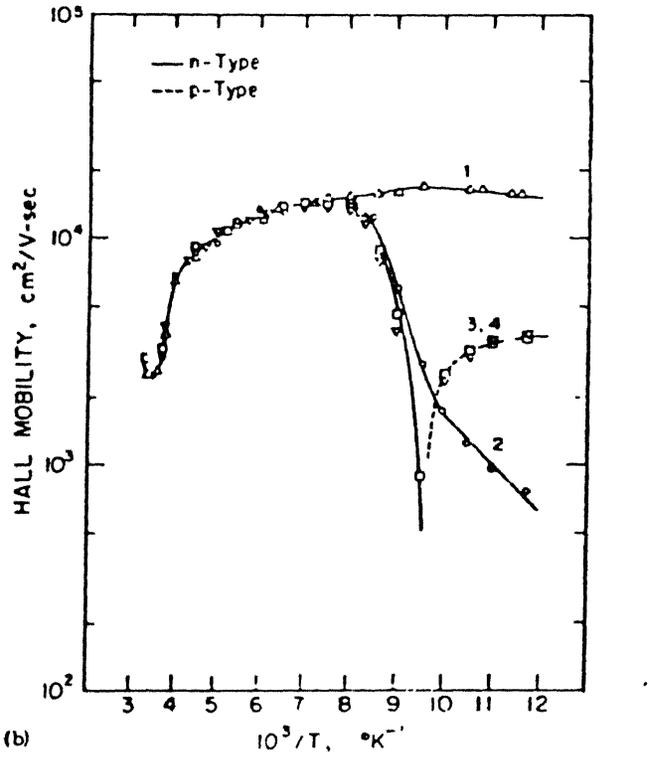

FIG. 4. (a) Temperature dependence of photoconductivity in GaAs:O for intrinsic photoexcitation after quenching 1 h with 1.08-eV (○) or 1.16-eV (□) photons at 82°K, measured while warming, and for simultaneous intrinsic and 1.18-eV photoexcitation (▽). (b) Temperature dependence of the photo-Hall mobility for GaAs:O. Symbols are the same as in (a)

Fig(3.5) Temperature dependence of Photo-conductivity in GaAs for intrinsic excitation after quenching 1hr at 82 while warming. Photo-Hall mobility is also shown.
Lin, Omelianovsky and Bube[15]

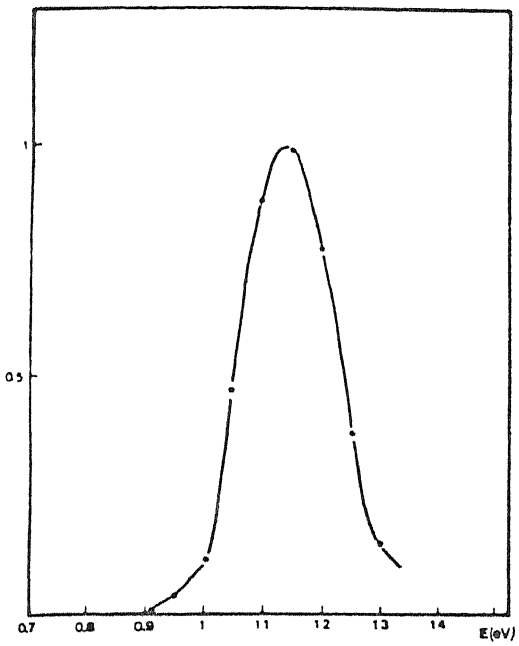

Fig(3.6) Spectral distribution of optical quenching
Lin, Omelianovsky and Bube[15]

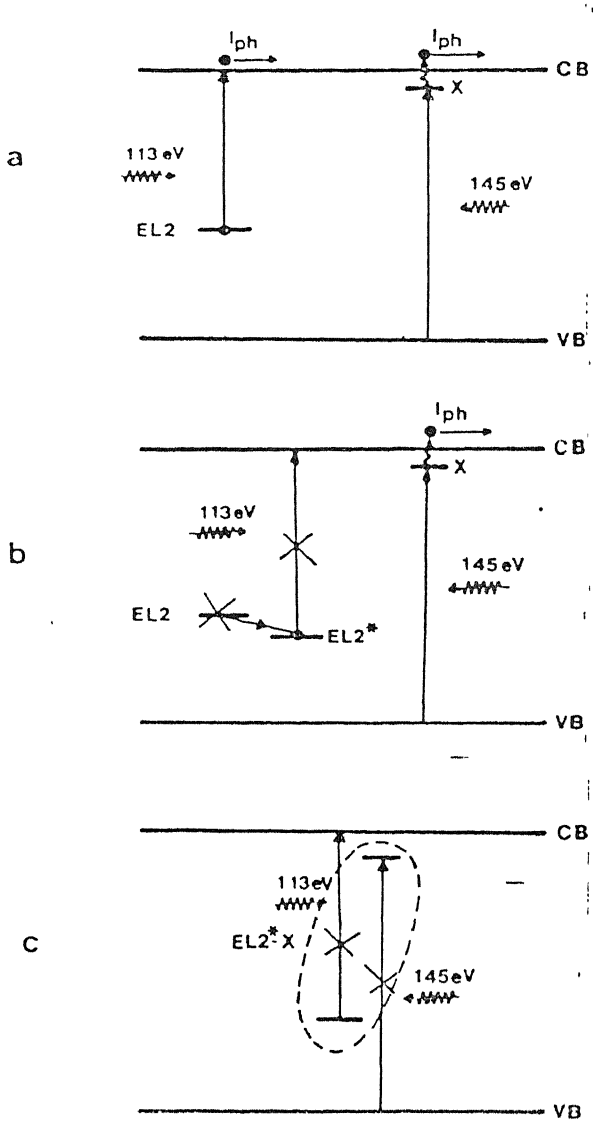

FIG 8 Single flat-band sketch, showing the successive steps involved in the defect reaction mechanism (a) Both transitions (EL2→CB and VB→X) are allowed giving photocurrent (b) EL2 transforms into EL2*, transition EL2*→CB is forbidden, and EL2*→EL2 transformation does not take place at temperatures below 140 K; these features induce the quenching of the extrinsic photocurrent Near intrinsic photocurrent is not still quenched (c) EL2* captures shallow donor level X, forming a complex, optically isolated from the bands, therefore the near intrinsic photocurrent is also quenched

Flat band model for the mechanism
Jimenez et. al. J. Appl Phys, vol. 57, June 1985

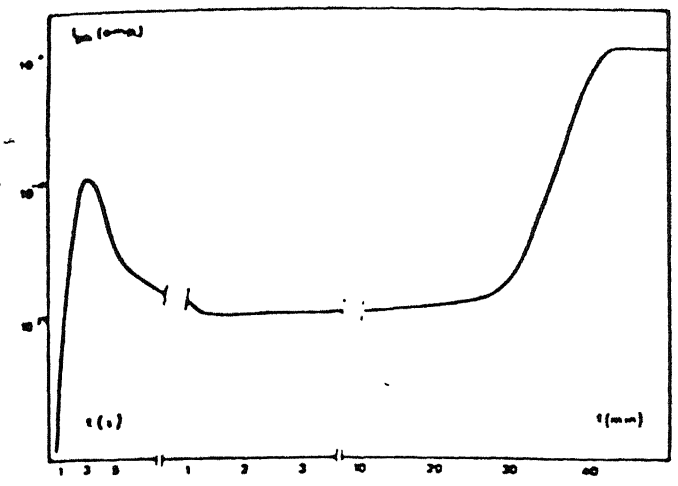

Fig 2. Time evolution of the 1.32 eV photocurrent at 77 K.

Fig (3.7) Optical enhancement of photo-current for 1.32eV.
Jimenez et. al. Sold-state Commun, 49, 917(1984).

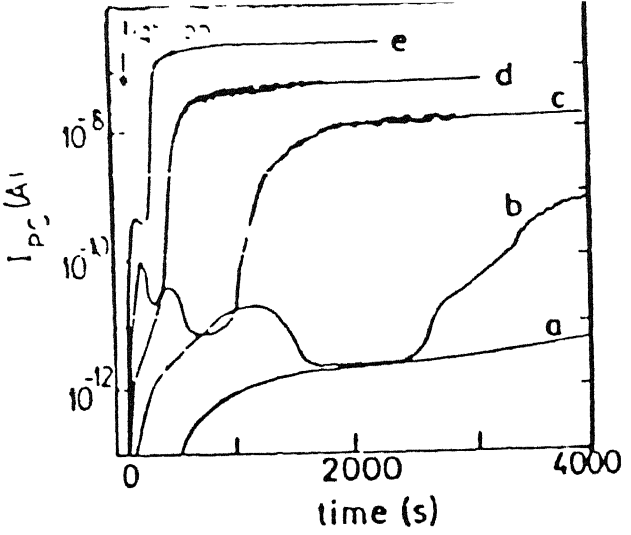

Fig(3.9) Time evolution of Photocurrent I_{PC} for different 0.7 eV photon Flux densities at 86K
Desnica et. al Sold-state Commun Vol 74 no 8, 1990

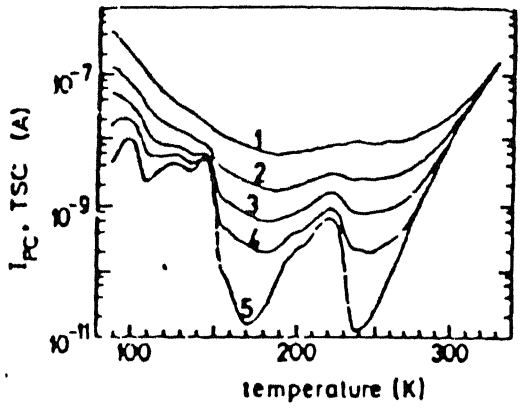

FIG 1. Photoconductivity vs temperature dependence for 1.55 eV illumination and various photon flux densities, for LEC SI GaAs sample with deep traps filled. Filling of traps is performed by preillumination at 80 K, with a 5×10^{16}/cm^2 total dose of 1.55 eV photons. Photon flux densities (photons/cm^2 s): 1—2×10^{14}; 2—8×10^{13}; 3—4×10^{13}; 4—2×10^{13}; a thermally stimulated current measurement is added for comparison (5)

Fig(3.8) Photoconductivity-temperature plot for initially filled traps for various intensities
Desnica et. al. J. Appl. Phys Vol 67, Feb 1990

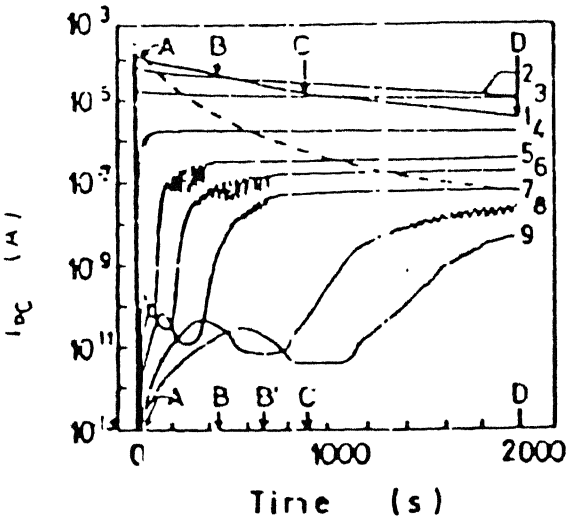

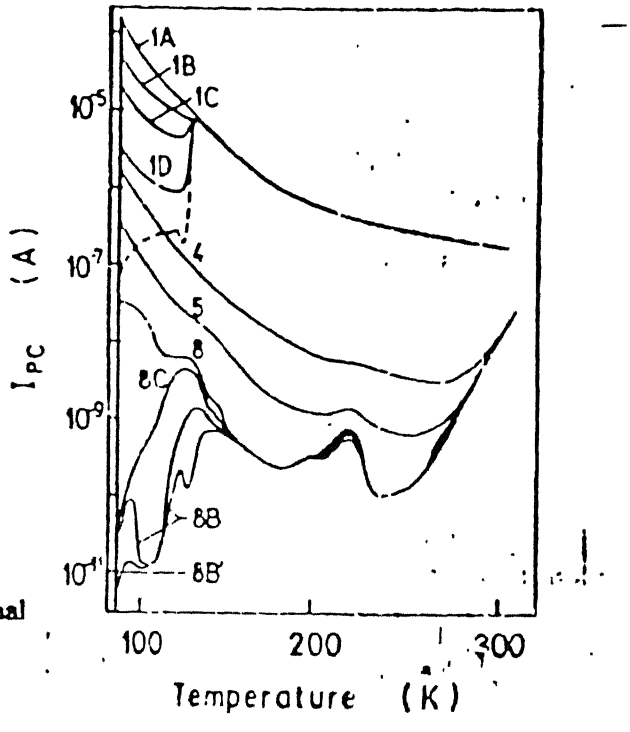

Fig(3.10) Optical quenching and thermal recovery as a function of light intensity

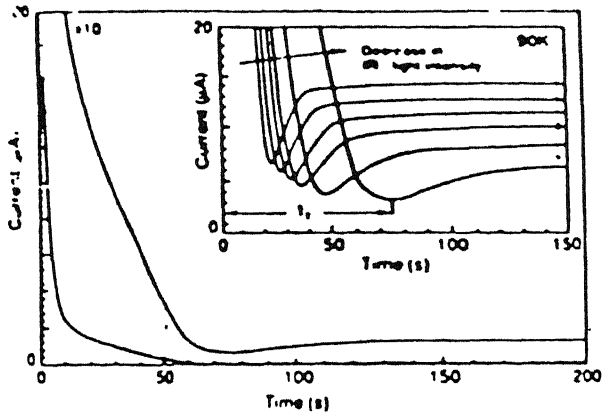

FIG. 1. Infrared quenching of the photocurrent at 90 K ($h\nu < 1.12$ eV), showing a minimum at a transition time t_T, which depends on the light intensity, as shown in the inset.

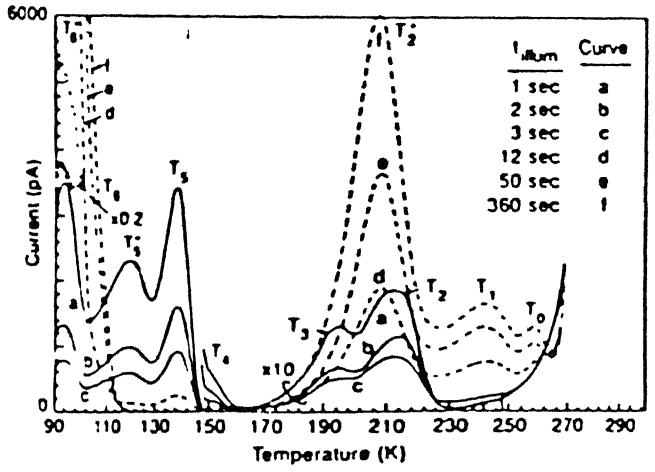

FIG. 2. TSC spectra under different illumination times from 1 to 360 s, showing a drastic change in the TSC spectrum from feature I to II at $t_{illum} \sim 12$ s (maximum light intensity used).

Fig (3.11,3.12) Infrared Quenching of Photocurrent at 90K. TSC quenching for IR illumination and unquenching by thermal anneal

Fang and Look, Appl Phys. Lett Vol 73 No 10 May 1993

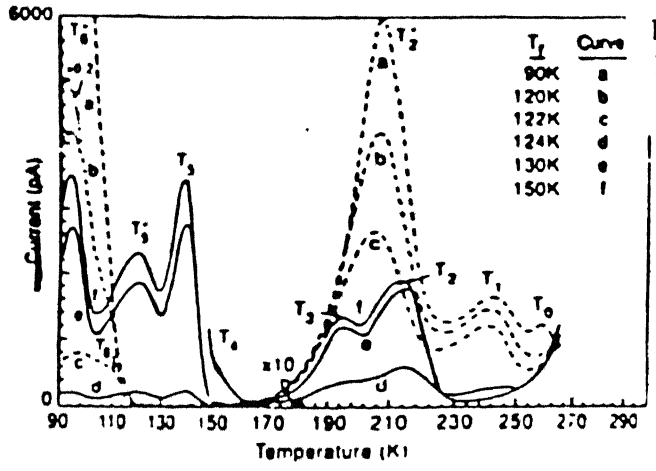

FIG. 3. TSC spectra following a soak at the different recovery temperatures T_r s and then a 1 s excitation at 90 K with the same light intensity as used in Fig. 2, showing a reversible change in TSC feature from II back to I at $T_r \sim 124$ K.

Chapter 4: Experimental Set-up

4.1 Types of experiments normally conducted to characterize deep traps in semiconductors.

4.2: Experimental procedures to look into the unique properties of SI GaAs.

4.3 Experimental set-ups and instruments used.

- 4.3.1 Experimental requirements
- 4.3.2 Instruments used
- 4.3.4 The set-up for current-voltage measurements
- 4.3.5 The set-up for quasi steady-state dark and photoconductivity measurements.
- 4.3.6 The set-up for transient measurements.

4.4 Specific Experimental Tips For the Present System

4.5 Details of the Sample

Chapter 4: Experimental Set-up

This chapter gives an account of the experimental set-ups developed for the purpose of this work. Since most of the experiments performed are rather involved, and are specific to such materials, we first provide a overview of the normal procedures usually carried out for the purpose of characterisation of trap related phenomena in photoconductors in general and in semi-insulating GaAs in particular.

4.1 Types of experiments normally conducted to characterize deep defects in semiconductors.

1. Spectral response of photoconductivity

The spectral response of photoconductivity for any material gives qualitative picture of the different imperfections present in the material. In a pure element, the photo-conductivity is maximum for light just under the band edge, and falls rapidly for smaller photon energies. The existence of photoconductivity for energies much lower than the band edge is a direct evidence of the presence of imperfections, and the low threshold of such a photoconductivity is a possible parameter for the estimation of the presence of the imperfection level in the energy bands of the host material.

2. Intensity dependence of photoconductivity

In a crystal with one principal recombination centre, the photoconductivity varies as the power of excitation intensity between 0.5 and 1. The exponent is a pointer to the distribution of trap density with trap depth.

If two types of recombination centres are present, and if one has cross section suitable for the its behavior as a sensitizing centre, a region is found where the photoconductivity increases with a power of excitation intensity greater than unity, a phenomenon called superlinearity. This occurs in the region where the sensitizing centres are changing from hole traps to recombination centres with increasing excitation intensity.

Thermal quenching of photoconductivity is a complementary phenomenon to that of superlinearity. Here the photosensitivity decreases rapidly with increase of temperature beyond a critical point. Here we look at the change in sensitizing centres from recombination centres to hole traps at a fixed excitation intensity, with increasing temperature.

3. Thermally Stimulated Current

If a crystal is subjected to photoexcitation at low temperature, then the carriers are trapped at imperfections in the crystals, in the absence of sufficient thermal energy to free them. If the crystal is now heated at an uniform rate, the trapped carriers will be freed when sufficient thermal energy is available, and the presence of the free carriers are detected as increase in the dark conductivity. The temperature at which the maximum thermally stimulated current is seen can be related to the trap depth, and the total charge freed is a measure of trap density.

Various methods of obtaining the trap parameters from the TSC spectra are present, and it is possible to cover a wide range of trap depth in a single measurement, and estimate the distribution of trap density in this range.

4.2: Experimental procedures to look into the unique properties of SI GaAs.

The unique properties of semi-insulating GaAs has been studied for over 30 years, and while each research group used their particular routines to go about the task of understanding them, the procedures used can be broadly categorised into several types. The modes of carrying out of some particular studies which are of interest to this work is now looked into in more detail.

A point to be noted is that while we are using the term SI GaAs to describe the material concerned, many of the properties looked into may be dependent on the growth procedures. The earlier works have used the Horizontal Bridgemann (HB) grown material while later LEC (Liquid Encapsulated Czochralsky) and Vertical Gradient Freeze (VGF) grown crystals are more common.

1. Optical quenching of photoconductivity.

This has been studied by several groups, since the 70's, and though there are various procedures, the main theme has been to study the effect of lower than band gap light on the photosensitivity at low temperature. Generally the temperature range of these studies has been liquid nitrogen temperatures. The sample is dark cooled to empty the traps, and is exposed to photoexcitation. Bube[15] has measured the spectral response of the sample from 1.6eV to 0.6eV, using two different waiting times 3min and 15 min at each wavelength. The time of exposure is significant specially as the time constants for low intensity light at that temperature can be several hours. This has been done in two directions, from higher to lower energies, and vice versa. The two runs effectively give the effect of the history of exposure on the photosensitivity of the sample, and particularly of the effect of the IR exposure on photocurrent due to visible light.

The quenching efficiency has also been studied by varying the wavelength of the secondary light. There are two different behaviour here, the quenching of IR light by itself, after long exposure, and the quenching of intrinsic light. The IR light has been found to have maximum quantum efficiency at 1.1 eV, and several different IR sources has been used. Martin has used white light from a 50-Watt tungsten lamp for 10 minutes, while Jimenez has used a 1.17 eV YAG laser. The point to be noted here is the possible diversity of intensity of the optical sources.

One way to study self-quenching and eliminate time constant effects at the same time is by using a temperature scan technique (Jimenez)[25]. Here the temperature dependence of photocurrent is studied separately for all the different spectral components.

The changes in the photosensitivity brought about by excitation, were neutralised by heating to a temperature higher than 120K. This is seen by a sudden rise in photocurrent at that temperature.

2. Optical quenching of thermally stimulated current peaks.

This has been studied by two groups, starting in the early 90's. The typical experiment done by Fang and Look has used a high pressure LEC grown Ga rich sample. The infrared source was a 25W tungsten lamp with a Si filter, which allows energies less than 1.12eV.

In order to measure photoquenching in the dark, the sample was quickly dark cooled, and in exposed to infrared light for different times from 1 to 360 sec, in different runs, and heated from 90 to 270k at a rate 0.2K/sec. To measure the thermal recovery, the sample was first illuminated for 5 min at 90K to ensure complete quenching of EL2, and the quenchable TSC traps. Then it was warmed to a certain recovery temperature T_r, ranging from 90K to 150K. Next it was quickly cooled back to 90K, and finally exposed to the same infrared for 1 sec to fill the traps before TSC scan.

4.3 Experimental set-ups and instruments used.

There are four essential components to each of the various systems used in this work and discussed in this section : Cryogenic, optical, electronic and software. Each of these has to be judiciously integrated to form *systems* which are capable to meet the various requirements that are imposed by the nature of the material under scrutiny and the type of data that are sought about it. We now present the various requirements that has to be fulfilled by the experimental set-ups, and the components, both hardware and software, that has been utilised for this purpose.

4.3.1 Experimental requirements

The three experimental directions talked about in the section 4.1 and 4.2 ask for diverse and sometimes contrasting requirements for the instruments.

The first and foremost requirement is dictated by the name of the material itself *: semi-insulating* GaAs. This indicates that the currents to me measured for low voltages to be extremely small, of the order of a ~ 10 nA at room temperature. The intention of measuring the temperature dependence of conductivity makes it necessary to use instruments capable of measuring the current for the entire temperature range, which for low temperatures falls to $\sim 10^{-14}$ Amperes. One way of increasing the *current* is to increase the voltage, which in this case is not permissible because of the limitation of the ohmic nature of the contacts to within 10 Volts at low temperatures.

The *photocurrent* is another parameter to be measured, and this is several orders higher than the dark current, and as such does not present too many problems. However, the

very fact that there is more than six orders of change between the dark current and the photocurrent due to high intensity (mW) laser source, is of importance, specially in the transient measurements. The transient measurements require the ability of the electrometer to measure the currents from 10^{-5} to 10^{-13} Amp, continuously, that is with fast and automatic change of scale. This is a tall order for any system.

The time of acquisition, that is the time of data integration + data conversion + data transfer is of prime importance in the *transient experiments*. Due to the small currents at the lower ends of a decay transient, the integration time cannot be made small without the noise predominating. Also if too long a acquisition time is used, the fast transients cannot be measured accurately. This leads to a stand-off and optimum conditions have to be found.

The spectroscopic measurements necessitate a continuously varying and remotely programmable monochromatic light source, which would have a strong intensity in the IR range for *photoquenching* experiments Also variation of monochromatic light intensity over several orders is helpful.

Measuring material parameters at low temperatures also imposes severe demands. The *cryogenic system*, that is the refrigerator and temperature controller, must be capable to cooling in a reasonable time to temperatures of 10-20K. Also it should be able to stay at any intermediate temperatures accurately (within a few K) for a long duration (several hours, if necessary). The thermally stimulated current measurements make it necessary that the temperature of the system be increased in a constant and controlled rate. Also, the *unquenching* experiments require that the temperature be increased rapidly to a pre-assigned value from low temperatures, held there indefinitely within a small error limit, and them cooled with a fast rate. This imposes strict conditions on the thermal mass of the system.

The various hardware components used in the experimental set-ups are now described in detail.

4.3.2 Instruments used

The instruments used can be categorised into three: (1) Electronic (2) Optical (3) Cryogenic and (4) Instrumental control and Data acquisition. We present the specific instrument parameters that are of consequence to our work.

Electronic

1. **Model 182 Sensitive Digital Voltmeter** *(Keithley Instruments)*

Mode of Operation: Measurement of Voltage

Resolution: 1μV for 30V range

1nV for 3mV range

Reading rate: 100/sec for 3msec integration time, 30 V

16/sec for IEEE-488 bus, Power Line Cycle (PLC) integration.

Buffer length: 1024

2. **Model 236 Source Measure Unit** *(Keithley Instruments)*

Source and Measurement of Current

Resolution: 100fA in 1nA range

Source and Measurement of Voltage

Resolution: 10μV

3. **Model 602 Electrometer** *(Keithley Instruments)*

Mode of Operation : Measurement of current

Range 10^{-14}A to 0.3A

Cryogenics

1. **Model 22C CRYODYNE Refrigeration System** *(CTI Cryogenics)*
2. **Janis VariTemp Variable Temperature Insert system** *(Janis research company)*
3. **Model DRC-91C Temperature Controller** *(Lake Shore Cryotronics)*

The three instruments together form a close-cycle He refrigeration system, where the sample mounted can be controllably cooled to a temperature in the range of ~15 K to

320K, the lower limit depending on the thermal mass of the sample head. The temperature controller is a PID type, and is capable, on external control through a IEEE interface, of varying the temperature as a function of time. There is a quartz window which allows light to be focused on to the sample.

OPTICS

1. DSP-275 Double Monochromator *(Acton Research Corporation)*

Resolving power of Monochromator: 0.1nm, programmable, remotely controlled through RS232 interface.

2. Optical Sources:

Diode Laser (676 nm) Battery operated

He-Ne Laser (643 nm) Red, (10mW)

QTH (Quartz Tungsten Halogen Lamp) 50 watt, with power supply.

IR Lamp 200 Watt, tungsten filament *(Philips)*

3. Filters, low-pass, and narrow-band interference type.

CONTROL & DATA ACQUISITION

1. PCL 236 IEEE-488 interface card. *(DYNALOG Corporation)*

2. RS232 interface

4.3.4 The set-up for current-voltage measurements (fig 4.1)

The sample is mounted on a low thermal mass holder as shown in figure in the *Janis* cryogenic insert system, which is cooled by a helium low temperature close cycle refrigerator. The temperature is maintained to the desired value by a PID controller, which is remotely set by a IEEE interface. The incident light to the sample is controlled by a monochromator, whose exit slit is mounted on the optical window of the cryogenic head. Light from various sources are incident on the entrance slit of the monochromator. Which is controlled remotely from the IEEE-488 interface.

Measurement of current-voltage or voltage-current data is done by use of the K-236 source measure unit, which has a voltage range of +/- 100V. This constraint does not allow for the measurement of dark conductivity at low temperature, as the current

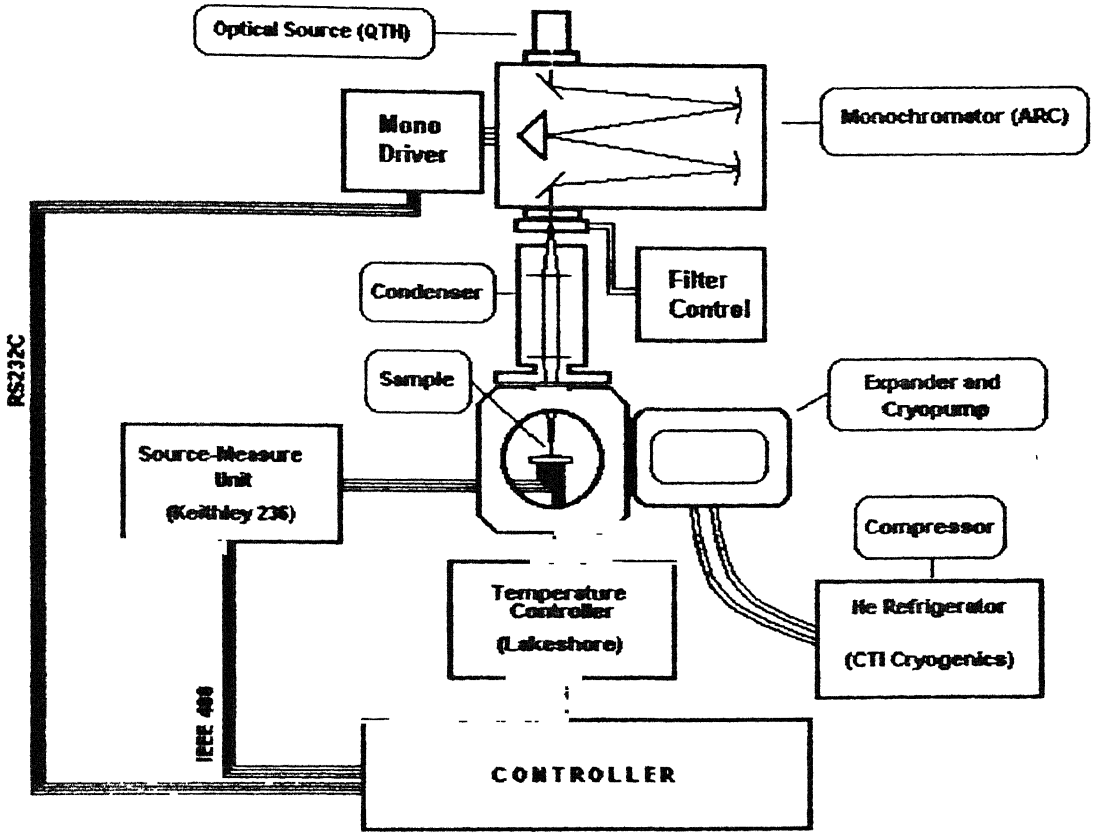

Fig 4.1 I-V Measurement Set-Up

sourcing/measuring is limited to 1nA, below which the instrument shows low S/N ratio. So, the system has been is used to measure photocurrent at low temperatures, and the dark photconductivity is restricted to room temperature measurements. In the normal working range, the integration time is set to line-cycle, and the digital filter is set to 32.

A computer s/w has been developed to control the entire process of setting the monochromator, temperature controller, and the source-measure unit. Here it is necessary to ensure that enough time is given after setting the current on voltage, and measurement of the relevant parameter, in order that the system reaches the steady state condition. Also, the temperature should remain constant throughout the current or voltage scanning.

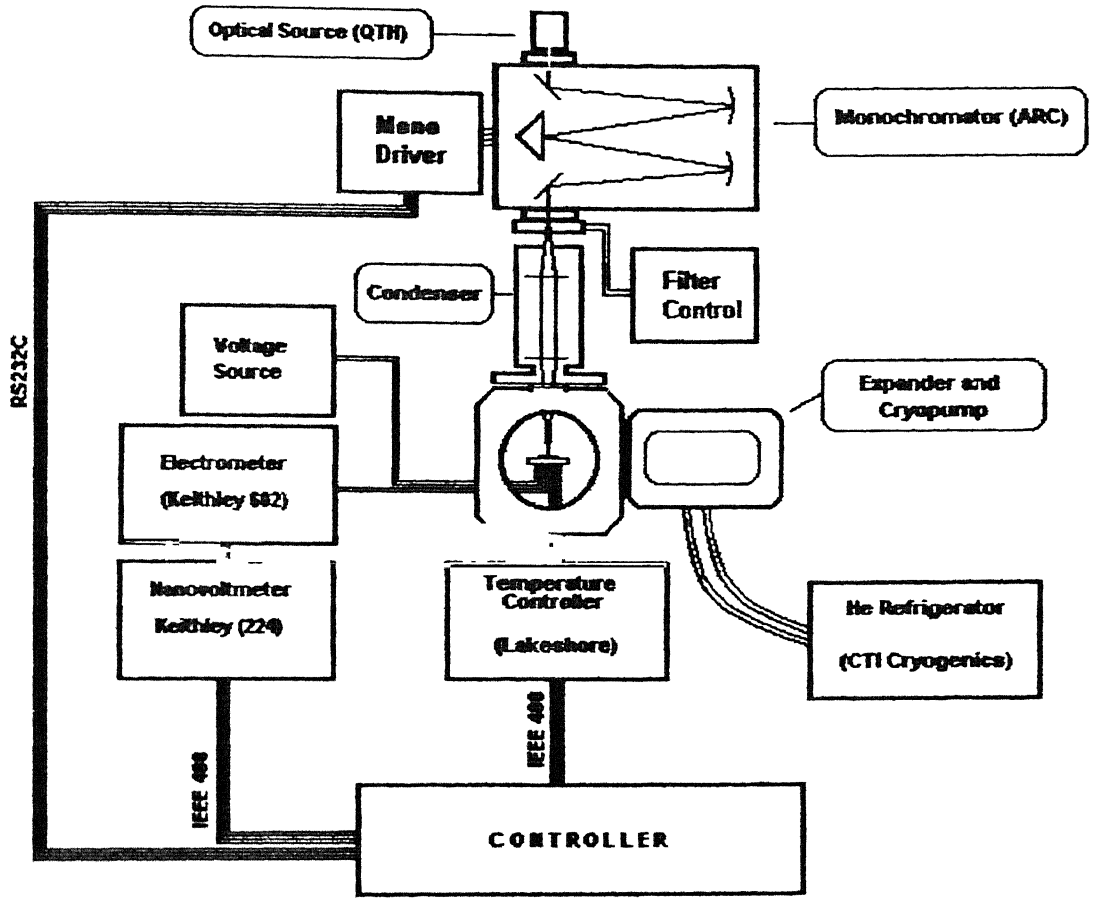

Fig 4.2 Steady-State Measurement Set-Up

4.3.5 The set-up for quasi steady-state dark and photoconductivity measurements.

Most of the data taken has been of this type, and this system (fig 4.2) has vital significance on a major part of the current work. The difficulty of this type of measurements has already been stressed in an earlier section, and a lot of effort has gone in to make the measurements reliable and reproducible.

The set-up essentially measures current passing through the device when a steady DC bias is applied across it, either in the dark, or when exposed to a light of a specific wavelength. The DC bias is supplied by a alkaline cell, to reduce line-frequency noise.

The current is measured by K602 analog electrometer, and the data is taken by using a nanovoltmeter (K224) to sense the position of the needle, by measuring the analog output from the K602, which is a signal between 0 and 1 volt, depending on the position of the needle. The accuracy of the data is enhanced by use of the nanovoltmeter, which at 1 V scale has a resolution of 1μV, with high stability for an integration time of 100msec. Thus the data is accurate up to at least $10^{-11}\times10^{-5}$Amperes. Further integration is brought about by the software after the data acquisition, by averaging over large data.

All cables are shielded, with Teflon insulation, and the grounding conditions are very stringent. The system is very sensitive to noise picked up by capacitive coupling, so care has to be taken that there are no such disturbances while the data-taking is on.

The thermally stimulated current (TSC) measurements and TSPC measurements require very strict control in the temperature, especially in the linear heating rate. This is brought about by two simultaneous processes. The computer, through the GPIB interface varies the temperature set-point as a function of time, as required by the experiment. The parameters of Gain, Rate and Reset (PID) are preset so as to allow the temperature to reach the set-point without oscillations. In all cases the best linearity in the heating curve is obtained by keeping the Gain low so that the set-point is increased just before the temperature rises to that level. However in this system, small deviations from linearity cannot be ruled out.

4.3.6 The set-up for transient measurements

The difficulty in transient studies in semi-insulating GaAs is that there are several time-scales involved in transient data taken in this particular material. In most rise or decay curves, there can be demarcated at least three different portions: (1) fast change, which is over within a few seconds, (2) slow change, which can take minutes, and (3)a slow tail, which usually at low temperatures can take several hours.

The second difficulty is that for optical transients, and for light of large intensities, the change in photocurrent is over five orders of magnitude at low temperatures. These two conditions compounded make an extremely difficult requirement to fulfil.

The nature of the transient measurements in GaAs depend heavily on the intensity of incident light, therefore our experimental set-up can be divided into two categories : one used for high intensity light, such as a laser, and the other for low intensity light, such as that obtained from a monochromator.

Set-up1: Transients due to high-intensity light

The switching on or switching off transients for HeNe laser show a very fast transient, within 100msec, followed by a slow one, till about 30 sec. Therefore two conditions are necessary : (1) The light is switched off/on in less than 1 msec, and (2) The data is taken immediately afterwards, by automatic triggering.

The K236 in used in this set-up as it has auto-ranging facility, storage buffer length of 1000 and fast mode of operation. Even though the instrument can take data at the interval of 1 msec, using an integration time of 416μsec. However during operation it was found that the S/N ratio is within the satisfactory range only if we use a 4msec integration time, with a digital filter of two. This gives a data interval of not smaller than 20msec.

The autoranging facility was found not usable in recording fast transients, as the scale changing time is of the order of ~200msec. Therefore we were forced to keep the scale fixed, losing in accuracy of data at the lower part of the transients. This effectively reduced our span to the middle portion of the transient, which is present for several seconds.

The laser light was switched on /off with a mechanical chopper system developed by us, having a switch-off/on time less than 0.3msec. This chopper is connected to an electronic circuit which produces a low-to-high digital signal, which is then used to externally trigger the K-236.

The data is first stored in the buffer and after the transient, is transferred to the computer. A buffer length of 1000 is used, and the time interval is set by the operator through the s/w developed, and can have a value higher than 20msec.

Set-up2: Transients due to low-intensity light

The transients due to low intensity light are much slower than those described above, and can range from a few seconds to a few hours at low temperature. Keeping in mind

these time-scales and the fact that the currents associated are extremely low, it is necessary that the measurement is done through the K602-K224 electrometer-nanovoltmeter system as described earlier. The integration time used in this case is 20msec, and it is possible to get a data at 70msec interval.

There are two modes of operation, one used to track relatively fast changes, and the other used for transient data that are either very slow, or if the data for a sequence of operations are stored, over the space of an hour or more. The first mode uses the storage buffer of the K224 to store the data for the entire transient, and then transfer it to the computer. The instrument also allows simultaneous retrieval of data, while the storage is taking place. This allows data to be taken in relatively fast, up to 70 msec, but it is difficult to monitor the progress of the transient or the quality of data.

The normal mode of operation, which allows the data to be taken in the computer one at a time, and plotted to show the progress, has been used for all slow changing transient data. The interval can be as low as 0.3 sec, and up to any desired value. The additional advantage is the possibility of s/w controlled integration/smoothening of data which allows us to selectively look at or remove any oscillatory behaviour, which are sometimes present in low temperature transients.

4.4 Specific Experimental Tips For the Present System

The earlier section describes the broad operating principles for the instrumental set-up. However, other than these very general criteria, there are also certain features specific to the system currently used, which can either enhance the quality of the data or introduce systematic errors which have to be carefully eliminated. Therefore it is important to keep these in mind while taking in or processing data. It is with this in mind that several important points are now enumerated.

1. The CTI cryogenic refrigerator requires that the cold head chamber be evacuated to better than 5×10^{-2} Torr before the cooling is started. It has to be noted here that in the current system, a rotary pump is used to evacuate the chamber through a narrow side tube. The tube is fitted to a T-junction, in which one arm is connected to the pump, while

on the other is mounted a thermocouple gauge for measurement of pressure. The pressure thus measured from the gauge is essentially that of the narrow side tube, and does not indicate a proper measurement of pressure inside the much larger chamber. Therefore cooling should not be started immediately after the gauge shows the required pressure. Ideally a pressure gauge should be directly mounted on to the chamber.

2. The controllability of the temperature of the cold head, and the lowest temperature attainable depends on the thermal mass of the cold head, and specifically on that of the sample holder. This depends not only on the holder geometry, but also on the material used in making it. This can be of importance while trying to obtain specific parameters at temperatures near 20K.

Anther aspect of the problem is the temperature gradient along the sample holder, which makes the exact temperature of the sample slightly indeterminate.

3. The stability of low intensity photocurrent data, normally in the range of 1×10^{-12} A $\rightarrow 5\times10^{-12}$ A depends on various factors. Some of them have been mentioned earlier, and the importance of grounding has been stressed.

(a) Actual operation of the instrument has shown that the sample holder has to be electrically connected to the casing of the shielded cables. These have to be connected together in turn to the casing of the K602 electrometer through the body ground connector.

(b) The K182 nanovoltmeter, while taking data from the analog output of the K602 electrometer must be put in the scale of 0 to 3 Volts. Autoscaling in not to be used as this shows large fluctuations in the data.

(c) The changing of scale of K602 has to be done manually, and this incorporates errors in the data as the instrument takes some time to settle. Thus it may become to separate temperature dependence of low intensity with photocurrent with the switching on characteristics of the instrument. An important offshoot of using the 5V as DC bias during TSC in that most of the region of interest lies in the span of one scale, that is there is no need to change the scale.

(d) The K602 is sensitive, even in the well grounded state to capacitive coupling to the objects near it. Therefore it is not advisable to approach the instrument while taking the data, other than to change the scale, as there may be fluctuations in the measurements.

4. The use of s/w has to be done judiciously while taking in data, specially when the program asks for the user to specify the number of data that is to be averaged to form a single data point, that is the s/w integration. In this material, specially for low excitation intensities and low temperature, cutting noise fluctuations by large averaging will also filter out the slow oscillations that are generally present.
In the I-V characteristics, it is necessary to set the waiting time necessary at each voltage, before the corresponding current is recorded, depending on the nature of the transient. This will further be a function of temperature, spectral range and excitation intensities. Another way is to do a scan up and down and to look for hysterisis loop.

5. The HeNe Laser source used shows very slight but discernable fluctuations in the intensity, which may arise from the power supply. This may tend to make the photocurrent a little noisy.

6. The development of interface s/w also requires understanding of various difficulties, which are specific to the instruments used. The instruments individually possess their device-dependent commands, which are usually terminated by a particular character. For the monochromator, the parameter is the carriage return. It has been noticed however that GPIB programming requires the passing of an extra carriage return command without which the program may hang.

4.5 Details of the Sample

The material used in this study is commercially sourced (Hewlett-Packard) liquid encapsulated Czochralski (LEC) grown undoped semi-insulating gallium arsenide (SI-GaAs). From earlier studies, the sample is known to be lightly n-type with resistivity ~10^7 Ω-cm. The contacts are made using AuGeNi alloy which is vacuum evaporated and annealed in flowing H_2 at 450°C. The contact geometry is planar, and distance between

contacts is 3mm. Gold wires are epoxy bonded onto the contacts. The sample is mounted

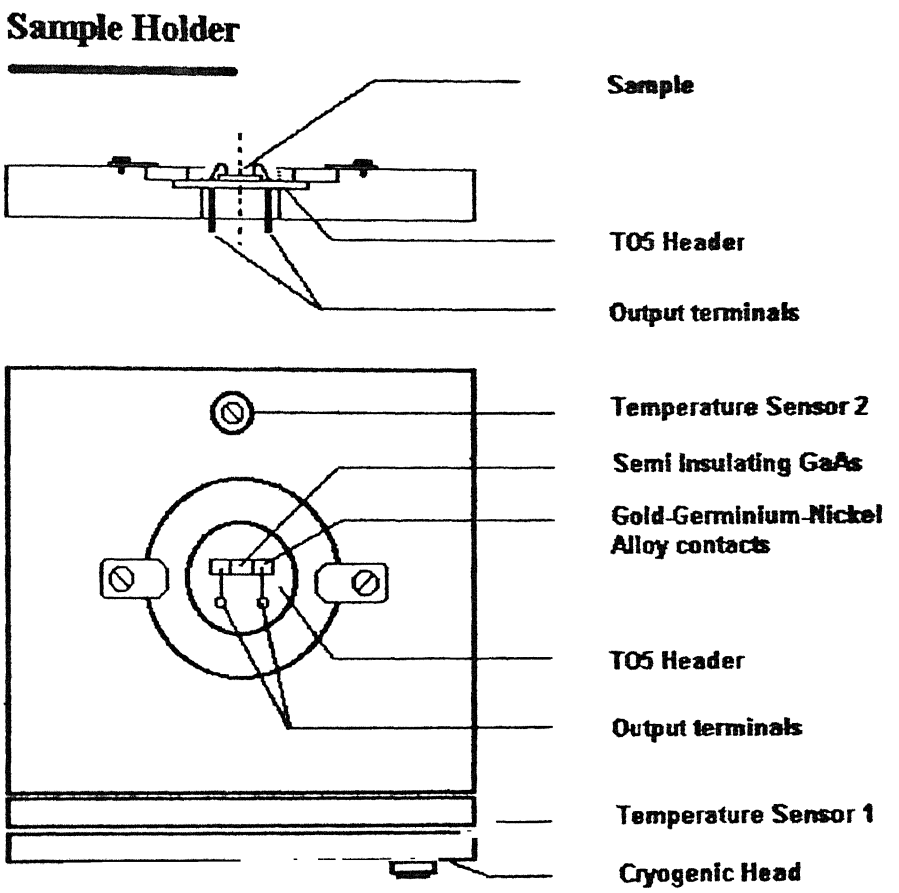

on a TO-5 header, and annealed at 170°C for 30min prior to the experiments.

The sample is mounted on the holder as shown in fig(4.3(a)) in the chamber (fig(4.3 (b))), and the experiments described in the next chapter are performed.

Sample Chamber with Sample Mount : Top View

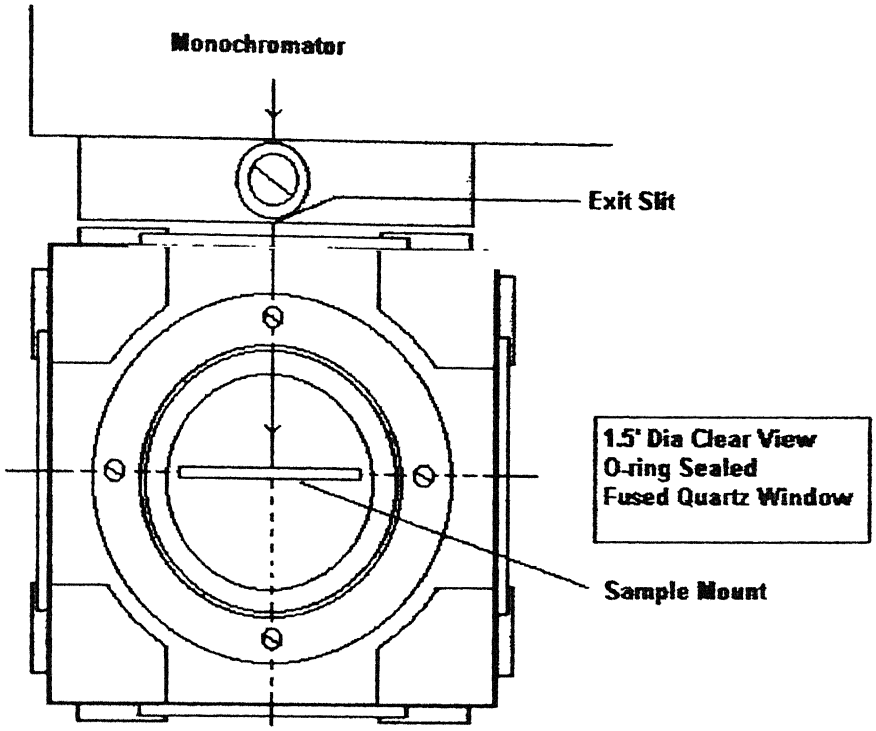

Fig 4.3(b)

Chapter 5: Results and Discussion

5.1: Previous work

5.2 : Experiments Conducted for Preliminary studies

1. Set Current-Measure Voltage 'I-V' plots
2. Photocurrent-Voltage plots for different excitation intensities

5.3: Experiments Conducted: Main

5.3.1 Thermally Stimulated Current Measurement

5.3.2 Design of Experiments:

5.3.2.1 High Photo-Intensity Studies

1. Traps initially empty. Temperature dependence of photocurrent for different excitation intensities
2. Traps initially partially or completely filled with much larger than band gap light

TSC studies

3. Initial trap Filling with sub-bandgap light

Effect of IR exposure prior to laser TSC

TSC with IR filling only.

Absence of EL2 related photoquenching

TSPC after IR exposure

5.3.2.2 Low photo-intensity studies

Effect of IR on response times

5.4 Other Experiments

1. Observed instabilities during TSC measurements
2. Switching-off transients at different temperature
3. Observation of low frequency oscillations (LFO).

Chapter 5: Results and Discussion

The results of photoelectronic characterization experiments performed in this work on Semi-insulating GaAs are described in three distinct parts. First we show briefly the results based on an earlier work, and then devote several sections to the main body of the work. In the last section we collate interesting results which can form the basis of a full-fledged future study.

5.1: Previous work

The sample and its geometry used in all the experiments have already been detailed in the last chapter.

The experiments previously conducted in our laboratory tried to give an overall picture regarding the various trap levels in the sample under scrutiny. It also provided the basis for choice of experimental conditions such as ohmic nature of the contacts and the photocurrent levels.

Current-voltage scans conducted for both photocurrent and dark current at various temperatures shows that contacts are ohmic only for a narrow voltage range (-9 to 9 volts, typically). Using this guideline, the photocurrent measurements as a function of temperature has been always conducted with a voltage source of 5V DC, which lies within this stipulated range.

Thermally stimulated current spectroscopy is a simple and efficient way to obtain a detailed and complete picture of the trap levels present in the sample. The various trap levels that has been obtained from the TSC measurements are detailed later.

The other important observation was that quenching of intrinsic photoconductivity with IR radiation at low temperature, as normally expected in such samples, was *not* obtained despite repeated attempts. The established understanding of the photoquenching phenomena, is that at low temperatures, the exposure of the SI GaAs to IR light causes a transition of the mid-gap level EL2, through a configurational change. The new state created called $EL2^*$ is metastable, and is insensitive to light. This very visible phenomena was not observed in our samples, necessitating a detailed study.

5.2 : Experiments Conducted for Preliminary studies

These studies are a continuation of the preliminary studies mentioned above, so as to delineate the region the region of I-V characteristics, where the properties of the contacts are least pronounced, and the parameters thus obtained are essentially those of the bulk material.

1. Set Current-Measure Voltage 'I-V' plots

This is a study which can be considered as complimentary to the set-voltage-measure-current data obtained earlier. The earlier data shows clearly that at low temperature, the current saturates very rapidly beyond the ohmic region. Therefore it is more convenient to set current and measure voltage in order (fig (5.1)) to look into the detail of the low current points behavior. The data obtained is however identical to that obtained by setting voltage and measuring current

2. Photocurrent-Voltage plots for different excitation intensities

It is necessary to obtain photocurrent I-V plots for different intensities of light to find a safe region of operation for later experiments. Fig (5.2) shows such plots for two different excitation intensities. The data shows that apart from the very large magnitudinal change, the nature of the plots remain same, for example the saturation voltage is seen to be independent of the excitation intensity. This eliminates the possibility that the photocurrent-temperature plot taken at 5 Volt DC biasing, will deviate from the ohmic region and show junction effects for any irradiation condition.

5.3: Experiments Conducted: Main

5.3.1 Thermally Stimulated Current Measurement

The essential feature of Thermally Stimulated Current (TSC) is that the trap level of the sample is selectively filled at a temperature where there is not enough thermal energy to re-emit the stored carriers. This filling of traps can be designed, such that selective traps are filled, or that the traps are filled only partially. The first is brought about by the

selection of excitation sources, which can be extrinsic, that is lower than the band gap, or intrinsic, that is, larger than the band gap. The filling intensity and time can be varied to partially or completely fill the traps.

The TSC is essentially the dark current measured after initializing the sample preparation by selectively filling the traps at low temperature. The rise in temperature gives the carriers enough energy to be freed, and the presence of these free carriers give rise to a peak in the current, indicating the presence, and state of filling of the traps. The TSPC is similar in nature, except that the photocurrent is measured instead of the dark current.

A standard TSC plot for SI GaAs obtained by us is shown in fig (5.3). From such plots by varying the rate of heating the trap parameters such as the activation energy and the capture cross-section can be obtained. The results thus obtained are seen to be identical to the reported values for this material, and are presented in table (5.1). The TSC result shows that our sample is similar in characteristics to those reported in the literature for undoped semi-insulating GaAs.

Peak	Our Result		Reported Result	
Temp	ΔE (eV)	σ (cm^2)	ΔE (eV)	σ (cm^2)
95	0.14	6.76×10^{-16}	0.16	10^{-16}
120	0.32	2.38×10^{-12}	0.24	4×10^{-17}
145	0.30	4.16×10^{-16}	0.32	4×10^{-15}
200	0.45	1.71×10^{-15}	0.44	2×10^{-14}
220	0.65	9.16×10^{-12}	0.53	3×10^{-13}

Table 5.1 Trap parameters obtained from TSC measurements on undoped SI-GaAs

The phenomena of photoquenching in SI GaAs, have been described earlier. Standard literature indicate a presence of a very large concentration of a defect state at the mid-gap level, called EL2, whose concentration pins the Fermi level at this center giving rise to the semi-insulating property. The excitation of intrinsic light, especially light in the range

of 1.0-1.2 eV, has a very distinct effect on this trap level. There have been three contrasting reports in this regard. Bube[15] has shown that the 1.1eV excitation quenches the photocurrent completely, and the photocurrent reduces by over 99%, and can be only generated by a thermal annealing process over 120K. *Jimenez*[27] has shown a different phenomena, that the sample on exposure to light shows first a partial quenching, and then an *"optically enhanced defect reaction"* which shows a rise in photocurrent after long exposure. *Desnica*[32] has tried to explain the diverse phenomena, stating that the low intensity intrinsic light shows an enhancement and then a quenching, which does not come out of any structural change in the defect levels, but is due to a change from the nature of the defect state from a trap level to a recombination center.

The distinct feature that indicates the involvement in the metastability of the EL2 level has been the sharp regeneration of the photocurrent at a temperature over 120K, where the metastable configuration becomes unstable. The attempt has been here to understand the interaction of different lights, both extrinsic and intrinsic, on the state of the trap levels present.

5.3.2 Design of Experiments

The distinct feature of our sample is that while it behaves as any normal undoped SI-GaAs as far as trap characteristics observed in TSC, the photoquenching signature is not observed. All experiments are designed keeping this difference in mind. Some of the experiments were originally designed to test whether for some reason of experimental artifacts we are not being able to observe photoquenching in the sense of conversion to $EL2^*$. However it must be borne in mind that EL2 distribution in wafers of SI GaAs fluctuates widely even in the same wafer, and characterization of positions of wafer having low EL2 concentration have not attracted that much attention, though EL2 mapping is a standard industrial procedure today. Before we go into details of the results we give below a classification of experiments that are discussed in the following sections to give a helpful guide-map of what follows in the rest of the chapter.

The various initial conditions can be divided into two broad divisions: High intensity studies and low intensity studies, depending on excitation intensities

High photo-Intensity studies

The direction has been generally to look at the optoelectronic properties of the sample through either TSC or TSPC after different initial preparations.

1. Traps initially empty

   Photoconductivity-Temperature studies with different photocurrent intensities

2. Traps initially partially or completely filled with much larger than band gap light

   TSC studies

3. Traps initially partially or completely filled with sub-bandgap light

   TSC studies

   TSC studies after exposure to high intensity larger than band-gap light

   TSC studies after partial or complete unquenching by annealing at higher temperatures, and then exposure to high intensity larger than band-gap light

   TSPC for 676nm light

Low Photo-Intensity studies

Here the stress is on transient measurements, after suitable sample preparation, and on TSPC, both of low intensity 676nm light. The sample initial conditions used are:

1. Traps empty
2. Sample exposed to sub-bandgap light
3. Sample exposed to high intensity white light to fill all traps, and then sub-bandgap light.

5.3.2.1 High Photo-Intensity Studies

1. Traps initially empty: Temperature dependence of photocurrent for different excitation intensities

The temperature dependence of photconductivity of GaAs, with the intensity of excitation source as a parameter, brings out several interesting features. The temperature dependence can be broadly broken into three parts, a fall in photocurrent with decrease in

temperature in the range of 300 to 200K, peak-like features in the range 100 to 200K, and a low temperature (< 80K) sharp rise in photocurrent with lowering of temperature. Figure (5.4) shows typical plots, where the current is plotted in logarithmic scales, to facilitate comparison of photocurrents differing in magnitude by five orders. Similar peak-like features were reported for GaAs in the 60's but were not analyzed in detail.

The important point to note is that these peaks or shoulders observed are not due to thermal activation, as in TSC, as there is almost no difference in the data taken while heating at different rates as well as between the heating and cooling curves. (fig(5.5))

These results are different from those reported by Desnica [30-34], who has shown a direct link between the thermally stimulated current peaks and those present in photoconductivity due to low intensity excitation. Later, we do show similar results for low intensity excitation. In an earlier work in our laboratory, the major peak at 140K in the photoconductivity-temperature plot for high intensity excitation, was linked to the dependence on mobility, assuming that the lifetime does not play a significant role. However in low intensity data the lifetime dependence is brought out in detail, as it shows that there are two shoulders present and the position of these shoulders shifts to higher temperature for higher intensities (fig (5.6)). These shoulders which represent transition from higher to lower sensitivity has been termed thermal quenching, and occurs when an impurity level changes from acting as a trap to acting as a recombination centre[2]. In a material in which the majority carriers are electrons, the change from a recombination center to a hole trap with decrease of temperature causes the number of free holes to decrease, thereby increasing the electron lifetime. This causes the sensitivity to increase sharply. This change in the nature of an impurity center can be alternatively understood as the motion of the hole demarcation level, which crosses the trap level at this transition temperature.

In our data, we can see the presence of two such transitions in two different temperature ranges. The transition temperature is present where the demarcation level crosses the defect level, and the condition satisfied can be expressed as

$$\ln(n) = \ln\left(\frac{N_v S_p}{S_n}\right) - \frac{E_I}{kT} \qquad (1)$$

so, if the photocurrent is taken as a measure of n, we can plot ln(*photocurrent*) vs. $1000/T$ (fig (5.7)). This has been fitted to a straight line and the energy of the trap level E_I can be obtained from the slope. Such studies have been earlier done in great detail for several photoconductors such as GaSe, GaAs, CdS and CdSe much earlier[15].

The energy values obtained from the process described above for the two transitions present is found the be very similar to the activation energy for the two major traps seen in the TSC data, and the shoulders are present at roughly the same temperatures as the relevant stimulated current peaks. Also the TSC plots show that these two peaks, at ~130K and 200K are ***the*** two major peaks present, and hence represent the major traps in the sample. Therefore it is logical to suggest that the thermal quenching data and the TSC point to the same traps.

The low temperature rise of photocurrent with decrease in temperature (fig (5.8)) is due to the change in trap filling, due to the shift in the quasi-Fermi level, rather than the change in capture cross-section of the dominant EL2 traps. This can be understood by the progressive change in slope of the plots with change in excitation intensity, which would have remained constant, that is the lines would have remained parallel, if the quasi-Fermi level did not shift. The change in quasi-Fermi level is calculated from the slope of the log of photocurrent vs. 1000/T plot

The temperature dependence of photocurrent in this region can be written as

$$I = C\exp\left(-\frac{E_f - E_I}{kT}\right)$$

From fitted results shown in .(fig (5.9)), the $\Delta E = (E_f - E_I)$ is obtained for five different excitation intensities (fig (5.10)), The change in ΔE with excitation intensities is shown for five different intensities. The shift in Fermi level is seen to tend to saturate for large intensities.

2. Traps initially partially or completely filled with much larger than band gap light

TSC studies

This has been carried out earlier, using a diode laser (676nm), and the results are tabulated in Tab (4.1). The attempts to obtain quantitatively the trap filling times by progressively increasing the low temperature exposure time, and trying to obtain the number of traps filled from the height of TSC peaks showed the there are some unusual behavior associate in the process, and that the traps have distinctly different filling rates.

3. Initial trap Filling with sub-bandgap light

Effect of IR exposure prior to laser TSC

Since TSC is a convenient tool to monitor traps in SI samples, it is natural to ask what changes, if any, occurs to TSC spectrum due to laser filling if the sample is exposed to IR band prior to conventional TSC. This is shown in fig (5.11) for progressively increasing IR exposure time, keeping all other parameters such as filling time with intrinsic light and heating rate constant. It clearly shows that he TSC spectra remain qualitatively same, except for the fact that all the trap related peaks show a decrease in current with increasing IR exposure time. Note that none of the peaks get selectively photoquenched. The process of decrease in TSC peaks can be reversed by heating the sample to a higher temperature such as 120K and 110K. This is demonstrated by fig (5.12) where the sample is annealed for varying durations at 120K after IR exposure and then cooled down to 25K to begin the conventional TSC measurements after laser filling. Note again that all the peaks recover similarly.

Fig (5.13) shows a similar behavior for another annealing temperature of 110K. The undulations in the spectra at around130K is due to oscillations to be described later in detail, and is not to be confused with changes in the peak structure.

Since the TSC spectra quench with IR exposure and unquench with annealing at higher temperatures, and further the peaks show similar behavior, we are left with choice between the following alternative explanation.

Either (i) *all traps observed through TSC spectra have similar origin so as to display similar photoquenching behavior.*

Or (ii) *none of the traps are individually affected, but occupation of a recombination centre controlling the lifetime of the carriers are altered so that the current level recorded is different only because of change in lifetime and not due to concentration of carriers emitted.*

Clearly the first explanation is physically implausible, since it requires same chemical origin for all traps. The second explanation is much more natural, since it is quite possible that one is being able to change the occupation of the lifetime controlling recombination center (by IR induced transitions and their annealing), thereby changing the lifetime of carriers released from all traps. Clearly, photoquenching accompanied by a transition to a metastable state as such need not be invoked here.

TSC with IR filling only.

It is interesting to ask the question what happens to the TSC spectra if the traps are filled only with IR band, and the step corresponding to the band to band generation with laser light is eliminated. This is shown in fig (5.14) for two different filling times. It is to be noted that the filling times in this case is much larger than those used in the previous section. The dominant peak in the spectrum is now at 135K. This is a trap distinct from those observed in the TSC spectra for filling with intrinsic light. Filling the traps in this case occurs through a band to trap radiative transition rather than thermal capture of photogenerated carriers from the band. This confirms that the IR radiation is able to fill a different set of traps than those filled by intrinsic light.

Absence of EL2 related photoquenching

As explained in chapter 3 , the quenching of photoconductivity in the IR is considered to be the signature of dominant EL2 traps in the undoped SI GaAs. Fig (5.15) shows a typical photocurrent transient at sufficiently low temperature when irradiated with

subbandgap IR band (<1.1eV). Clearly the photocurrent saturates without giving rise to any quenching. Note that the level of current is as high as 44nA, and hence absence of photoquenching cannot be attributed to insufficiency in the intensity of IR light.

Our experiments to observe quenching of photoconductivity is best summarized in fig (5.16) photocurrent with intrinsic light increases with cooling as shown in A→ B portion of the figure. At point B the radiation is changed to high intensity white light which included IR. The IR component is so intense that we see heating of the sample with larger photoconductivity as in B→C. Any quenching is expected to have occurred during this phase. At a point C the radiation is switched back to 676nm (intrinsic light). The photocurrent is now lesser by a small factor, and continues to be less than the AB portion on cooling (D→E).

The negligible difference can be attributed to change in lifetime of photogenrated carrier due to change in occupation of life-time controlling recombination center than that of any metastable removal of traps due to quenching.

TSPC after IR exposure

Any thermally stimulated processes related to photoconductivity can also be studied in experiments similar to TSC. They are referred to as thermally stimulated photocurrent (TSPC) experiments. The information obtained from TSPC is different from that of a TSC in so far as it does not relate to thermal release of carriers from the trap. Any thermally activated process controlling the lifetime of the photogenrated carriers would show up as peaks.

Since we have obtained evidence of change in lifetime on IR exposure, the process can be further studied using TSPC. A typical plot for different exposure times of IR is shown in fig (5.17). For unquenched sample (no IR exposure), the PC shows a broad maxima at about 125K. On progressive increase in quenching time, the photocurrent peaks decrease and separate out into resolvable features. However the proof that the peaks indeed correspond to thermally activated processes would come from dependence on heating rates as in TSC. TSPC plots for different heating rates for the same amount of prior

quenching (10 minutes of IR exposure) are shown in figure (5.18) where the curves are shifted in the y axis for convenient comparisons. Note that the peak at 125K (labeled A) does not shift with heating rate while the higher temperature peak (labeled B) shifts as expected of a true TSPC feature.

The observation points to the fact that peak A corresponds to occupancy changes with temperature due to the position of the quasi-Fermi level; while peak B is related to a thermally activated trap parameter such as photoionizaton, capture cross-section etc.

5.3.2.2 Low photo-intensity studies

Effect of IR on response times

We now go on to further investigate the role of IR in controlling the response to intrinsic light using temporal development of photocurrent. We limit the intensity of both the intrinsic light and IR to low levels, so that the switching times are slow enough to be within the range of our experimental set-up. These experiments are conducted at 25K in order to suppress any thermal generation effects.

An intense white light is used to change the occupation distribution of traps and recombination centers needed for some of the cases described below. The sequence of operations to isolate the role of IR is as described below and shown in figure(5.19).

(i) The sample is heated to 320K to empty all traps, and then dark cooled to 25K, and kept at that temperature to ensure thermal equilibrium.

(ii) It is then exposed to light of λ=676 nm from a tungsten lamp, using a monochromator. The rising transient has a long time constant, and therefore the exposure is switched off after 1000 sec, before the steady-state condition is reached.

(iii) The sample is then exposed to low intensity (as given by the photocurrent) broadband IR radiation. The IR photocurrent reaches a saturation level, and is seen to decay very slowly. The IR is then switched off, and the sample is again exposed to low intensity 676. The transient is seemingly identical to that of the first, indicating total absence of any change in response time due to IR exposure (Fig (5.20)).

During the IR exposure, the nature of the transient suggests that the photocurrent is due to the photoionization of the filled centers. From these measurements, it would appear that the exposure to IR light has no effect on the PC transients using intrinsic light.

However since the transients involved in the figure was too slow, a source with two orders of more magnitude of intrinsic light was also used for a similar sequence. The result is shown in (fig(5.21))

The switch on transient in this case became too fast to be recorded, due to the decrease in response times with intensity. Note that the PC level due to 676nm increases two fold following IR exposure. This is clear proof that the low intensity IR is able to sensitize the photoconductor by increasing the lifetime of photogenrated carriers. This also means that the occupation distribution of recombination centers get changed significantly due to band to defect transition during IR radiation.

Another independent way of changing the charge distribution in the band-gap would be through the separation of the quasi-Fermi level using a highly intense white light. This would lead to the filling up of many more levels in the gap. Next we describe the results of experiments similar to the last two except that this time the sample is exposed to intense white light at 25K prior to another excitation to achieve a completely different initial condition in occupation after white light exposure is shown in Fig (5.22). Note that the results are in sharp contrast to the last two as shown in fig (20,21) and listed below.

(a) Even for low intensity intrinsic light, the response time is much faster and the transient saturates quickly.

(b) Photocurrent transients during IR exposure are similar in nature but faster.

(c) Surprisingly though the photocurrent level after IR exposure due to 676 nm is very small. The insert in the figure shows that the PC transient response increases very slowly indicating that it is the response time that has become too high.

From these experiments it is clear that the lifetime of photocurrent carrier with intrinsic light gets enhanced by IR radiation acting alone. However if a different set of traps are filled by using an intense white light, then the same IR irradiation leads to drastic increase in response time.

The observations described earlier are also borne out by low intensity TSPC experiments and their comparison with TSC results. Figure (5.23) shows two low intensity TSPC plots (for 15K/min heating rate) in which the curve with open circles indicate the one obtained after initial white light exposure.

A comparison of these with TSC curves is shown in Fig (5.24) From the comparison it is obvious that the peaks obtained in these low intensity TSPC curves are the same ones as in TSC and are due to thermal generation of carriers from the traps. At low temperatures the lifetime is higher and hence current levels are larger.

Therefore there is no abrupt increase or unquenching of TSPC, as would be expected if the quenching had been due to a structural change, that is due to metastability. Therefore it can be concluded that this phenomena is due to the variation in the lifetime of carriers, which depend on temperature. For the very low intensity of excitation, the heating to higher temperatures cause the quasi-Fermi level to come close to the equilibrium Fermi level, thus emptying the traps. This will in turn cause the lifetime to decrease and the photocurrent level to come down and merge with the dark current in form of thermally stimulated current peaks..

In conjunction with TSC results obtained earlier, these are strong indicators of the fact that there are many discrete traps levels present in sufficient concentration so as to control lifetime at low temperature when filled. Also under different circumstances the role of lifetime controlling center is assumed by different set of recombination centers. This is also in keeping with our TSPC, and temperature dependence of photoconductivity results, wherein the shifting of demarcation levels brings about a change in the nature of the center from trap to recombination centers.

Therefore in undoped semi-insulating samples having low or insignificant amount of EL2 concentration, many of the so called unusual behavior depend on the simple SRH kinetics rather than any special configurational change of defects to a metastable state. In fact Desnica et. al. in a set of recently published papers seem to further argue that even the phenomena associated to EL2 could be traced to normal SRH kinetics with photoexcitation. However similar set of experiments by Look et. al. have been identified as that there are many traps with arsenic antisite as a chief constituent so that all of these display common response to photoexcitation, specially in the IR.

The tenor of arguments by Desnica et.al seem to be more in line with the results obtained in this work, We have shown conclusively that portions of undoped semi-insulating do behave as normal high resistivity photoconductors with many trap levels in large concentrations.

5.4 Other Experiments

1. Observed instabilities during TSC measurements

We have been able to isolate consistent occurrence of instability linked time variation of current during TSC measurements for some very specific experimental conditions. A typical example of this instability is shown in figure (5.25), which is a ISC plot following IR exposure for 20 minutes at a heating rate of 15K/min. Note the sharp drop of current at 60K and again large variations of current where the TSC peak corresponding 130K would normally have been expected. These unexpected changes are due to time variation being superimposed on the otherwise well characterized temperature dependence of current. The oscillating feature have also been repeated in the literature[37] The conditions under which these oscillations are observed are as follows:

- They are most consistently observed only when the heating rate is high (specifically 15K/min). As the heating rate is reduced, the effects diminish and then slowly vanish. Fig (5.26)
- No such oscillations are observed if only intrinsic light is used to fill the traps initially. It is observed only when preceded by IR irradiation.
- The occurrence of instability diminishes if the effect of IR is annealed by heating to a high temperature (say 110-120K) and then cooling back to 25K before starting the experiment. This is demonstrated in fig(5.27) where the control parameter is the length of annealing time at 20K following IR irradiation before conducting conventional TSC. This can be compared to a data taken without the annealing. (fig(5.28))

Hence, these instabilities are certainly IR induced and have complicated dependence on heating rates. Similar features have in the past been observed with the quenching of TSC peaks.

2.Switching-off transients at different temperature

The raw data in presented here, for two different experimental runs (fig5.29). Each transient has a very fast decay portion which is below the scope of the current set-up, followed by a slow decay which is shown here, and finally a very slow decay to the dark current value, which is again difficult to record with the present set-up.

In SI GaAs the slow current transients that are observed on cessation of light is normally due to emission of carriers from traps that get filled during illumination. This aspect is one of the most studied for this material. It has been popularly investigated using signal analysis techniques such as Photoinduced Transient Spectroscopy (PITS) and more recently using Time analyzed Transient Spectroscopy[38-40]. Decay transients are of importance as they provide an alternative route to quantitative understanding of the various traps present in a material. Such results can be complimentary to the different trap properties investigated by steady-state analysis. However, as has been mentioned earlier, the problems encountered in obtaining good quality transient data, which is vital in the mentioned spectroscopic studies, are many, and arise out of various factors.

In this work, a beginning has been made in this direction, and decay transients have been taken after exposing the sample to high intensity intrinsic radiation from a HeNe laser. The experimental set-up has been discussed in detail earlier. The data is taken at intervals of 20msec, through K236 source-measure unit, at various temperatures during the cooling cycle of the sample. Care has been taken to ensure that the sample temperature remains constant throughout the transients.

There is very high reproducibility in the data, as the two runs show almost identical features. It is seen that firstly the decay in far from exponential and also the decay time constant varies similarly in the two runs. The decay time-constant increases as the temperature goes down, and reaches a maximum at around 130-110, and then again falls off at low temperatures. This can be qualitatively linked to the presence of the major trap,

as seen from TSC data, at around 130K. Also the photoconductivity shows a peak at that temperature.

The other observation of importance is the presence of oscillations in the decay curve, in both the cases. These oscillations present a major hurdle in obtaining meaningful and quantitative data out of the decay transients. The next section looks at these oscillations in more detail.

3.Observation of low frequency oscillations (LFO).

It is now known for some time that non linear current oscillations are caused due to instabilities in high resistivity semiconductos[40-42]. Such behavior has been observed in a wide variety of materials including the one under observation here. They have been linked to both trap and contact injection related phenomena, though no cogent explanation of mechanism has been forthcoming. We will only show some of the conditions under which we observed such LFO.

- Figure(5.30-31) Shows that photocurrent oscillations are dependent on the wavelength of radiation; and that this wavelength is itself dependent on temperature. If the wavelength of photoexcitation is being changed with time, it is possible to confuse these LFO with only wavelength dependent photocurrent oscillations. Our results indicate that level of photocurrent is in itself a parameter in controlling oscillation.
- Oscillations observed in photocurrent decay transients

These studied fall outside the scope of this work, and we will be content with displaying raw data of such transients for different temperatures for sake of completeness of records as regards this sample.

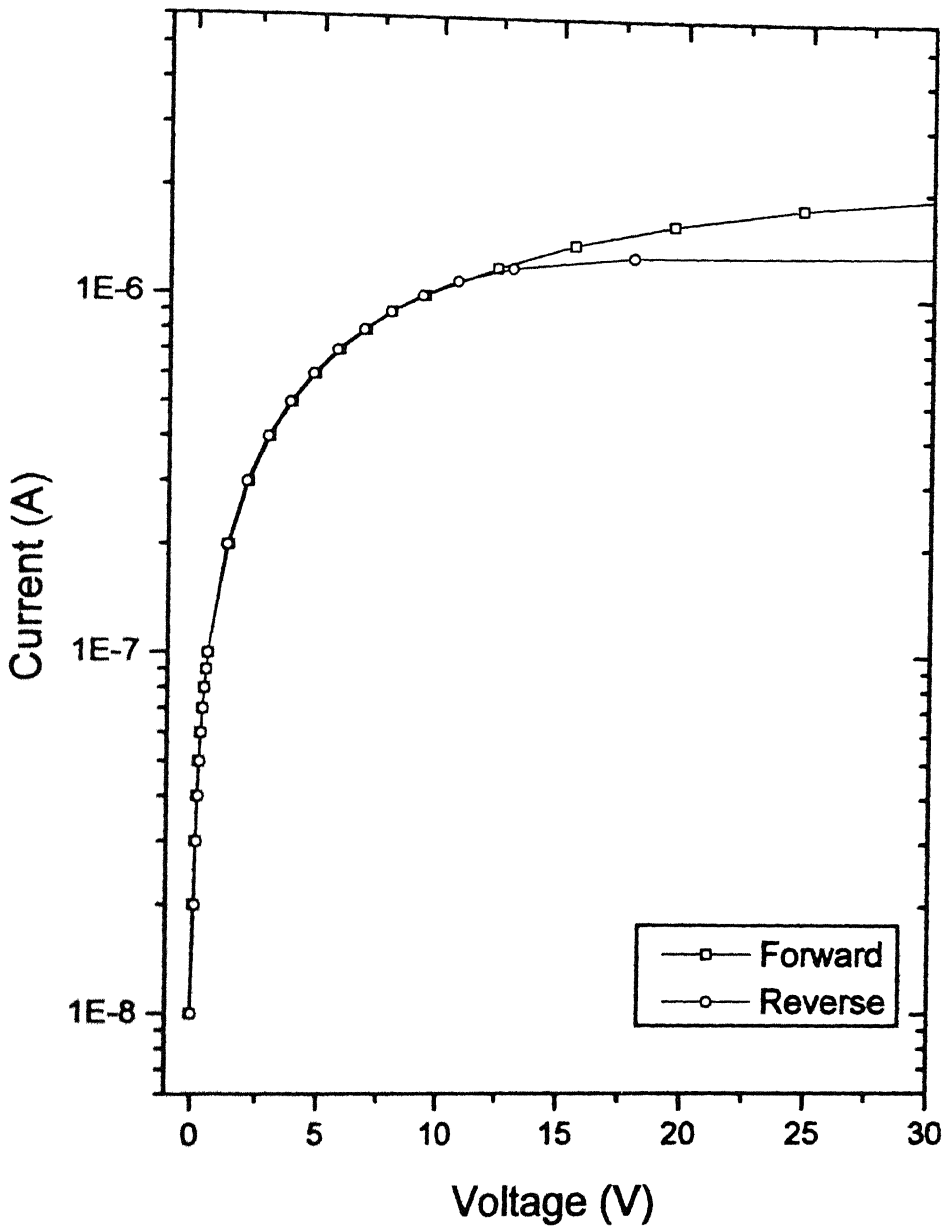

fig 5.1 V-I Characteristics (forward and reverse) at T=30K
Excitation source: Diode laser (676nm)

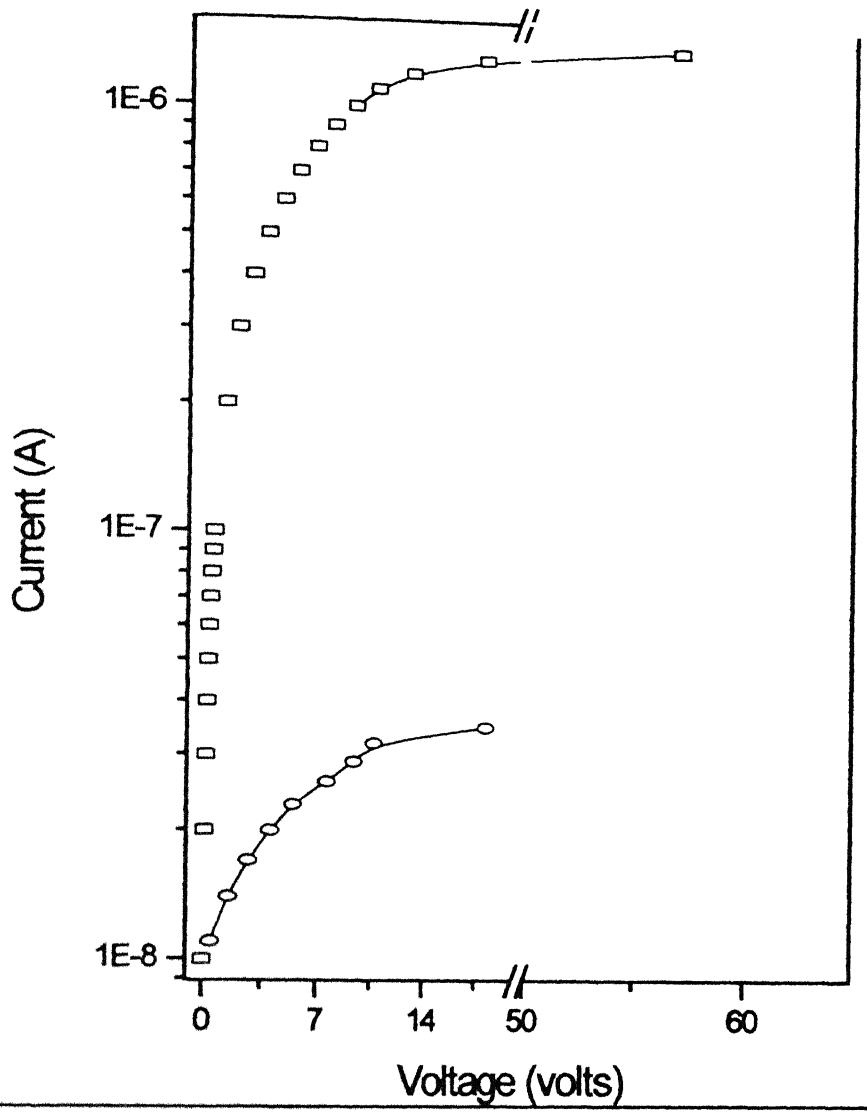

fig 5.2 V-I Characteristics at T=30K for 2 different excitation intensities
Excitation source: Diode laser (676nm)

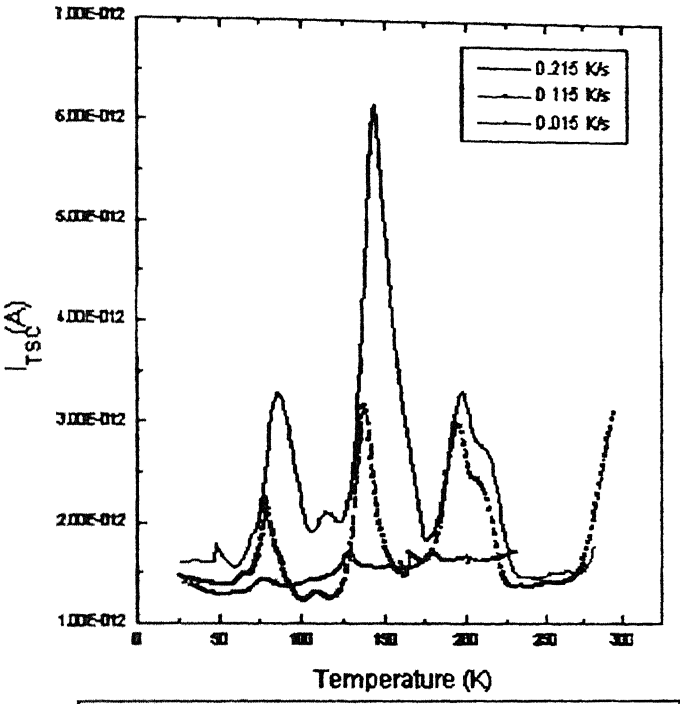

Fig 5.3 Thermally Stimulated current spectra for three different heating rates. The low temperature excitation (at T= 25 K) was done using photons of energy 1.86 eV (676nm)

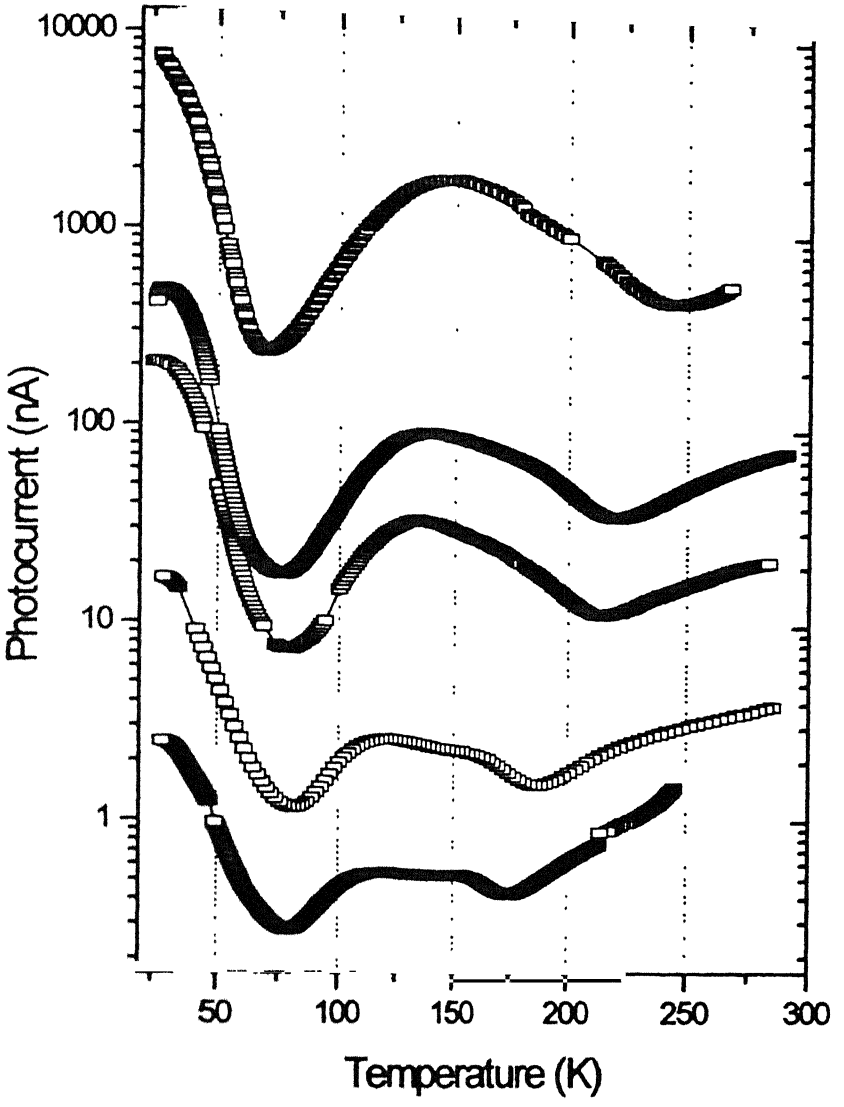

Fig 5.4 Intensity dependence of photocurrent-temperature plot
Source = Red diode laser (676nm)

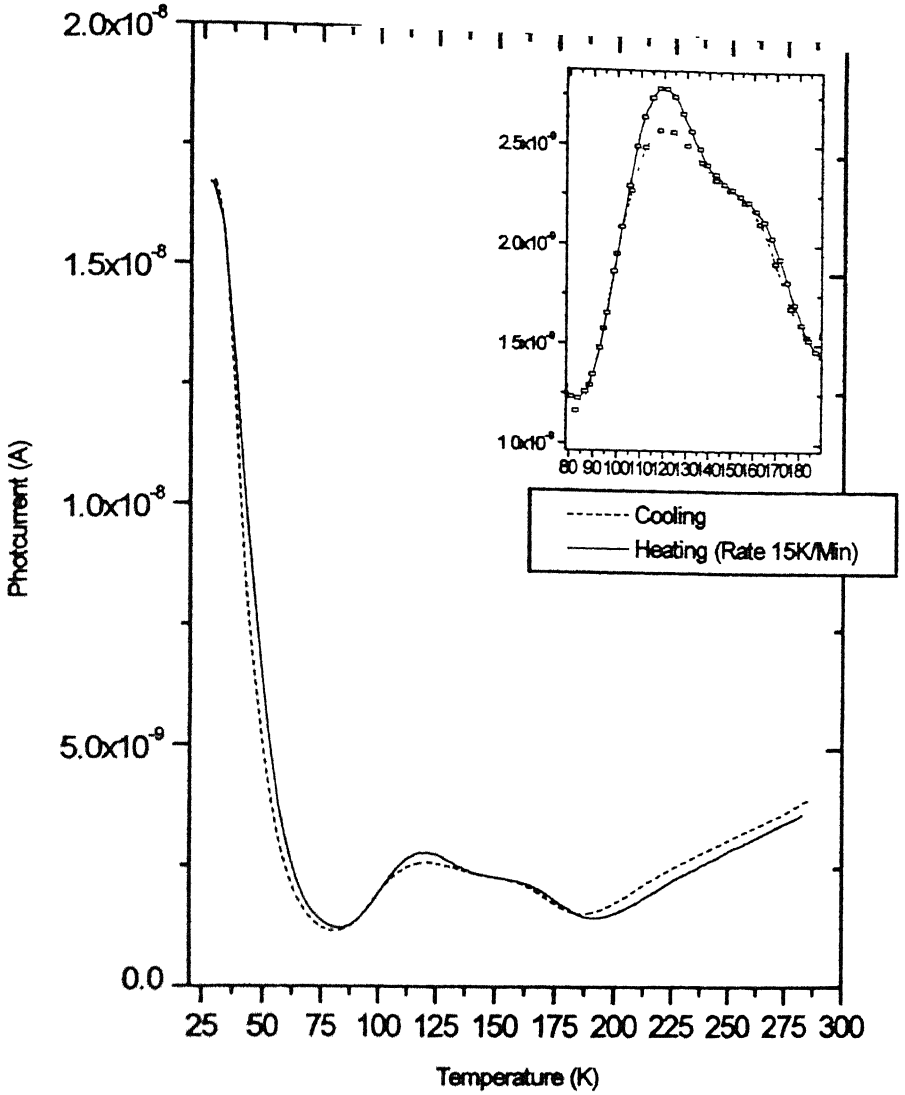

Fig 5.5: Photocurrent-Temperature for low intensity laser (676nm) light, shows similarity between the heating and cooling curves

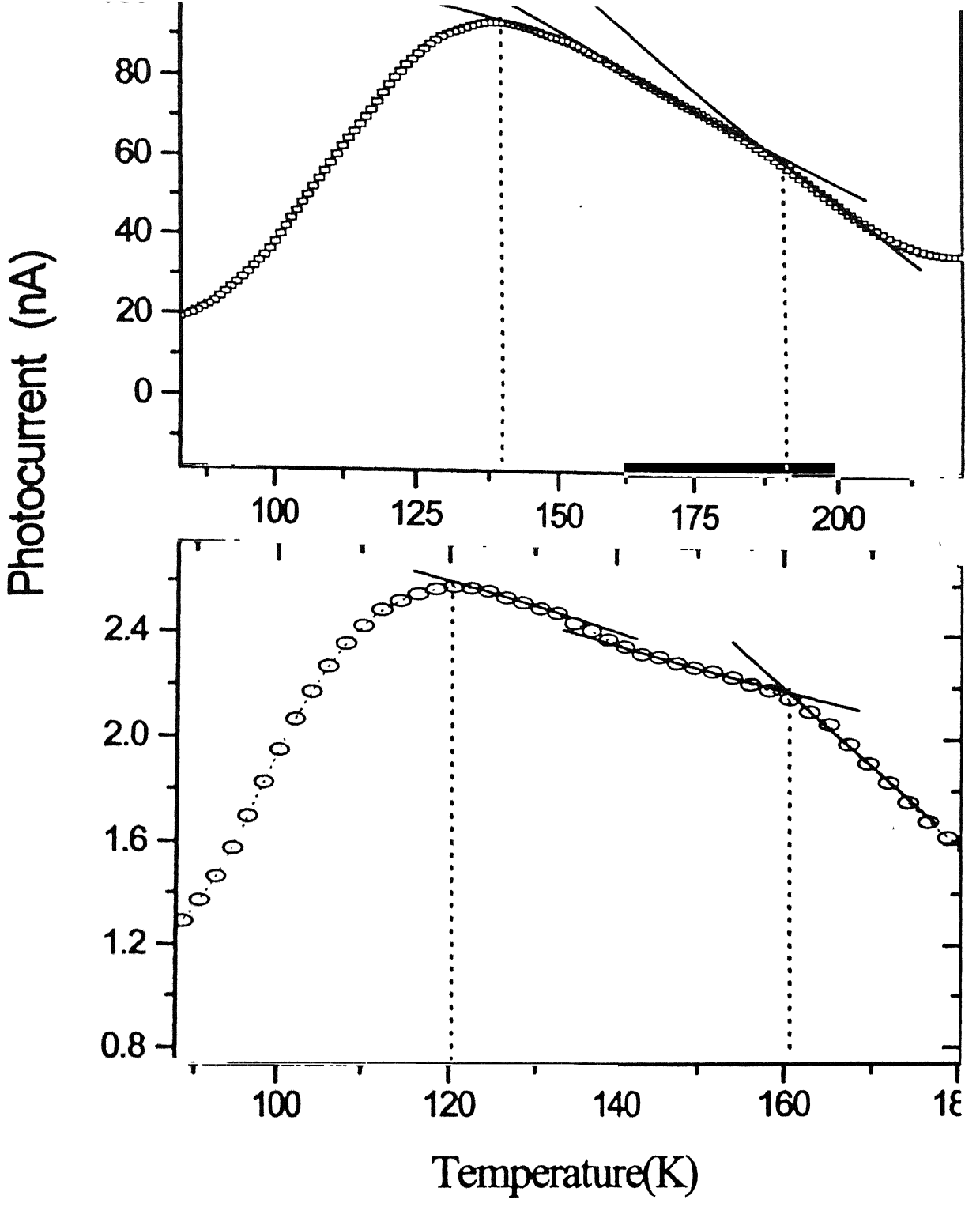

fig 5.6 The shoulders in Photocurrent-Temperature graph shifts with increase in excitation intensity

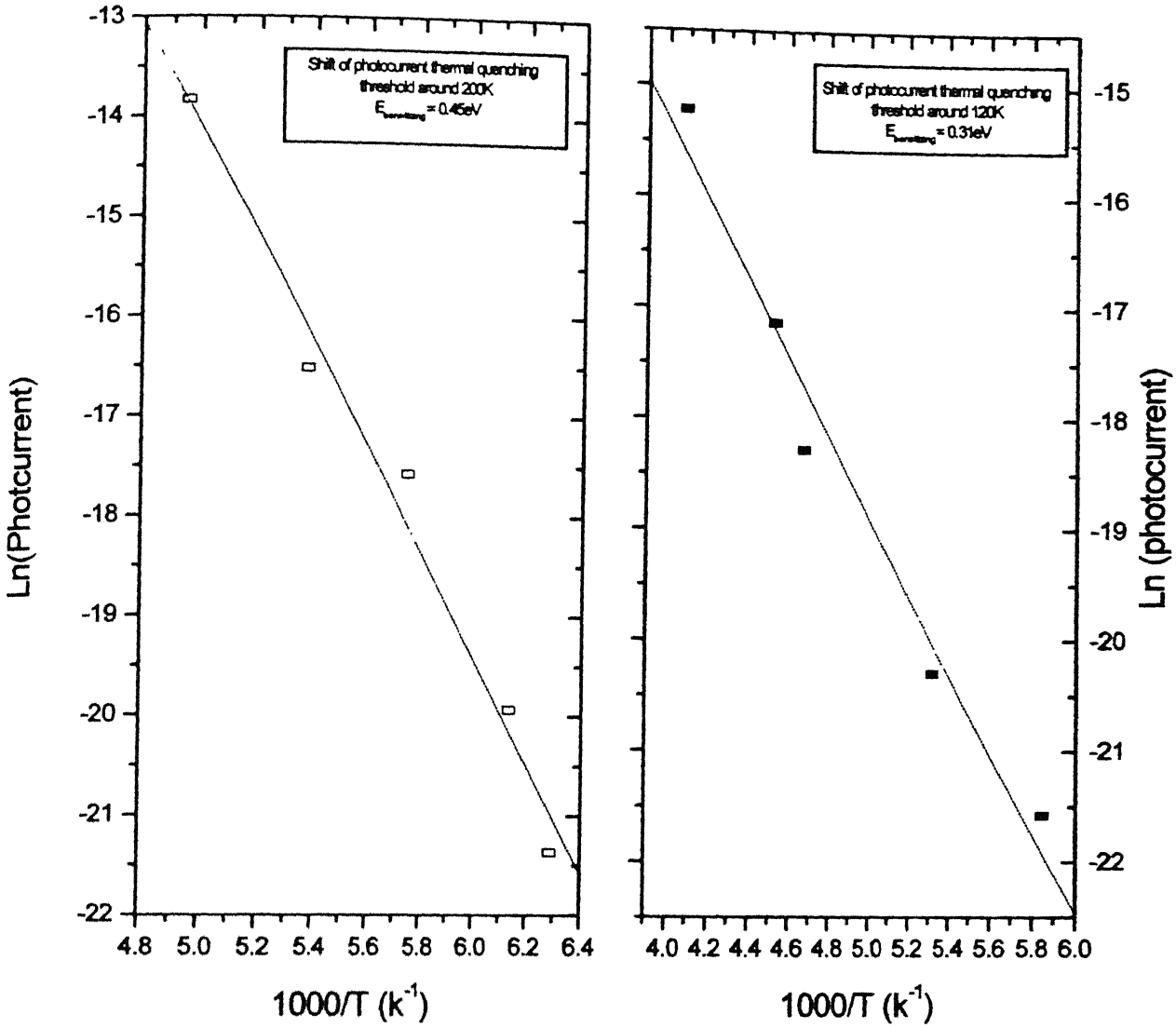

fig 5.7 ln(photocurrent) vs. 1000/T plot taken for transition temperature. Trap energy found from the slope of straight line fit, For two temperature regions

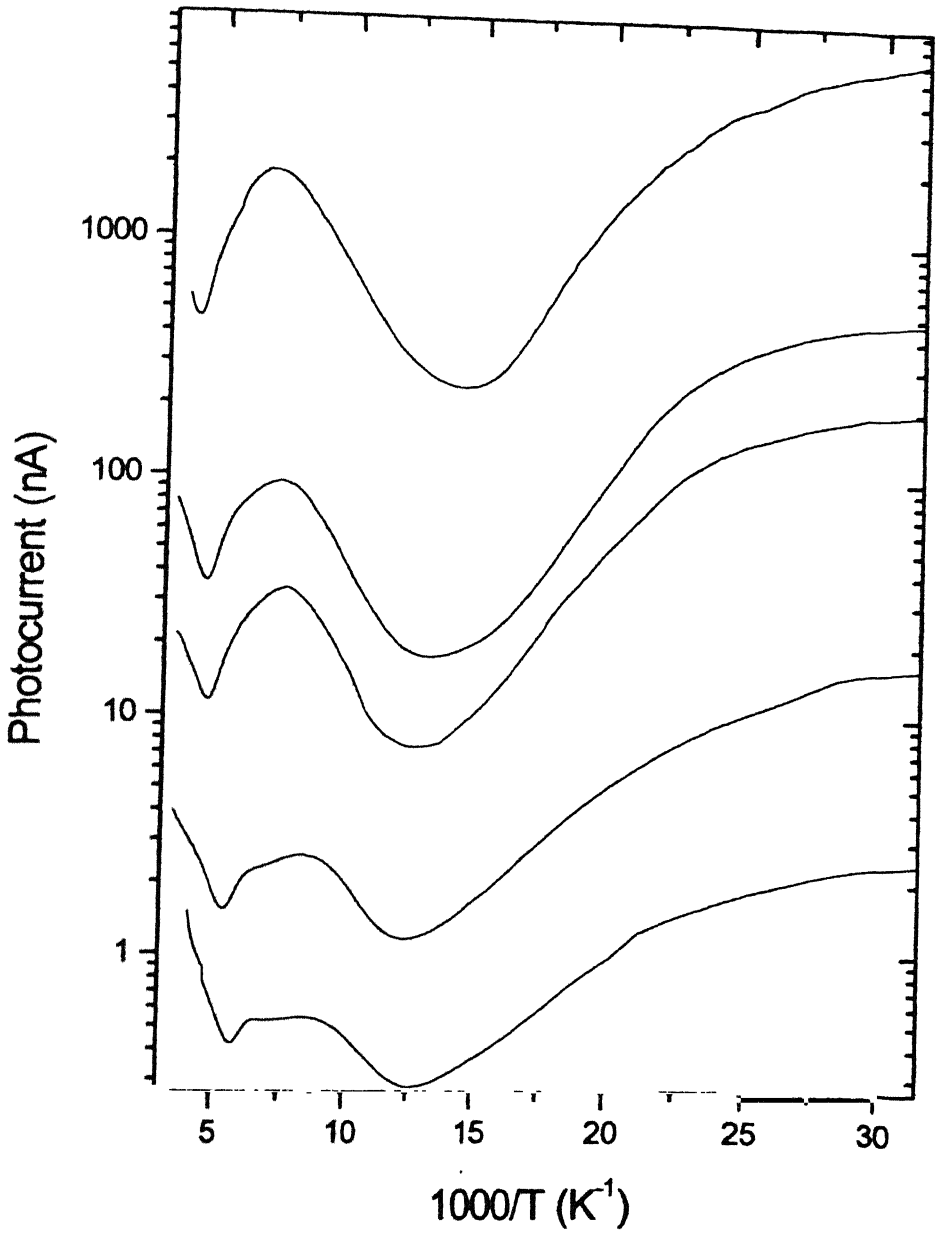

Fig 5.8 Low temperature rise in photocurrent for different excitation intensities

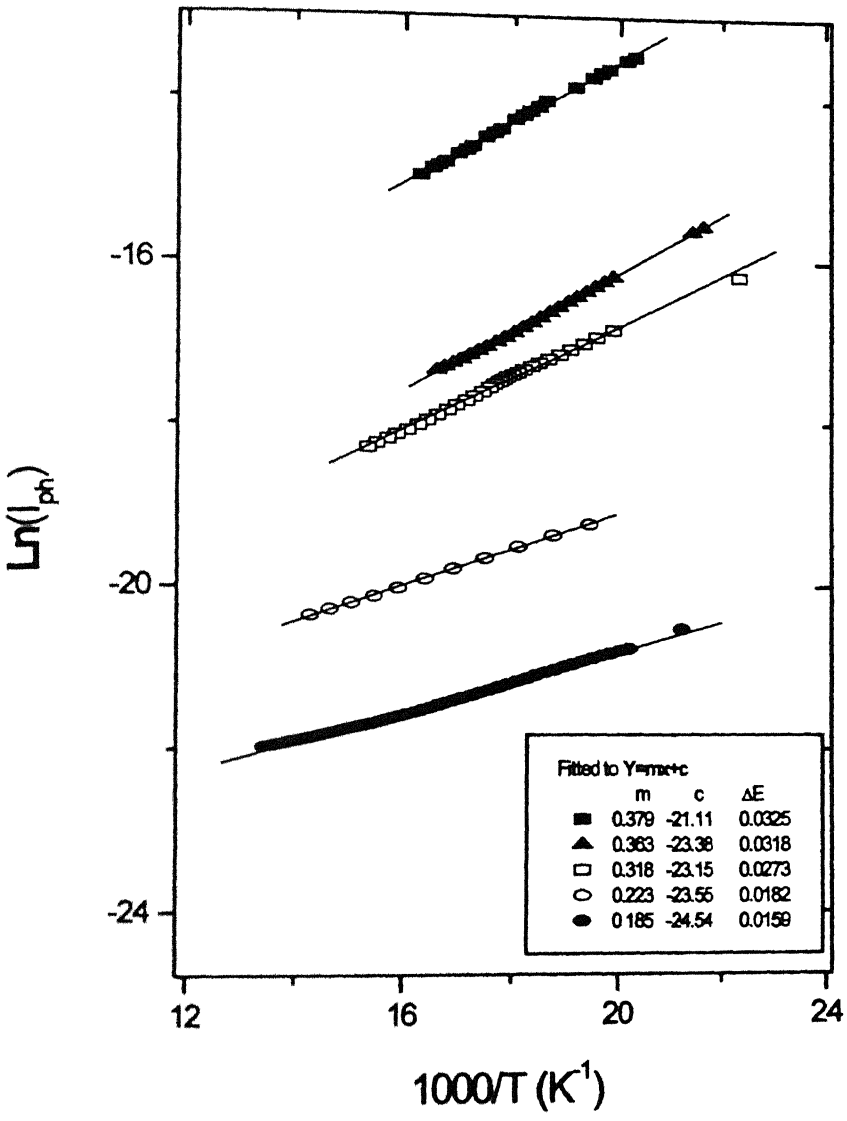

fig 5.9 Data for photocurrent-temperature plot for different excitation intensities

Plotted $\ln(I_{ph})$ vs. 1000/T lor low temperatures fitted to straight line, $\Delta E = E_i - E_F$ obtained from slope

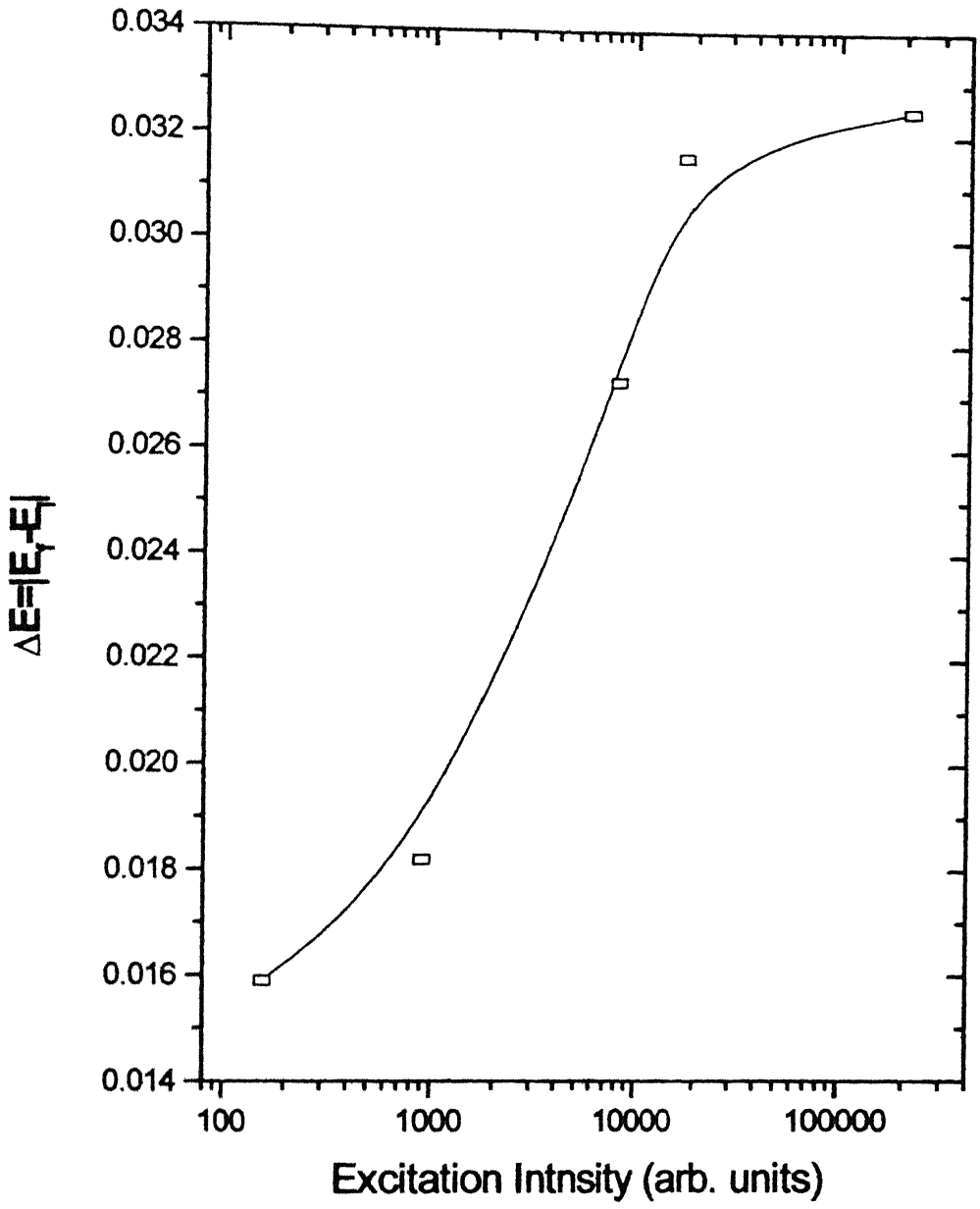

fig (5.10) Change in $\Delta E = (E_1 - E_2)$ for change in intensity of optical Excitation

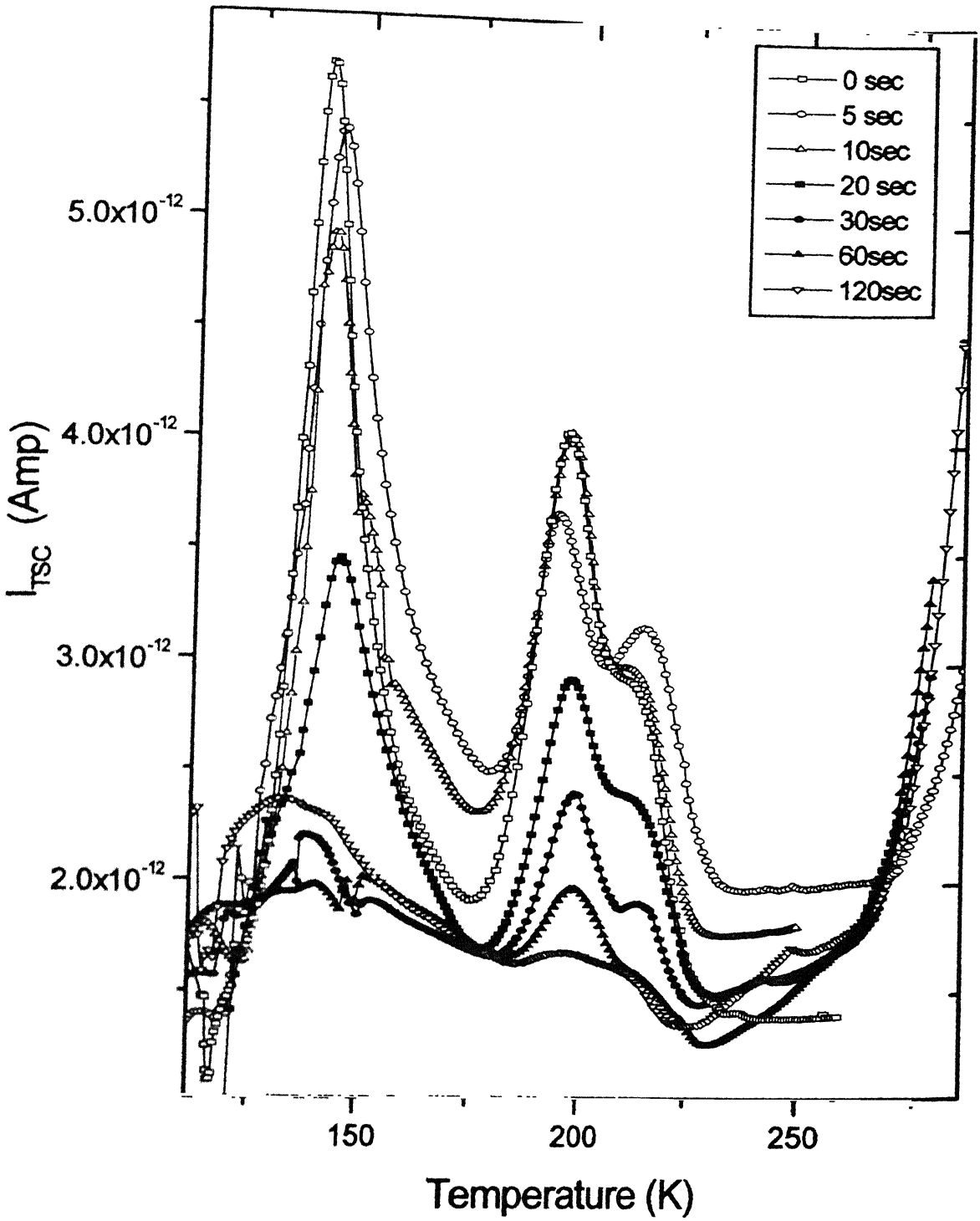

Fig 5. 11 The TSC for a 5 min exposure of HeNe Laser is taken after being exposed for different times to subbandgap radiation fron an IR source With a Si Fiter and a thermal Filter Rate of temperature rise = 15 K / min

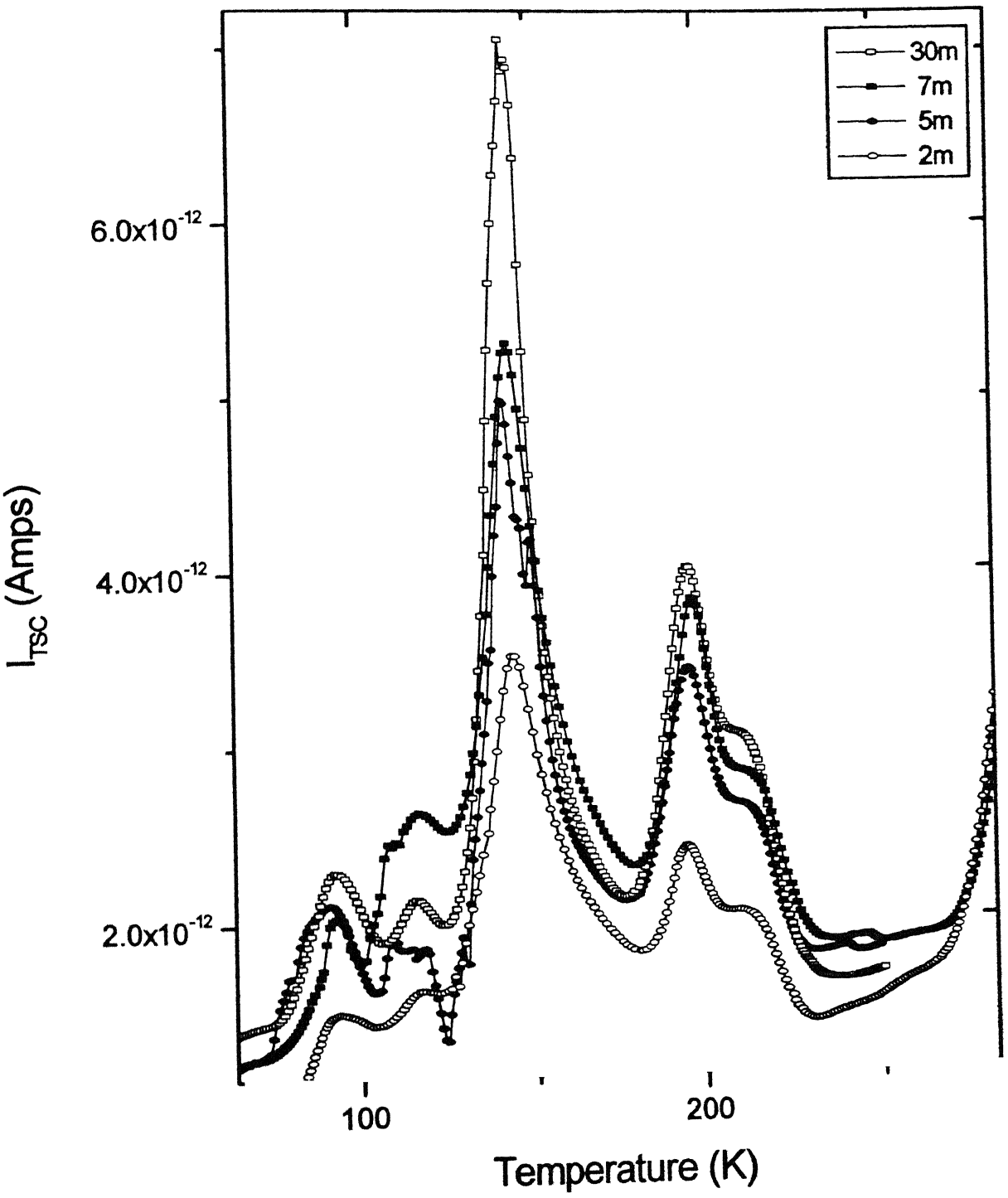

Fig 5.12 The Sample is Exposed to IR (Si Filter + Thermal Filter) for 10 min at ~26K
Heated to 120K and kept fot varying lengths of time
Cooled to ~25K, exposed to HeNe laser for 5 min
TSC measurements are done @ 15K/min

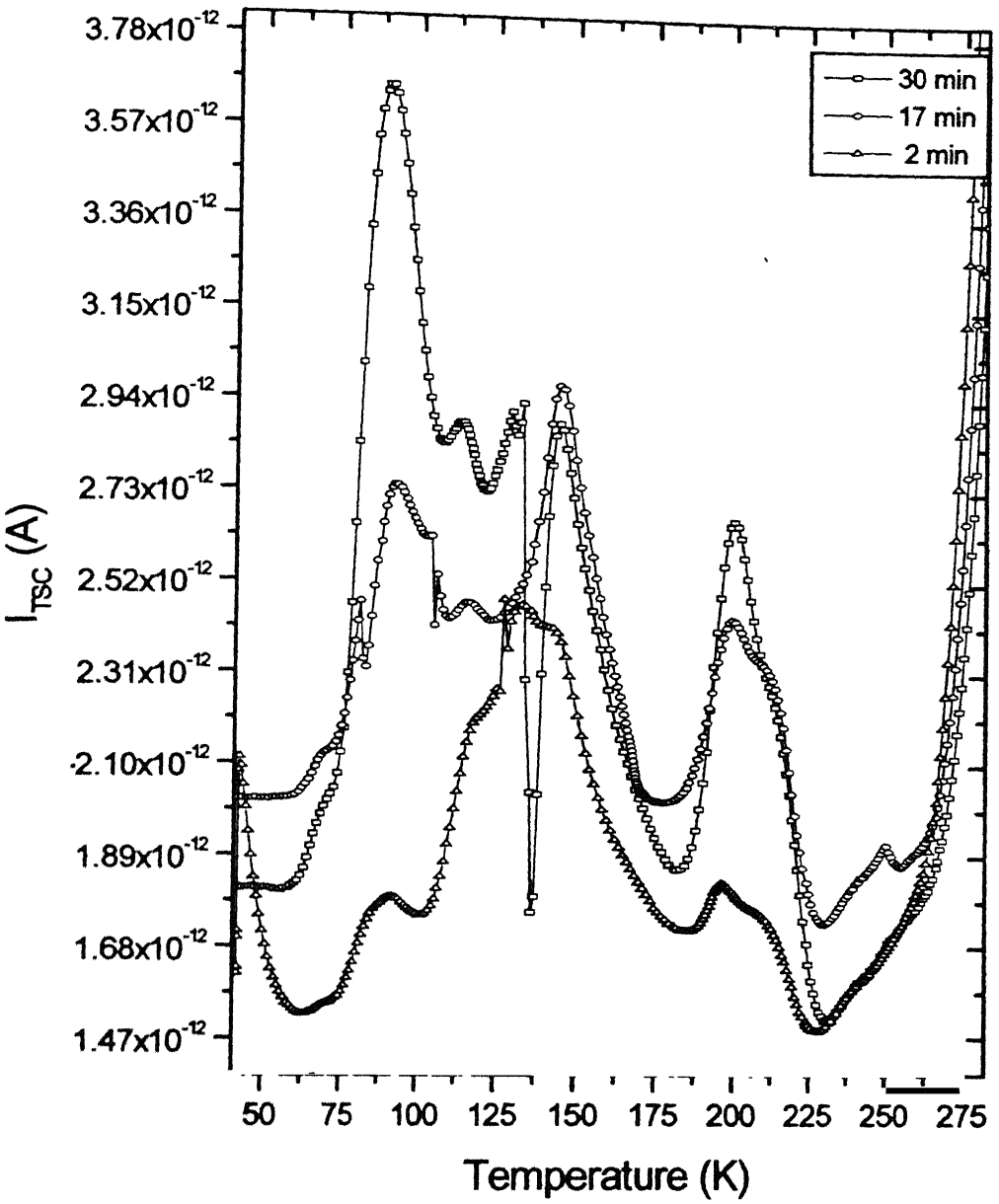

fig 5.13 The sample is exposed to IR (WL with Si filter+Thermal filter)
For 10 min at ~20 K
Heated to 110K, and held for different times
Cooled to ~25K, Exposd to Laser (HeNe) for 5 min,
TSC measurements taken

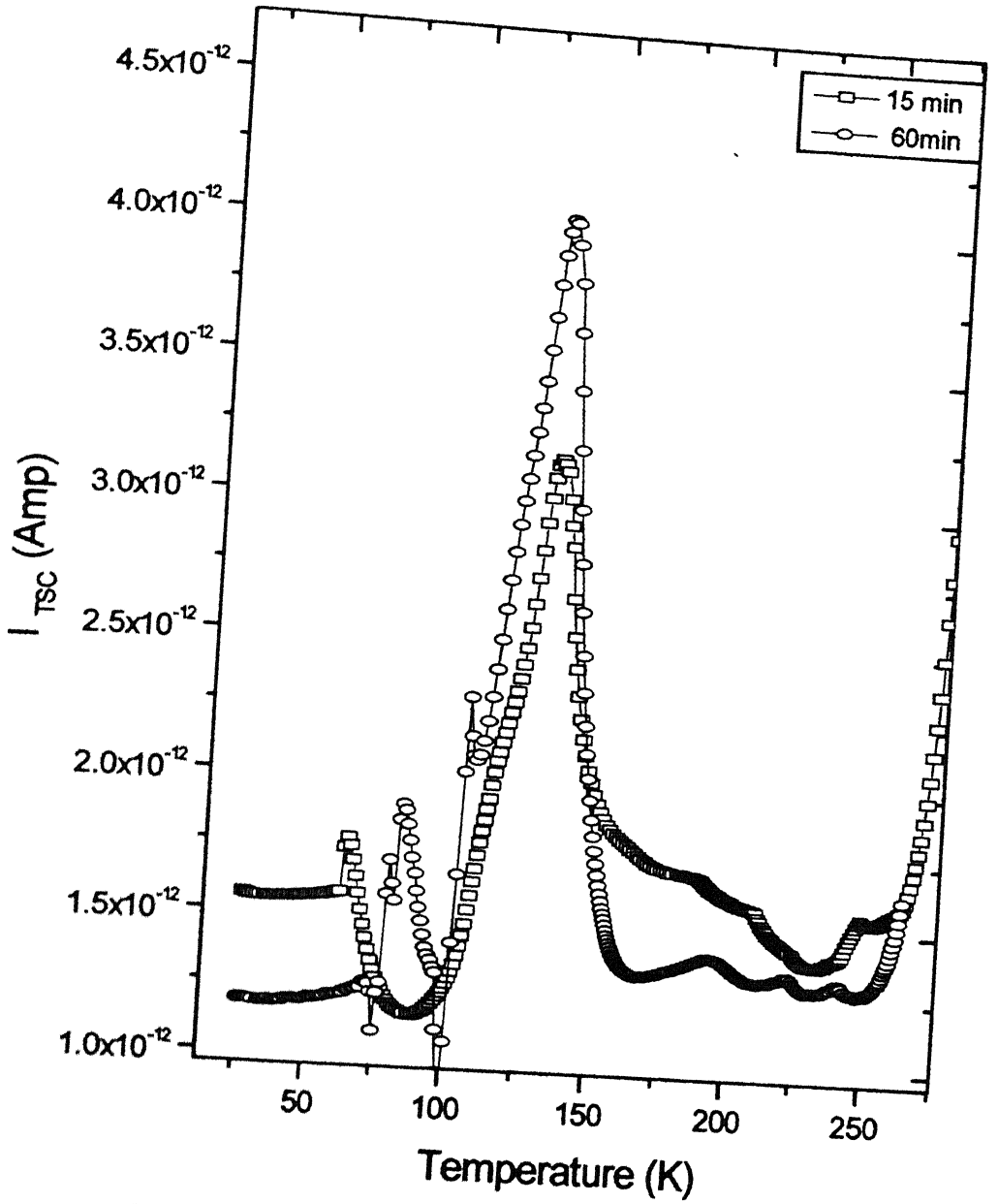

fig14 Sample exposed to IR
(White light with Si Filter+thermal filter)
For different exposure times, TSC taken with rate 15K/min

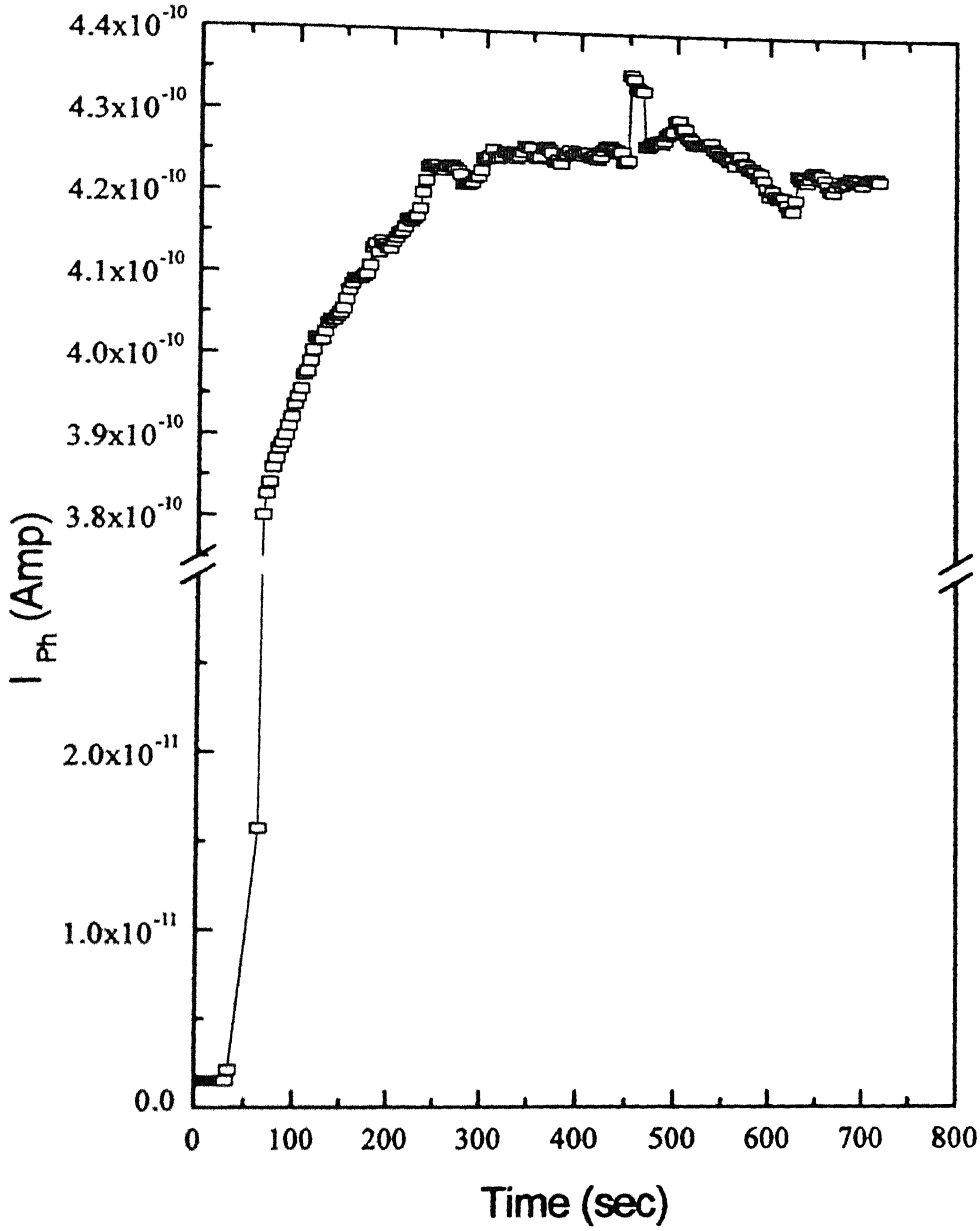

fig 5.15 Sample dark cooled to ~25K, exposed to IR light (White light with Si filter + Thermal Filter) under a voltage of 5V. Photoconductivity measured as a function of time

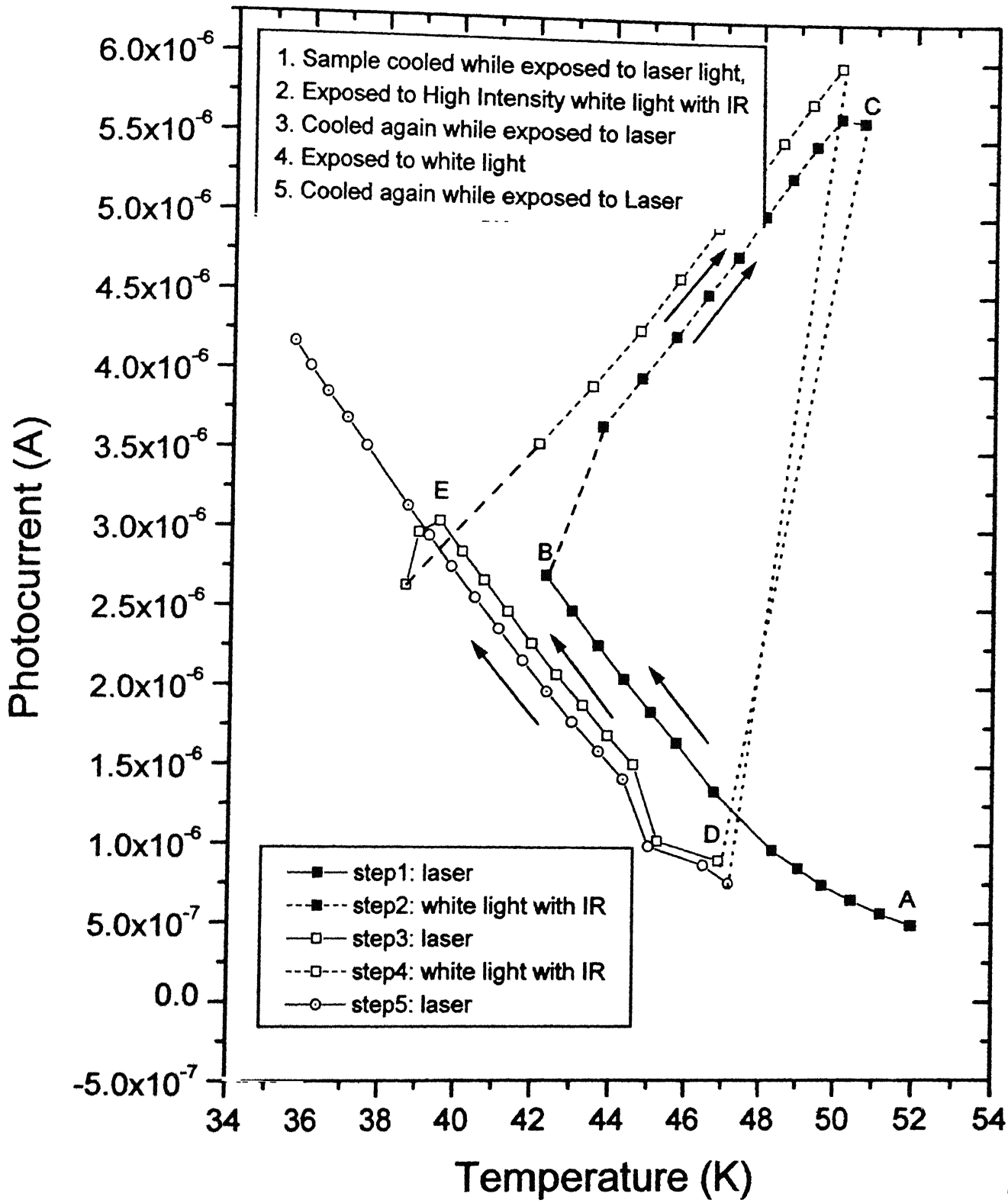

fig 5.16 Experimental plot to show the absence of large photo-quenching

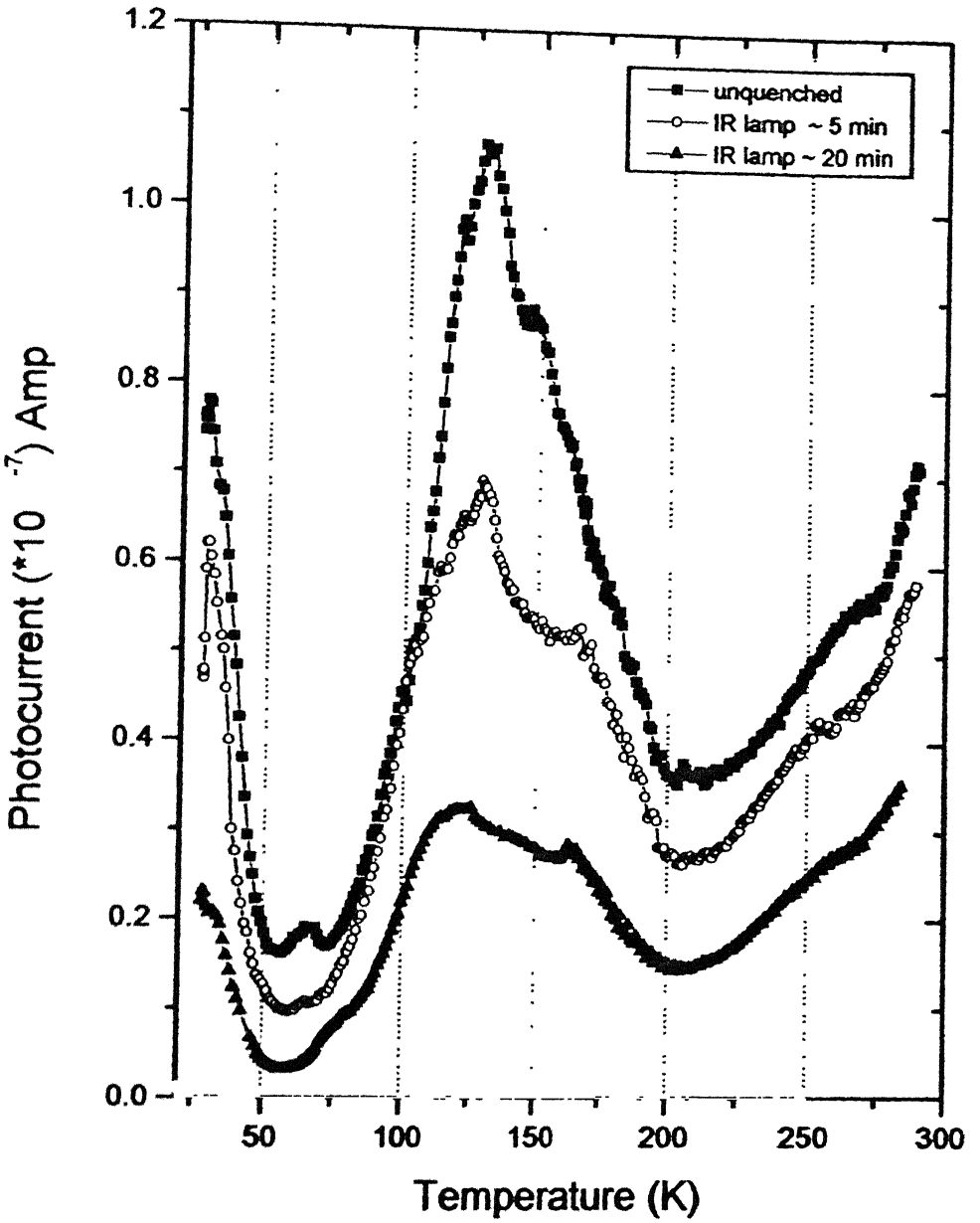

fig(5.17) The sample is exposed to IR raiation at low temp for various lengths of time
TSPC taken @15K/min

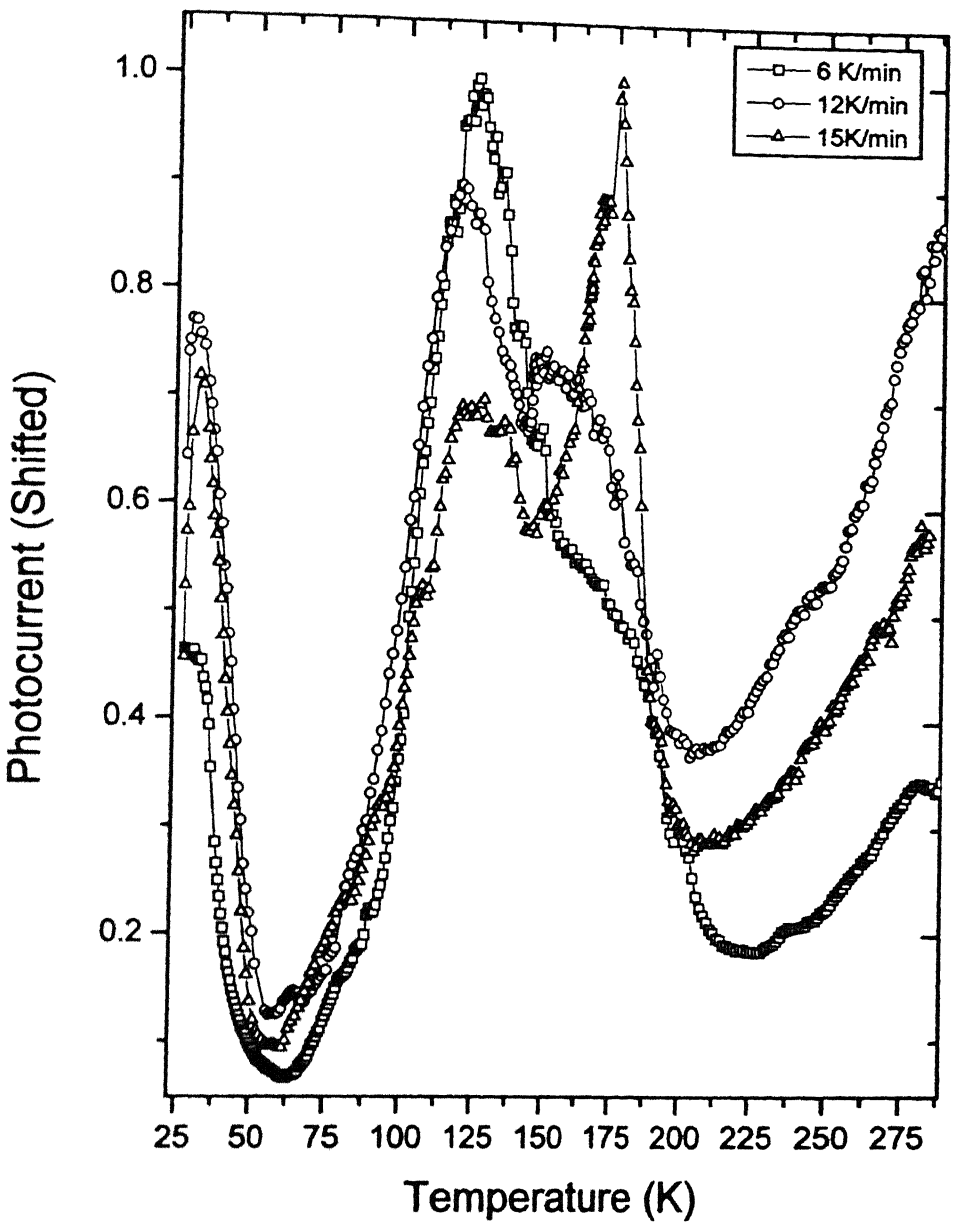

Fig 5.18 The Sample is exposed to IR radiation at low temperature Using a IR lamp with Si filter and Thermal Filter for 10 min The Photocurrent are recorded for different heating rates.

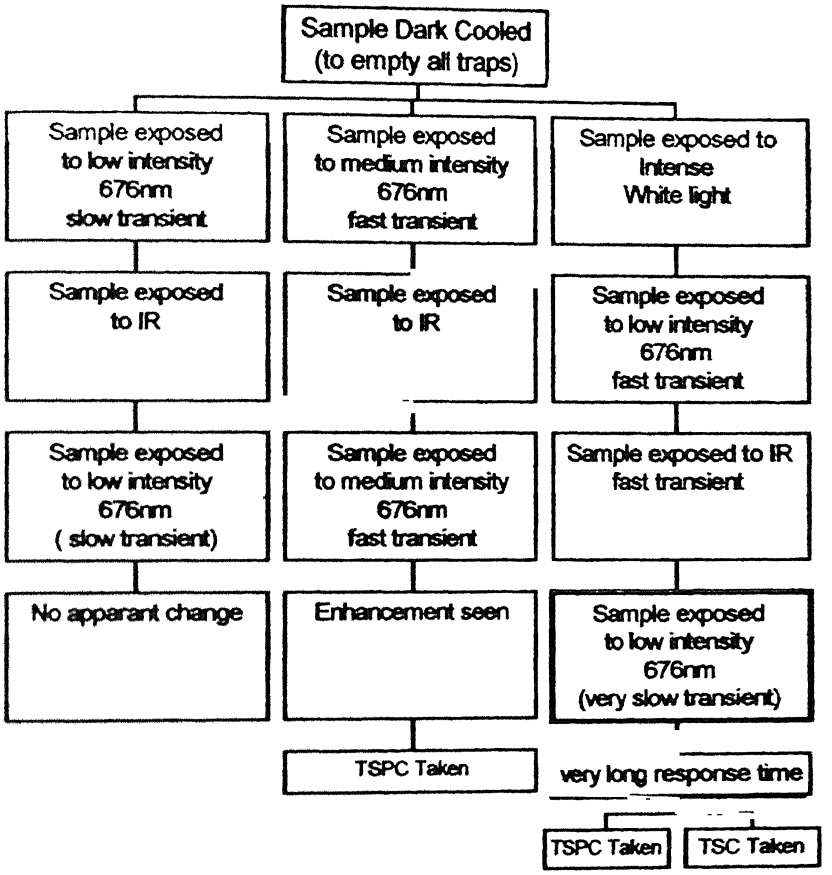

fig (5.19) Low intensity experimental procedure

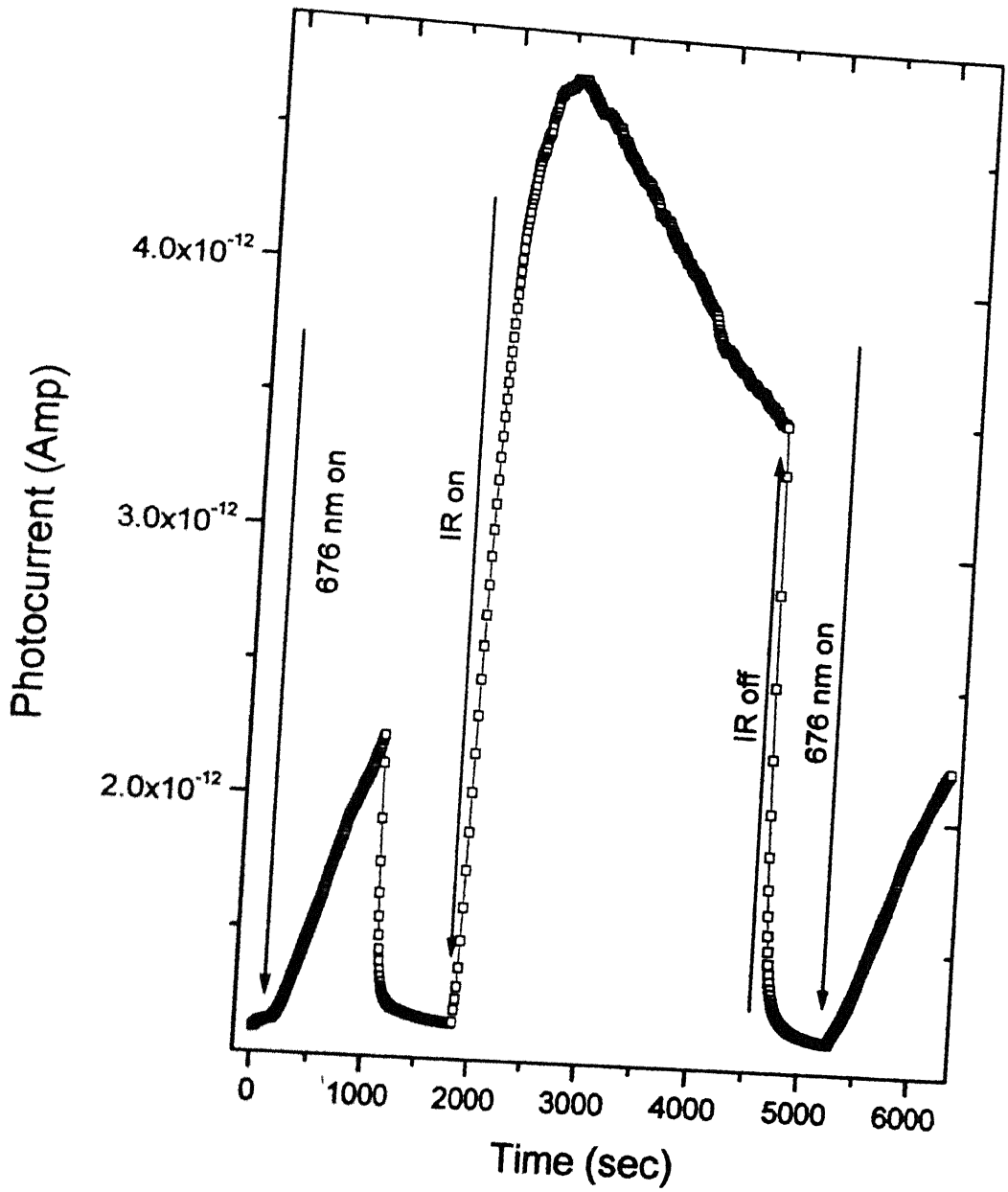

fig 5.20 Sample dark cooled to 20K, Exposed to light in the following sequence 1) Monochromatic 676 nm, 2)Broadband IR, 3) Monochromatic 676 nm

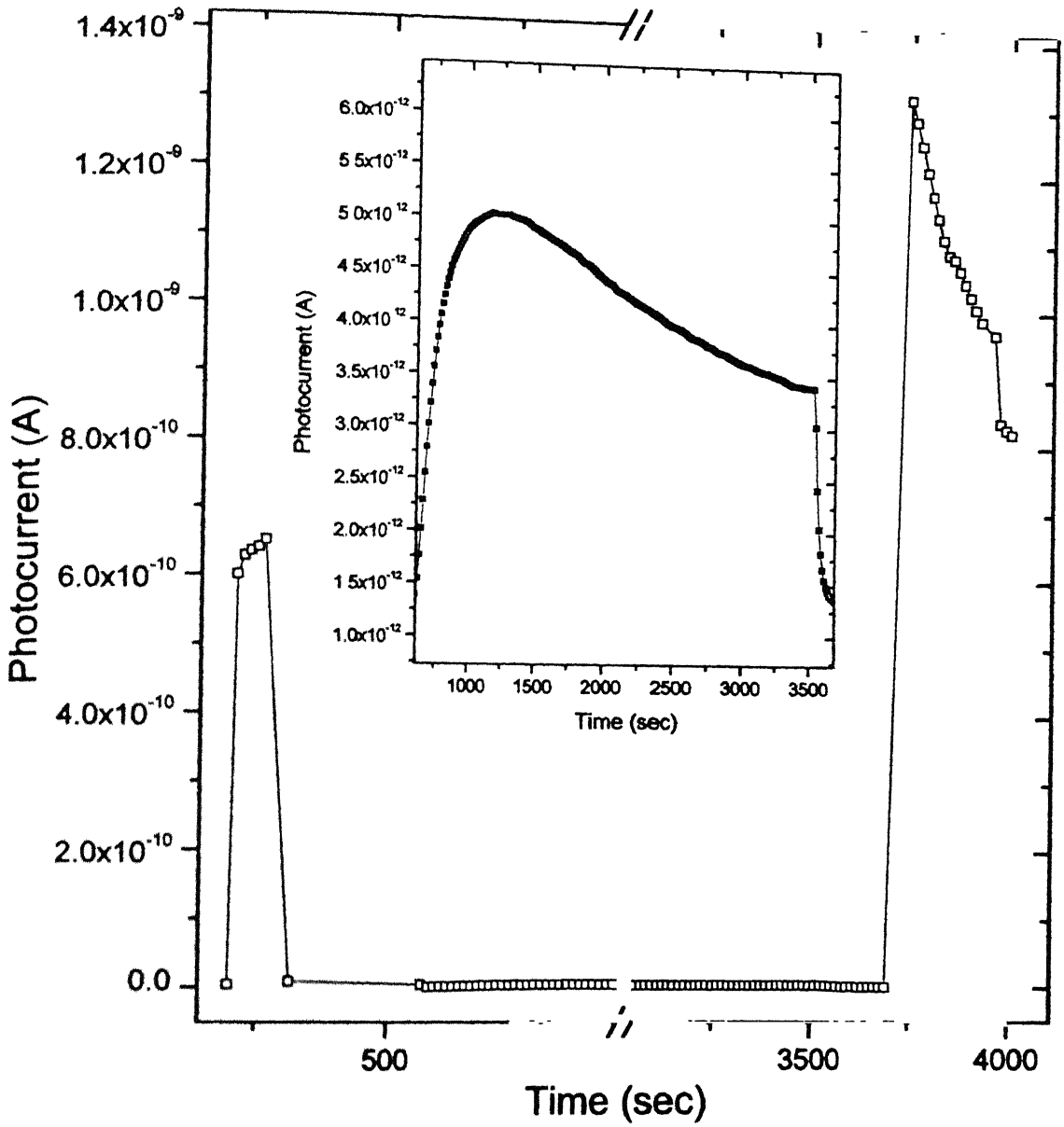

fig 5.21 Sample dark cooled, and exposed to 1) 676 nm from halogen lamp, 2) IR, 3) 676 nm

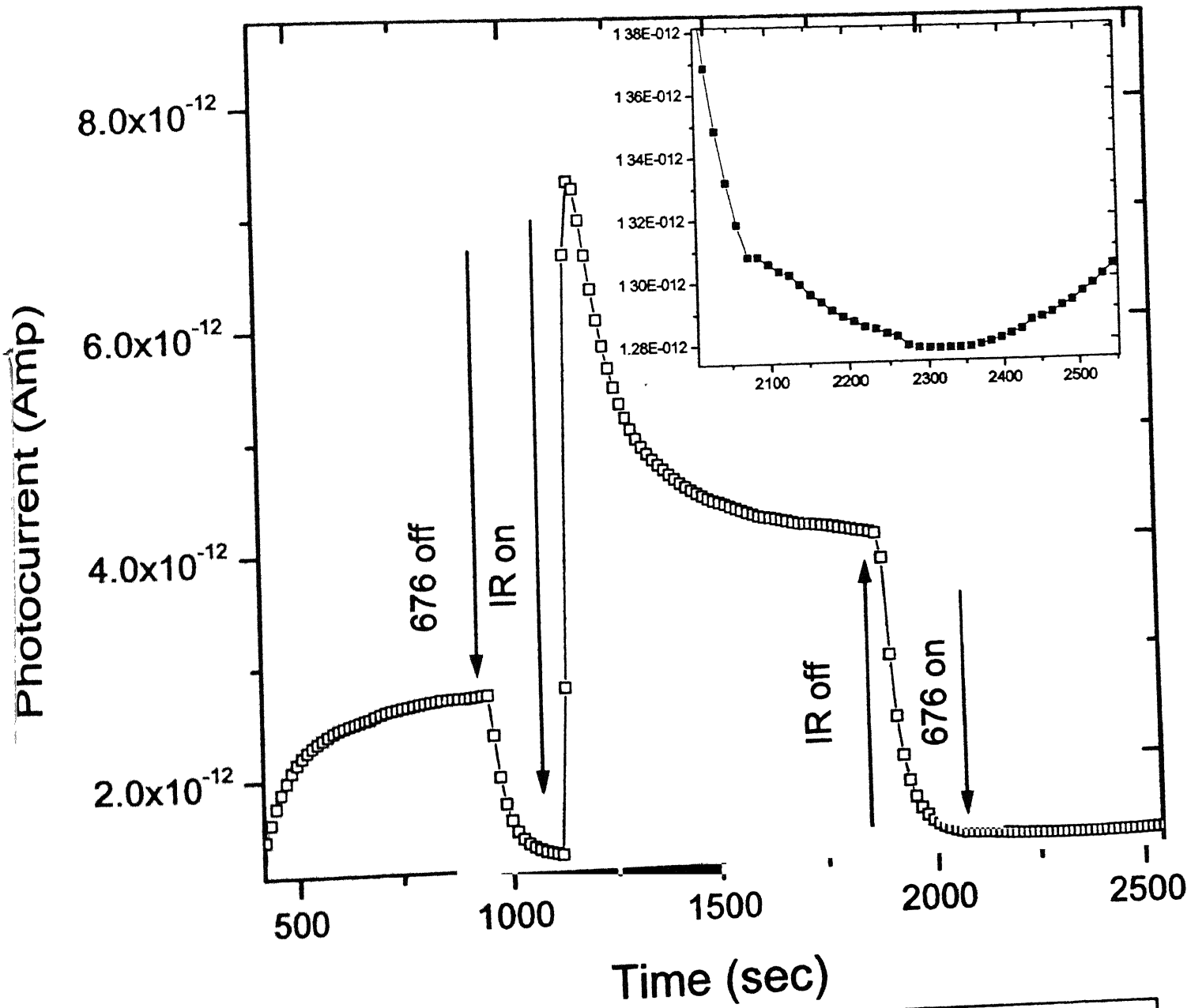

Fig 5.22 Sample dark cooled, exposed to White light of high intensity 676 nm light, IR lamp with Si filter and again 676 nm light.

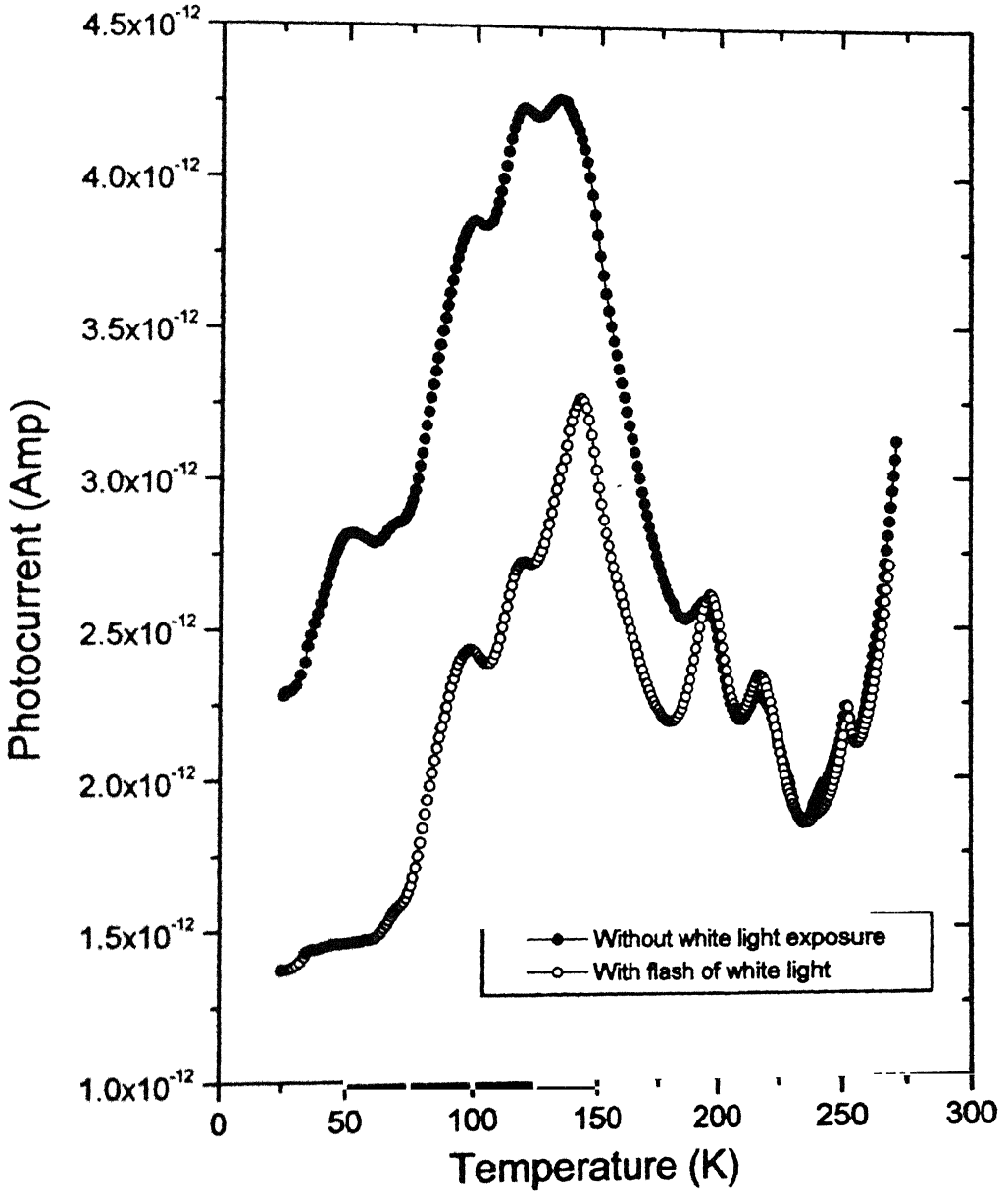

fig(5.23) The samples are dark cooled to 20K, and then exposed to:
sample1: 676 nm, IR, 676 nm in sequence
sample2: white light, 676 nm, IR, 676 nm in sequence
Photocurrent-Temperature data taken with 676 nm

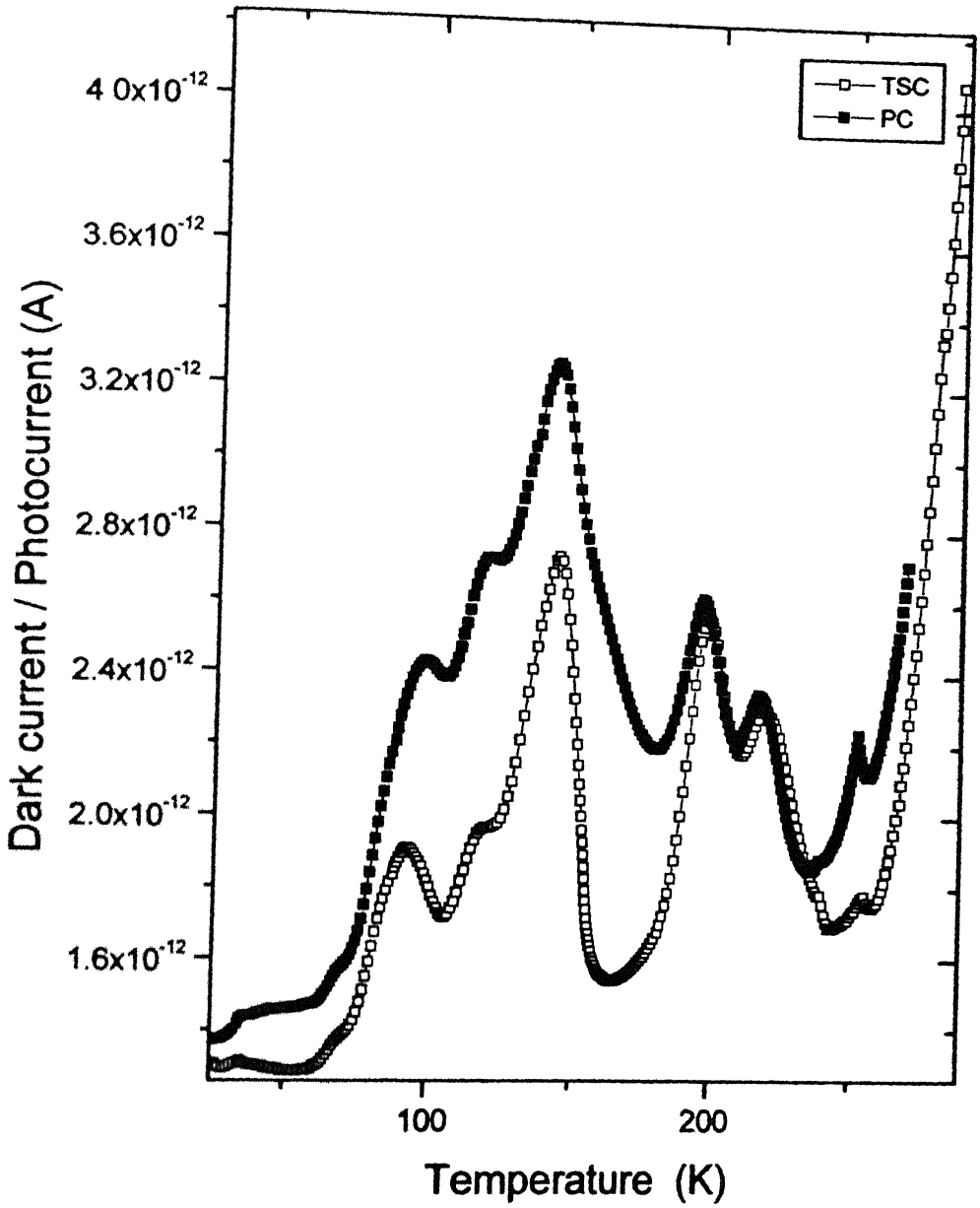

fig (5.24) Sample dark cooled, seguentially exposed to 1) Flash of white light 2) 676 nm, 3) IR, 4) 676 nm TSC, PC measured, heating rate 15K/min

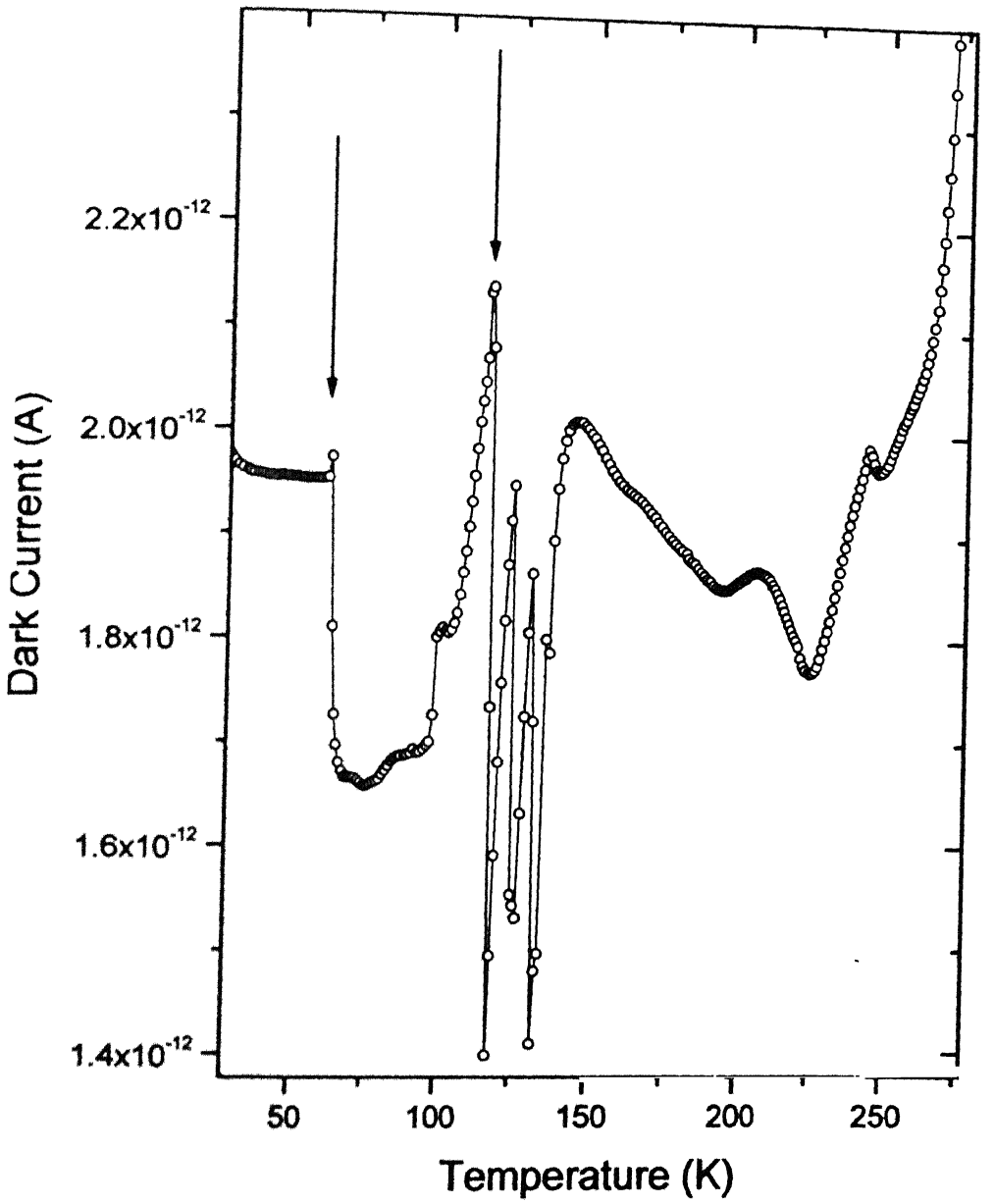

fig (5.25) Sample illuminated IR LAMP for 20 min at 25K
TSC taken with heating rate = 15K/min,
showing instabilities at 60K and ~130K

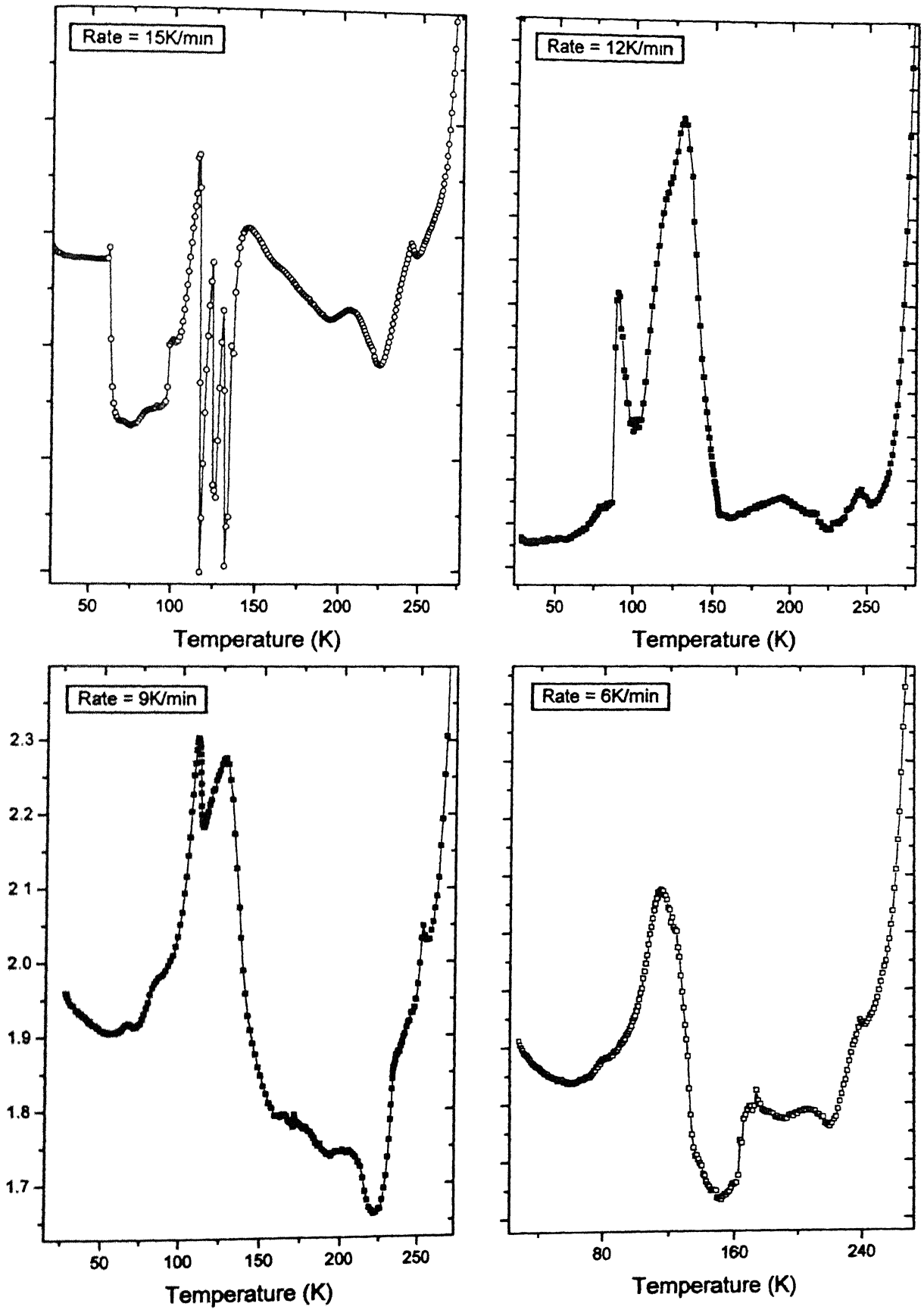

fig (5.25) Sample exposed to IR light for 20 min at 25K TSC taken at different heating rates

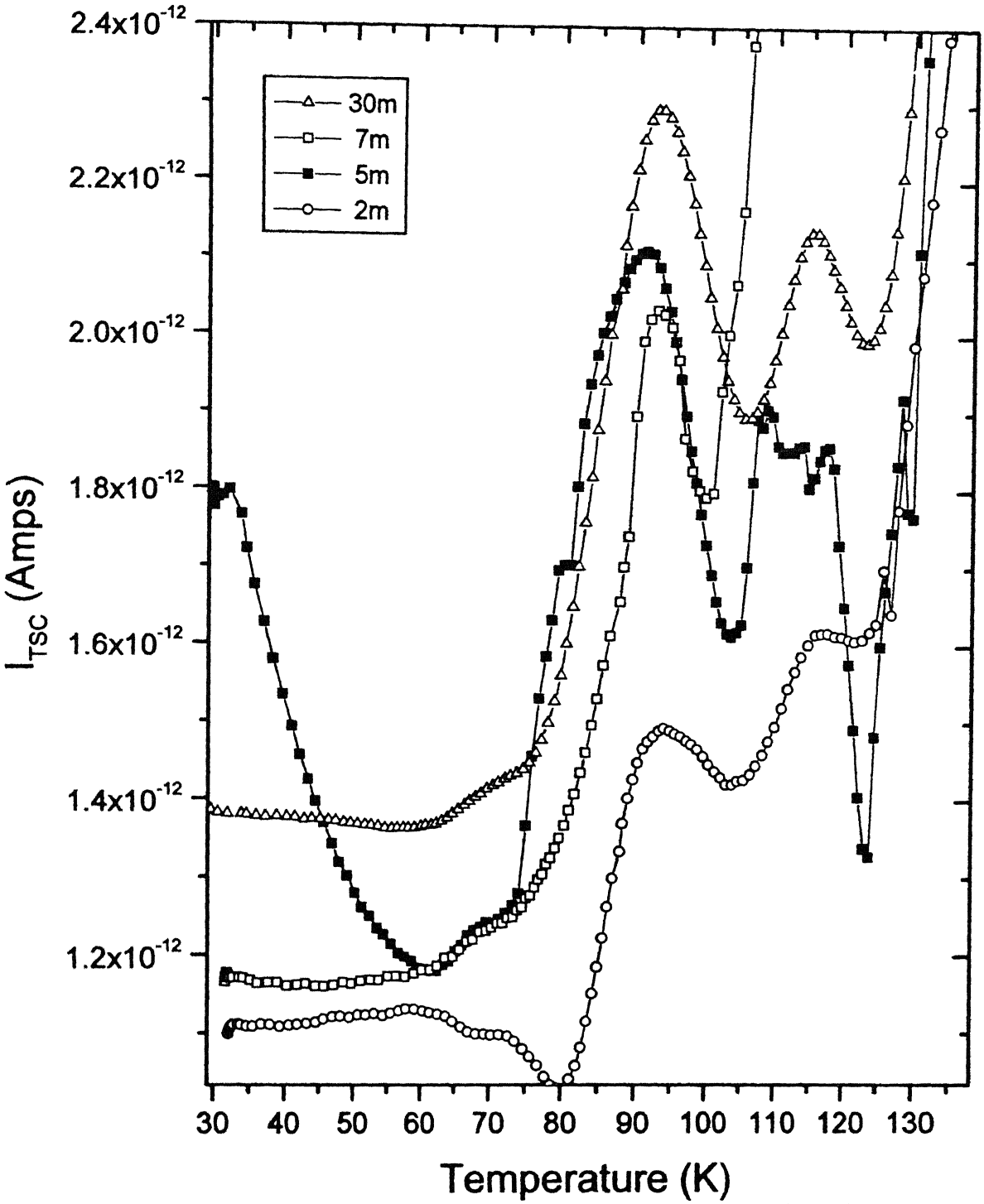

fig (5.27) The Sample is Exposed to IR for 10 min at ~26K
Heated to 120K and kept for varying lengths of time
Cooled, exposed to HeNe laser for 5 min, TSC done @ 15K/min
Shows lower occurance of instabilities at 60K

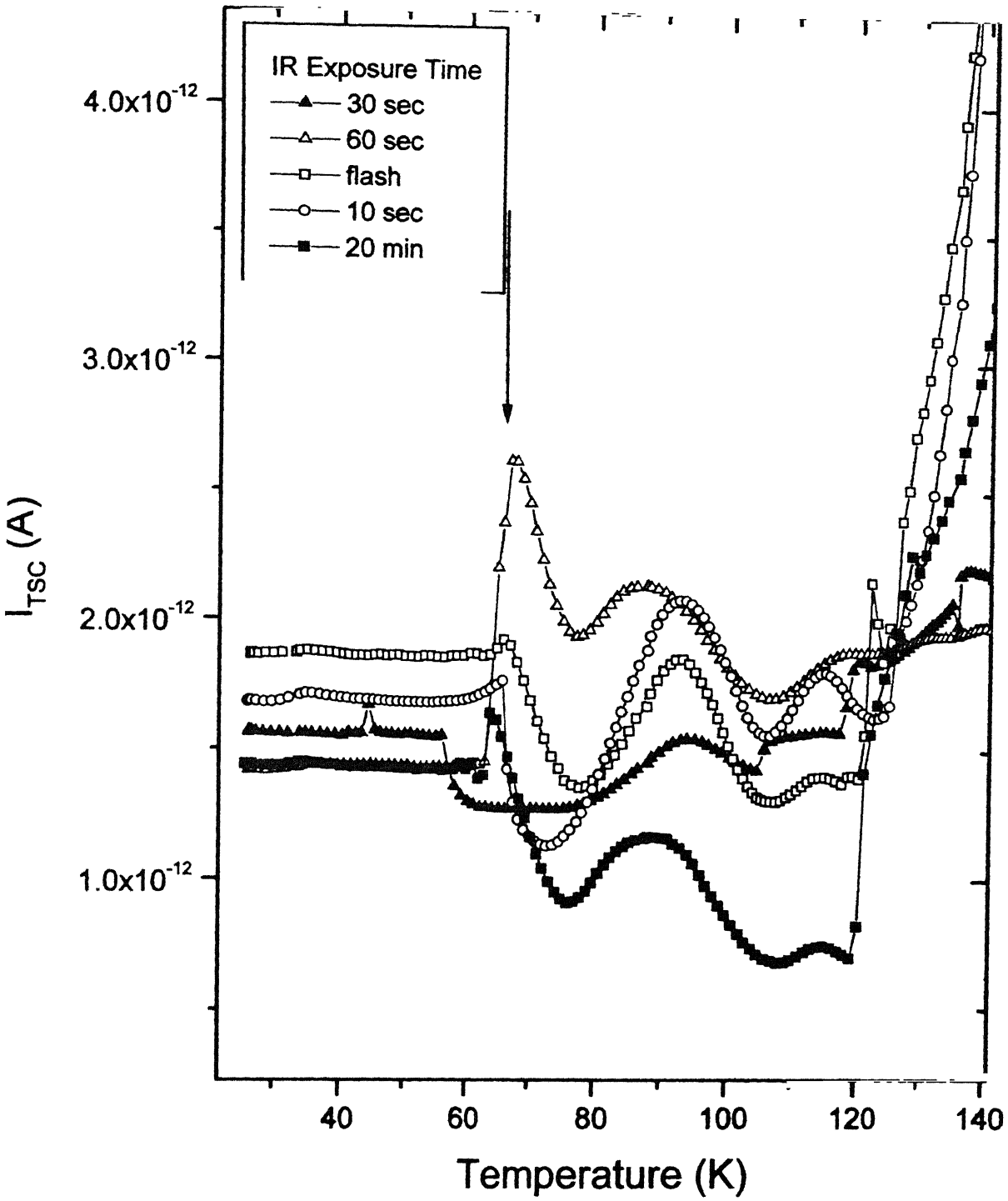

fig (5.28) Sample dark cooled, exposed to IR for varying lengths of time exposed to 5 min of laser, TSC taken at 15 K/min
Shows Instabilities at 60K

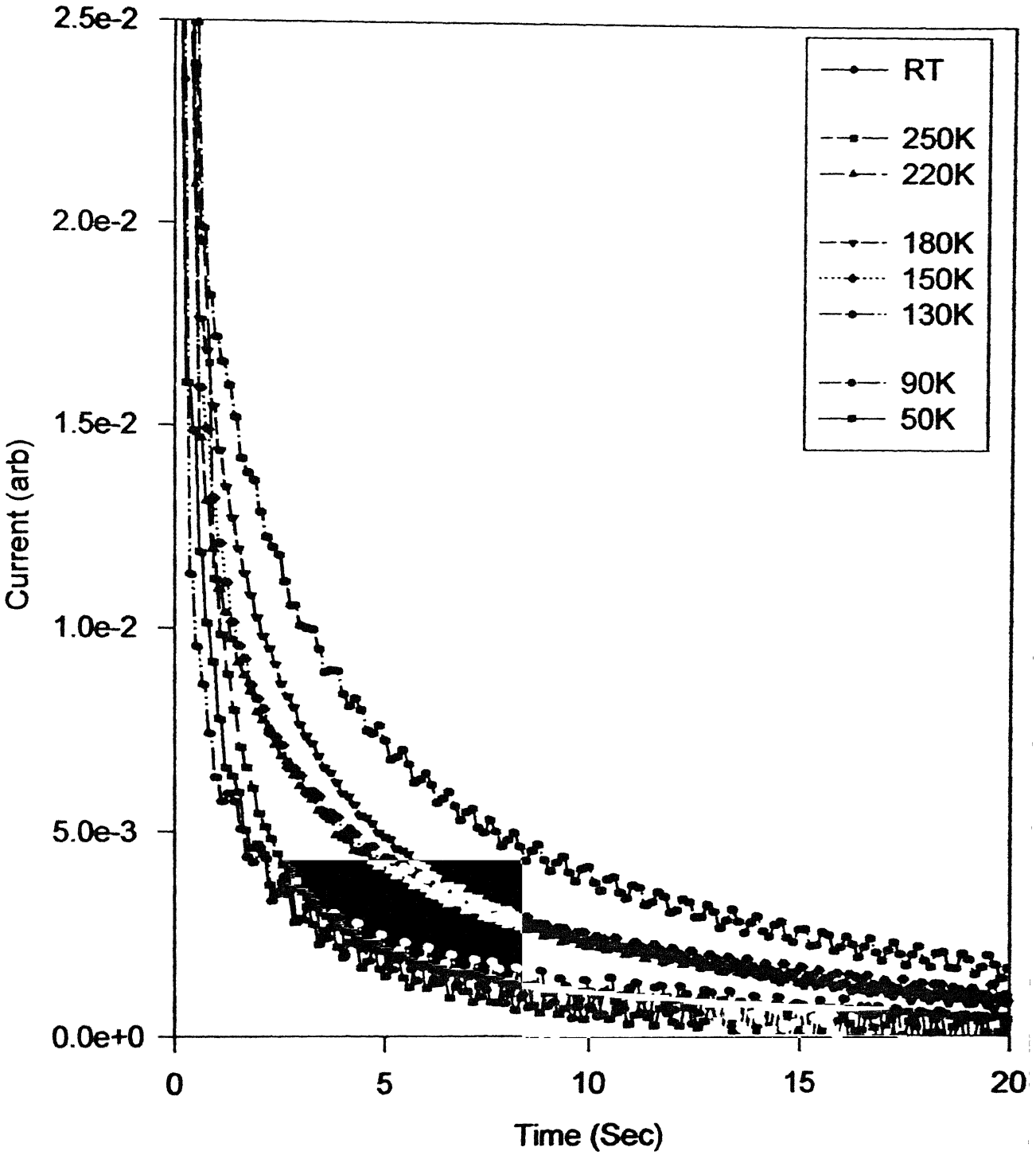

Fig(5.29) Decay transients at different Temperatures

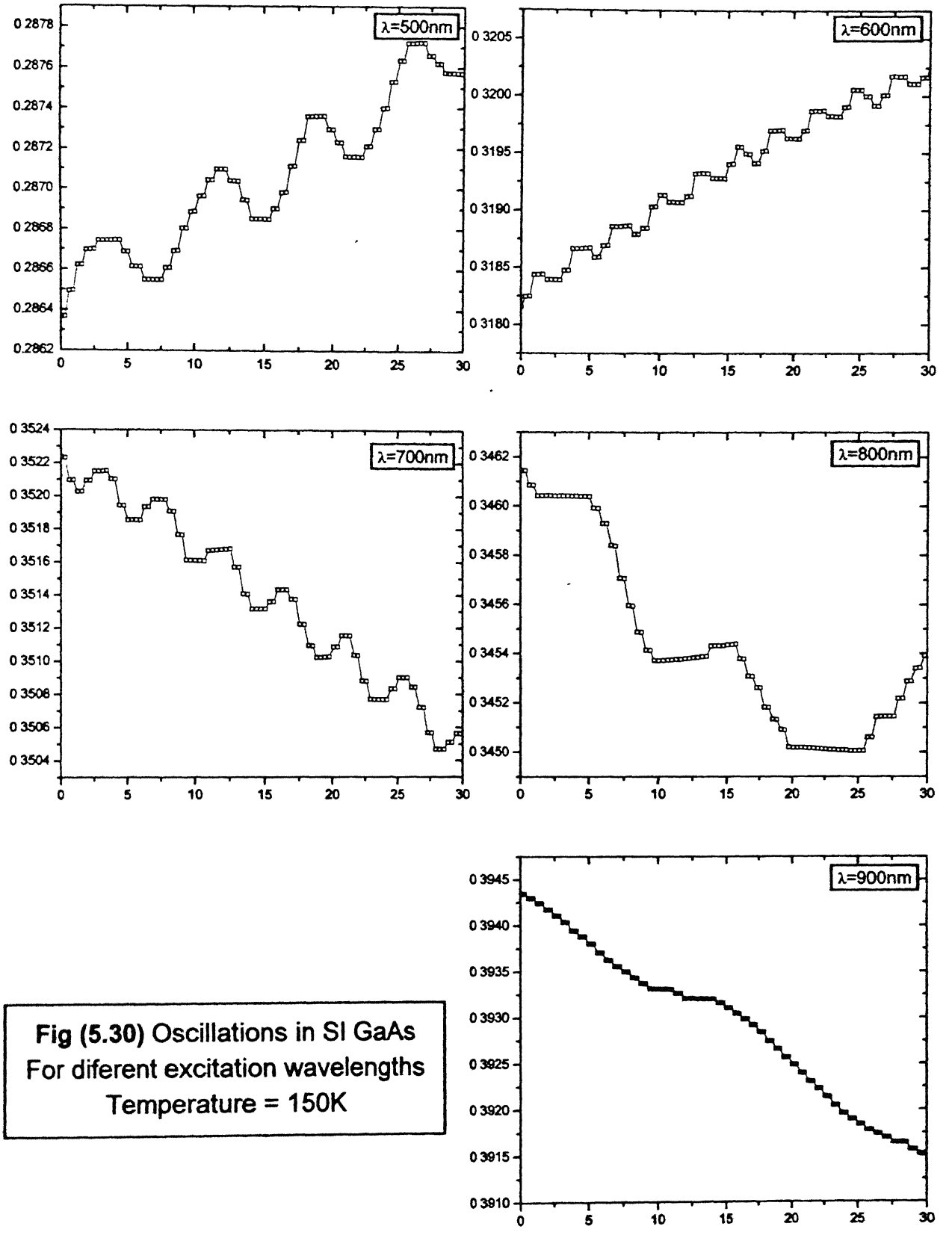

Fig (5.30) Oscillations in SI GaAs
For diferent excitation wavelengths
Temperature = 150K

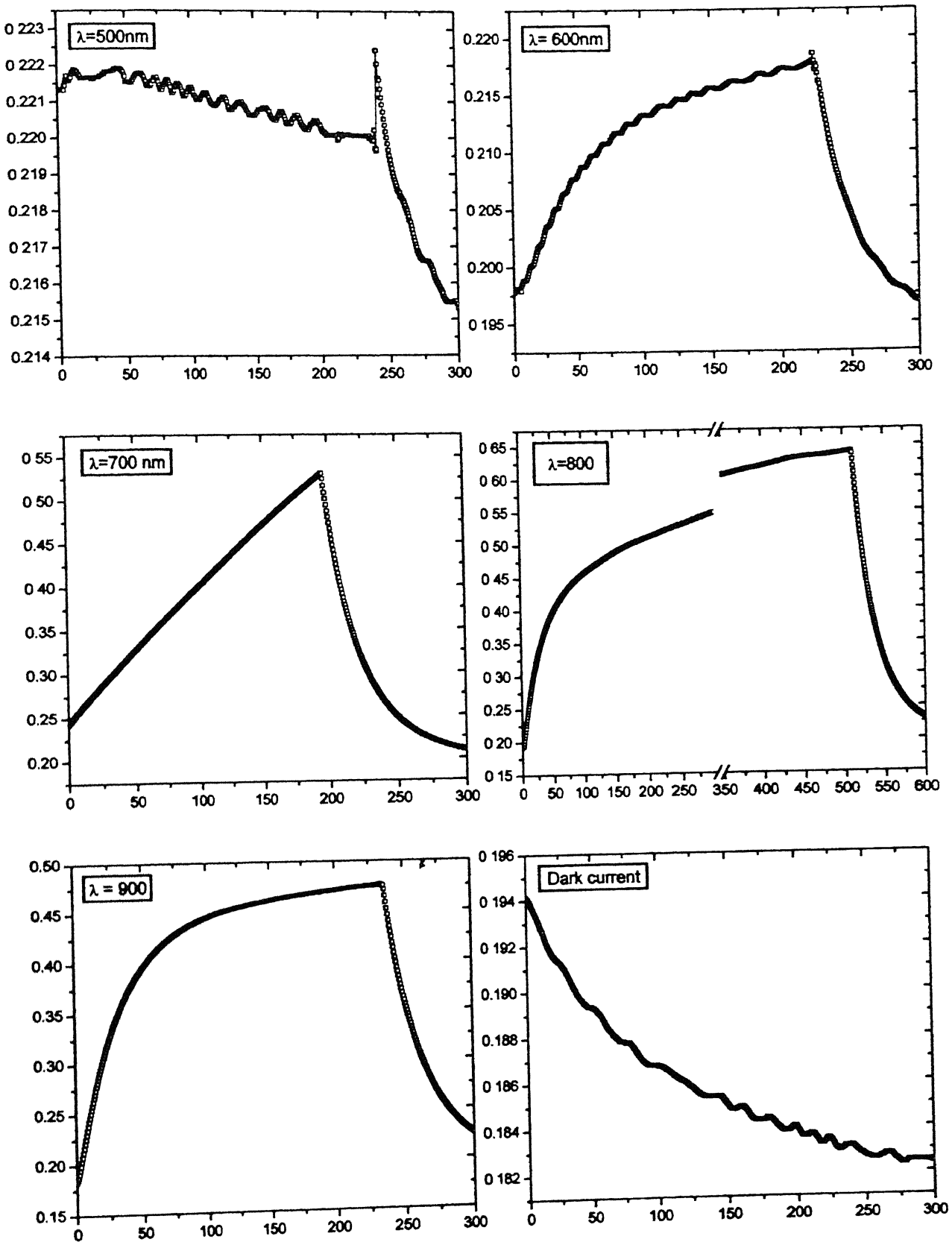

Fig (5.31) Oscillations in SI GaAs
For diferent excitation wavelengths
Temperature = 30K

Chapter 6: Conclusions

Semi-insulating gallium arsenide has been traditionally an enigmatic material, especially in its photoelectronic properties. Even after many decades of intense research, it is still defies a complete and coherent understanding. The history of research in GaAs has passed through various phases, and it has been the norm, since the mid eighties, to attribute most of its properties to the presence of a mid-gap level due to a native defect termed EL2. This level, which is indeed present in many samples in a very large concentration, and does indeed control the electronic properties of these samples to a very large extent, has been generally the focus of attention. However, in many samples depending on various factors such as growth conditions, and position in the wafer, EL2 is present in a very low concentration, and is no longer the dominant center. In such samples many other trap levels and recombination centers play important roles in determining the various properties of the material. The aim of this work has been to focus on such a sample, and investigate the various photoelectronic phenomena in order to understand the role of defect centers.

General characterization has been carried out to demarcate the experimental parameters, and also to obtain an understanding of the various traps present in the material trough thermally stimulated current measurements. Steady state photoconductivity measurements were carried out for a large temperature range from 20K to room temperature, and for a wide range of excitation intensities. Thermally stimulated current and thermally stimulated photocurrent measurements have been done for different initial conditions of trap filling at low temperatures. Time domain measurements have also been carried out in such cases.

The conclusions derived from the various experiments are itemized below.

1. The Thermally Stimulated Current measurements generally carried out to characterize the various trap levels present shows that the sample exhibits the presence of traps

normally present in semi insulating GaAs, showing six traps with two dominant ones with activation energies 0.32 eV and 0.45eV.

2. The temperature dependence of photoconductivity due to intrinsic light (676nm), with intensity as a parameter shows that
   (i) At low temperature (50K→25K) the temperature dependence is controlled by position of quasi-Fermi levels which in turn are controlled by light intensity.
   (ii) The two traps at 0.3eV and 0.45eV have been inferred from presence of two shoulders in the plot, which has been attributed to the temperature at which demarcation levels for these traps coincide with the trap level. These values are in agreement with the dominant traps observed in the TSC spectrum.

3. Little of no photoquenching is observed with high intensity IR light, an observation in direct contrast to behavior in samples containing large concentration of EL2
4. IR radiation tends to quench the TSC peaks simultaneously, but with slightly differing rates. An isothermal anneal at temperatures of 110K - 120K recovers the peak heights.
5. The quenching behavior observed can be explained on the basis of change in the occupation of lifetime controlling recombination centers with IR radiation and temperature. The observed IR quenching is not due to any configurational changes of defects or metastability.
6. The thermally stimulated photocurrent data for different heating rates show that of the two peaks observed in such a plot, only one of them presents a thermally activated process and the other only exhibits temperature dependence, being too fast a process for the heating rates used.
7. Low temperature photoconductivity transients with specially designed sequence of operation with white light, IR and 676nm shows that
   (i) Intense white light desensitizes the photoconductor due to filling of centers in the gap.

(ii) The sensitizing ability of IR radiation is dependent on the initial occupation distribution of centers, indicating that the dominant center controlling lifetime can be changed with proper choice in initial conditions

8. Temperature dependence of photocurrent due to very low intensity excitation show TSC peaks riding on the photocurrent. This further shows that the lifetime of carriers is a function of temperature and that the current levels associated with the traps are affected due to change in lifetime of carriers released from them.
9. During the course of the work, oscillating photoconductance at low temperature was observed under various experimental conditions. They need to be studied in detail in order to isolate the critical parameters and the nature of instabilities.
10. The photoconductivity decay transients at different temperatures have been measured. This shows that the decay is controlled by emission from different traps at different temperatures, and that low frequency oscillations ride on the transients.

In summary, we have set-up experimental facilities for a host of photoelectronic characterization experiments in the temperature range of 20K to 300K, and used this to characterize undoped SI GaAs using both conventional and designed experiments.

We have shown by focussing on a typical undoped SI GaAs sample that ***conventional Shockley-Read-Hall kinetics is adequate to explain IR quenching of trap activity in samples containing little EL2 centers.*** We have presented data which can form the basis for a full scale investigation into current instabilities and development of better characterization tools for SI GaAs

References

[1]Richard. H. Bube, *Photoconductivity of solids,* John Wiley & Sons, (1960).

[2]A. G. Milnes, *Deep defects in semiconductors*

[3]A. C. Lewandowski and S. W. S. McKeever, Phys. Review **B**, 43, 8163 (1991).

[4] A. C. Lewandowski, B. G. Markey and S. W. S. McKeever, Phy. Review **B**, 49, 8029 (1993)

[5]Saunders and Jewitt

[6]R. N. Hall, Phys. Rev, **87**, 387 (1952)

[7]W.Shockley and W. T. Read, Phys. Rev, **87**, 835 (1958)

[8]C. Hilsum in *Progress in Semiconductors Vol. 9*, ed. by a. F. Gibson and R. E. Burgess (Haywood, London, 1965).

[9]P. J. Dean, C. H.Henry, Phys. Rev. **176**, 928 (1968)

[10]J. Blanc and L. R. Weisberg , Nature (London) **192**, 155 (1961)

[11]C. H. Gooch, C. Hilsum, and B. R. Holeman, J. Appl. Phys. **32**, S2069 (1961)

[12]N. G. Ainslie, S. E. Blum, and J. F. Woods, J. Appl. Phys, **33**, 2391 (1962)

[13]I. Blanc, R. H. Bube and L. R. Weisberg, J. Phys. Chem. Solids, **25**, 225 (1964)

[14]S. M. Sze and J. C. Irvin, Solid-State Electron, **11**, 599 (1968)

[15]A. L. Lin, E. Cmelianovski and R. H. Bube, J. Appl. Phys, 47, 1852 (1976)

[16]D. V. Lang and R. A. Logan, J. Electron. Mater. **4**, 1053, (1975)

[17]M. Otsubo, K. Segawa and H. Miki. J. Appl. Phys, Jpn. 12, 797 (1973)

[18]A. M. Huber, N. T. Linh, M. Valladon, J. L. Debrun, G. M. Martin, A Mitonnaeu and A. Mircea J. Appl. Phys **50**, 4022 (1979)

[19]G. M. Martin, A Mitonnaeu and A. Mircea Electron. Lett, **13**,191 (1977).

[20]E. R. Weber et. al. J. Appl. Phys. **53**, 1332 (1985)

[21]J. Lagowski , D.G. Lin, T. P. Chen, M. Skowronski and H. C. Gatos Appl Phys Lett **47**, 929, (1985)

[22]B. Dischler F Fuchs and U. Kaufmanns. Appl Phys Lett, **48**, 1282, (1985)

[23] M. Baeumler , U Kaufmann and J. Windschief Appl Phys. Lett **46**, 781, (1985)

[24]M. Levinson , Phy. Rev. B**28**, 3660 (1983).

[25]J. Jimenez, P. Hernandez, J. A. de Saja and J. Bonnafe, J. Appl. Phys, **57**, 5290 (1985)

[26]J. Jimenez, P. Hernandez, J. A. de Saja and J. Bonnafe, J. Appl. Phys, **57**, 1152 (1985)

[27]J. Jimenez, M. A. Gonzalez and L. F. Sanz Santacruz Solid State Commun, **49**, 917 (1984)

[28]J. Jimenez, P. Hernandez, J. A. de Saja and J. Bonnafe, Phy. Rev. B**35**, 3832(1987).

[29]W. C. Mitchel and J. Jimenez J. Appl. Phys **75**, 3060 (1993)

[30]U. V. Desnica and B. Santic Appl Phys Lett **54**, 810 (1989)

[31]U. V. Desnica and B. Santic J. Appl. Phys **67**, 1408 (1989)

[32]B. Santic, Dunja I Desnica, B. G. Petrovic and U. V. Desnica Solid State Commun. **74**, 847 (1990).

[33]U. V. Desnica, Dunja I Desnica and B. Santic Appl. Phys **A 51**. 379 (1990).

[34]U. V. Desnica, Dunja I Desnica and B. Santic Appl Phys Lett **58**, 278 (1991)

[35]Z-Q Fang and D. C. Look Appl Phys Lett **59**, 48 (1991)

[36]Z-Q Fang and D. C. Look J. Appl. Phys **73**. 4971 (1993)

[37]Z-Q Fang and D. C. Look Appl Phys Lett **66**, 3033 (1995)

[38] R. E. Kramer, M. C. Arikan, J. C. Abele and J. S. Blackmore J. Appl. Phys **62**, 2424 (1987).

[39] J. C. Abele, R. E. Kramer, J. S. Blackmore. J. Appl. Phys **62**, 2432 (1987).

[40]P. K. Giri and Y. N. Mohapatra, J. Appl. Phys. 78, 262 (1995)